Spring 5-18-2019

Reversal of P-Glycoprotein and Breast Cancer Resistance Protein Mediated Multidrug Resistance In Vitro Using In Silico Identified Novel Compounds

Amila Nanayakkara
Southern Methodist University, ananayakkara@smu.edu

REVERSAL OF P-GLYCOPROTEIN AND BREAST CANCER RESISTANCE PROTEIN MEDIATED MULTIDRUG RESISTANCE *IN VITRO* USING *IN SILICO* IDENTIFIED NOVEL COMPOUNDS.

Approved by,

_____

Prof. John Wise
Associate Professor of Biology

_____

Prof. Pia Vogel
Professor of Biology

_____

Prof. Steven Vik
Professor of Biology

_____

Prof. Alex Lippert
Associate Professor of Chemistry

REVERSAL OF P-GLYCOPROTEIN AND BREAST CANCER RESISTANCE PROTEIN MEDIATED MULTIDRUG RESISTANCE *IN VITRO* USING *IN SILICO* IDENTIFIED NOVEL COMPOUNDS

A Dissertation Presented to the Graduate Faculty of

Dedman College

Southern Methodist University

in

Partial Fulfillment of the Requirements

for the Degree of

Doctor of Philosophy

with a

Major in Molecular and Cell Biology

by

Amila K. Nanayakkara

B.S., Molecular Biology and Biochemistry, University of Colombo, 2011

May 18, 2019

ACKNOWLEDGMENTS

First, I would like to thank Dr. Pia Vogel and Dr. John Wise for giving me this wonderful opportunity to pursue my Ph.D. in their lab. This work would have been impossible to accomplish without their unlimited support. Especially I would like to thank Dr. Vogel for responding to my email 7 years ago and arranging for me to shadow senior graduate students in the lab initially. I think that gave me an opportunity to get exposure I needed very much. Both Drs. Vogel and Wise you provided me the guidance exactly I needed to fulfill this task.

I would like to thank my committee members Dr. Steven Vik and Dr. Alex Lippert for their guidance throughout the past 5 years. Also, I would like to acknowledge collaborators of our lab, Dr. Noelle Williams from UTSW and Dr. Ashlee Moses from OHSU for their support. I was blessed to have received their expertise that heavily benefitted my research.

My present and past lab colleagues have been very supportive of my work. Specially, I am grateful for the guidance and mentorship by Dr. Courtney Follit. Further, I would like to thank Dr. McCormick, Maisa, Gang, Collette, Maha and Lauren. Also, I would like to thank two undergraduates who worked with me, Kasi and Beau, who were wonderfully supportive. Further, I would like to acknowledge both academic and nonacademic staff in SMU Biology department who were supportive to me in many ways. Outside the laboratory, I had the opportunity of getting to know wonderful new friends in Dallas who were supportive in various ways to my life and special thank goes to Aditi, Elnaz, Shruthy, Tetiena and Lena.

Last but not least my main gratitude goes to my family. My parents always believed in my skills and gave me the freedom to follow my dreams. Finally, I am so grateful to my loving wife, Nipunika Somatilaka. She has shared all the good and bad times with me and supported me throughout my studies.

Amila K. Nanayakkara B.Sc. Molecular Biology and Biochemistry, University of Colombo, Sri Lanka

REVERSAL OF P-GLYCOPROTEIN AND BREAST CANCER RESISTANCE PROTEIN MEDIATED MULTIDRUG RESISTANCE *IN VITRO* USING *IN SILICO* IDENTIFIED NOVEL COMPOUNDS.

Advisor: John G. Wise, Ph.D.
Doctor of Philosophy conferred May 18, 2019
Dissertation completed April 15, 2019

Multidrug resistance (MDR) is a major cause of chemotherapy failure. Overexpression of ATP-binding cassette (ABC) transporters, P-glycoprotein (P-gp) and breast cancer resistance protein (BCRP) are two well-studied drug transporters which are associated with MDR. These two transporters also act as a major functional unit of the blood brain barrier to protect the brain from xenobiotics and toxins. Lack of clinically approved P-gp and BCRP inhibitors renders chemotherapy treatments of many MDR cancers ineffective and obstructs drug uptake into the brain.

Using computational methods, we have identified new compounds that inhibit P-gp (Brewer *et al*., Mol. Pharmacol. 2014). Several of these compounds show successful MDR reversal in the drug resistant DU145TXR prostate cancer cell line (Follit *et al*., Pharmacol. Res. Perspect. 2015). Here, we further analyze these P-gp inhibitors **29**, **34** and **45** in a P-gp over-expressing ovarian cancer cell line, A2780ADR, and a P-gp over-expressing prostate cancer cell line, DU145TXR. Treatment of chemotherapeutics with the *in silico* identified inhibitors led to a higher mortality in MDR cancer cells in tests conducted with both conventional 2D and 3D-spheroid cell-based assays. Using a novel assay based on cellular accumulation of compounds in a P-gp overexpressing cell line, we report that **29**, **34** and **45** do not function as P-gp transport substrates. It was found that the efficacy of chemotherapy can be enhanced by initial cotreatment

of chemotherapeutics with P-gp inhibitor **29** followed by an extended treatment using only inhibitor **29** without having chemotherapeutics in the media. Further, we describe the effects of chemical variants of the P-gp inhibitor **29** in experiments aimed at improving the pharmacological characteristics of the inhibitor. The variants were generated using computational approaches or by structure-based design in attempts to improve P-gp inhibition. Multiple variants showed an improved efficacy in reversing paclitaxel resistance in the P-gp over-expressing DU145 TXR prostate cancer cell line. We achieved a 100% success rate using computational lead optimization in obtaining variants of P-gp inhibitor **29** which do not function as transport substrates of P-gp.

In related work, we developed a breast cancer cell line that overexpresses the BCRP transporter for the purpose of identifying inhibitors of the BCRP drug pump. Three of the variants of inhibitor **29** could reverse the BCRP-mediated MDR in this BCRP overexpressing breast cancer cell line. Further, we identified several other compounds that interfered with BCRP mediated transport *in vitro* screened from an inhouse library of small molecules.

The experimental inhibitors of P-gp and BCRP in this study appear to be promising candidates for further development into co-therapeutics to treat MDR cancers and modulate the blood brain barrier.

TABLE OF CONTENTS

List of Figures

List of Tables

I would like to dedicate this work to my wife Nipunika Somatilaka who shared this tough journey with me.

CHAPTER 1: BACKGROUND

1.1 Multi Drug Resistance and ABC transporters

multidrug resistance (MDR) is termed as the ability of a disease condition to develop the tolerance for multiple structurally or functionally different therapeutic agents simultaneously [1], [2]. Earlier, publications on this phenomena revolved around drug resistant bacteria, but later the development of MDR was discovered in other diseases such as cancers against chemotherapy [3]. Although chemotherapy is the most effective method for treating metastatic cancers, MDR is a major reason for chemotherapy failure, which can arise intrinsically or as a result of chemotherapy itself [4], [5]. There are multiple pathways of MDR in cancers including drug efflux, drug inactivation, alternation of drug targets, DNA damage repair and cell death inhibition [6]. The earliest and the most studied cellular MDR mechanism is drug efflux by transporters of the ATP-binding cassette (ABC) family [7]–[11]. Overexpression of these transporters can lower the intracellular accumulation of various anti-cancer drugs to decrease the efficacy of chemotherapy [12].

ABC-type transporters are found in almost all living organisms [13]. All these transporters belong to a superfamily of proteins with seven subfamilies (designated A to G) and 48 ABC transporters are found in humans [14]. These transporters are frequently located in cell membranes (transmembrane) and are involved in transporting a wide variety of both organic and inorganic substances across membranes against an electrochemical gradient utilizing the energy from of ATP hydrolysis catalyzed by the transporters [13]–[15]. P-glycoprotein (P-gp) and

Breast Cancer Resistance Protein (BCRP) are two important ABC-type transporters which confer MDR in cancers by extruding anti-cancer agents out of cancer cells [16]–[18].

1.2 P-glycoprotein (P-gp)

1.2.1 P-gp structure and function

After a series of studies based on drug resistant Chinese hamster ovary cells [19]–[21], Ling *et al.* in 1976 discovered a glycoprotein with a size of approximately 170 Kda and named it the Permeability-glycoprotein as it could alter the drug permeability of cells [22]. Permeability-glycoprotein commonly known as P-glycoprotein (P-gp) is also referred to as multidrug resistance protein 1 (MDR1) or ATP-binding cassette sub-family B member 1 (ABCB1) in the literature [23]. Human P-gp is encoded by the *MDR1* gene located at chromosome 7q21 with the genomic sequence size of approximately 209 kb [24]. Several polymorphisms are found in *MDR*1 gene which affect the pharmacokinetics of several chemotherapeutics [25].

Numerous transcriptional factors, including p53 [26] and many cell signaling pathways are also involved in the transcriptional regulation of the P-gp gene [27]. Among those signaling pathways, the PI3K/Akt pathway [28], the Wnt/ β-catenin pathway [29] and the MAPK/ERK pathway [30] have been reported to positively regulate the expression of P-gp . Contradictory studies showed that the JNK pathway is involved in both positive regulation and negative regulation of P-gp expression [31], [32] and the p38 MAPK pathway has been shown to negatively regulate the expression of P-gp [33]. Factors affecting the phosphorylation and glycosylation of the protein were reported to be involved in translocation and stability, while ubiquitination related proteins were involved in degradation of P-gp [27]. More recently involvement of micro RNA and long non-coding RNA have been suggested to be involved in post-transcriptional regulation of expression of P-gp [34], [35].

P-gp is a single polypeptide transmembrane protein with 1280 residues that contains two homologous halves. Each half contains a transmembrane domain (TMD) with six helices followed by a nucleotide binding domain (NBD). The two NBDs form the ATP binding sites where energy from ATP hydrolysis is provided to extrude molecules. Several helices from both transmembrane domains are responsible for forming the drug binding domain (DBD) which provides the binding site(s) for various molecules [36]–[40]. In addition, a flexible linker region between the two homologous halves of the protein plays a crucial role in bringing in two NBDs together to form ATP-binding sites [41]. The conformational changes that occur in the NBDs as a result of ATP binding and/or hydrolysis causes a rearrangement in transmembrane helices which triggers the transportation of DBD bound molecules out of the cells [42]–[44]. The glycosylation of P-gp occurs in the extracellular portion and may play a role in trafficking of P-gp into the cell surface, but this modification has not been observed to influence drug transport [45].

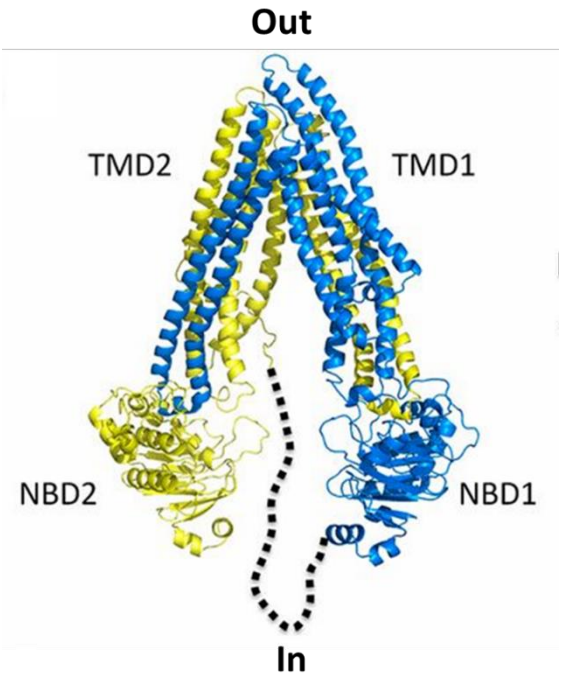

Figure 1.1- **3-Dimensional structure of P-gp**
The "open inward" crystal structure of P-gp with NBDs apart. The N-terminal half of the protein (blue) and the C-terminal half (yellow) are connected by a flexible linker region (black dashed line). TMD – Transmembrane domain; NBD – Nucleotide binding domain. Image is modified from Ward *et al*. [46]

After the discovery of P-gp expression in cell lines with MDR phenotypes, Fojo *et al*. in 1987 demonstrated mRNA expression of the *MDR1* gene in human tumors and healthy human tissues such as adrenal gland, kidney, lung, liver, lower jejunum, colon, and rectum [47]. Later, the expression of P-gp was discovered in blood capillaries involved in biological barriers such as blood brain barrier (BBB) [48], blood testes barrier [49] and placenta [50]. This expression pattern of P-gp in normal human tissues suggests that P-gp function may be to prevent the accumulation of detrimental substances inside human vital organs [47], [51], [52]. The tissue distribution patterns indicate that P-gp may play a significant role in excreting xenobiotics and metabolites into urine and bile and into the intestinal lumen, all processes which can affect the pharmacokinetics of drug availability in the human body [53]–[56]. Furthermore, it has been

shown that P-gp participates in the secretion of steroid hormones such as cortisol, testosterone, and progesterone from the adrenal gland [57].

Although humans have one *MDR1* gene expressing P-gp, mice express two P-gp encoding genes, mdr1a and mdr1b, which confer MDR [58]–[60]. It has been suggested that a double knockout mouse of both mdr1a and mdr1b is required to study the physiological role of P-gp in *in vivo* conditions to predict an equivalent impact of P-gp in humans [61]. Interestingly the double knockout mdr1a/1b (−/−) mice did not show physiological abnormalities in viability, development, fertility, and in a range of other biological parameters. This suggests the presence of the other proteins or biological systems that can mimic or complement the functions of P-gp. Most importantly, these observations suggested that transiently inhibiting P-gp in humans when P-gp is implicated in diseases like MDR in cancer might lead to increased chemotherapeutic efficacies [62]. Conversely, since the double knockout mdr1a/1b (−/−) mice exhibited altered pharmacological parameters such as increased drug accumulation in the brain and modulated activities in hematopoietic progenitor cells, therapeutic inhibition of P-gp will likely complicate the pharmacodynamics of chemotherapies [62], [63].

1.2.2 Role of P-glycoprotein in MDR cancers

The expression and function of P-gp was first demonstrated *in vitro* using drug resistant cell lines [19]–[22]. These drug resistant cell lines exhibited a simultaneous resistance to several drugs although the cells were originally selected for the MDR phenotype with only one anti-cancer agent. Overexpression of P-gp in various cancer cell lines has resulted in reduced accumulation of chemotherapeutics and exhibit resistance against various currently prescribed anti-cancer drugs such as taxanes (paclitaxel), vinca alkaloids (vinblastine), and anthracyclines (daunorubicin) [7].

Bell *et al*. observed the overexpression of P-gp in clinical cancer biopsy samples for the first time in 1985. They correlated the overexpression of P-gp in advanced ovarian cancer clinical samples with the patients' non-responsiveness to chemotherapy using a monoclonal antibody raised against P-gp [64]. Goldstein *et al*. later reported higher expression levels of P-pg before initiation of chemotherapy in solid tumors such as colon, renal, hepatoma and pancreatic cancers, and in both untreated or treated cancers such as neuroblastoma, acute lymphocytic leukemia (ALL) in adults and acute nonlymphocytic leukemia (ANLL) in adults [65]. Subsequent studies have also reported similar findings of elevated P-gp expression in clinical samples with either intrinsically or acquired resistance [66]. Poor clinical prognoses, treatment outcomes, survival rates and drug resistances have been connected with P-gp over expression in breast cancers [67], ovarian cancers [68], osteosarcomas [69], and acute myeloid leukemias (AML) [70], and the results from these studies have suggested that P-gp could be therapeutically targeted. The increased P-gp expression in human cancers after chemotherapy has been demonstrated using the *in vivo* experiments. Post chemotherapy doxorubicin resistance in a mouse model for hereditary breast cancer has been suggested to be caused by elevated levels of both mdr1a and mdr1b genes [71]. Most importantly, this doxorubicin resistance could be completely reversed by tariquidar, a P-pg inhibitor [71]. Unfortunately, tariquidar has shown only marginal success in clinical trials [72]. More details about current P-gp inhibitors are discussed in later in this chapter.

1.3 Breast cancer resistance protein (BCRP)

1.3.1 BCRP structure and function

A drug resistant breast cancer cell line that was selected with adriamycin (doxorubicin) and verapamil which was shown not to over-express P-gp or the multidrug resistance-associated

protein 1 (MRP1) led to the discovery of a new type of ABC transporter named the breast cancer resistance protein (BCRP) [73]. In concurrent work, a similar expression of BCRP was observed in a colon carcinoma selected in the presence of mitoxantrone. In this latter work, BCRP was reported as the "mitoxantrone resistance protein" [74]. BCRP belongs to the G subfamily of ABC transporter superfamily, hence it is called also ABCG2 in literature [75]. Human BCRP is encoded by the *ABCG2* gene located at chromosome 4q22. Expression results in a 2.4-kb mRNA encoding a 655- amino acid, 72 kDa polypeptide localized to the plasma membrane [76], [77]. In contrast to P-gp expression, p53 [78], [79] and MAPK/ERK pathways were reported to be involved in down regulation of BCRP, and upregulation of its expression was correlated with the JNK signaling pathway [80]. In addition, microRNA-328 has exhibited down regulatory effects in BCRP expression post-transcriptionally [81].

Unlike P-gp, BCRP is called a half transporter since the single polypeptide encoded from *ABCG2* contains only a single TMD and a NBD. Similar to several known bacterial ABC half-transporters, the BCRP l dimerizes to form a functional transporter [76]. BCRP is known to form heterodimers between wild type monomer with a variant monomer with mutations [82]. It is reported that cysteine (Cys^{603}) in the extracellular loop between TMDs participates in the stabilization of dimerization of BCRP by forming a disulfide bond [83] with its partner on the second monomer. Each TMD region composed of six α-helices is followed by a NBD region in the monomers. Like other ABC transporters BCRP also utilizes the energy derived from ATP binding and hydrolysis at its NBDs after dimerization into a functional transporter to extrude transport substrate molecules out of cells through the TMDs. Binding and hydrolysis of ATP in the NBDs triggers a conformational change in TMDs which enables the BCRP to bind with various structurally and functionally different molecules and release them to the outside of cells

[84]. Several mutations in BCRP have been reported to affect the transport activity of BCRP. Specifically, mutations in position 482, 557 and 630 can change the affinity and transporter activity towards anti-cancer drugs such as mitoxantrone, methotrexate, doxorubicin and reporter molecules like rhodamine 123 [85].

Beside the discovery of BCRP in drug resistant cell lines, in 1998 Allikmets *et al*. reported an ABC-type transporter that was highly expressed in human placenta, which was later discovered to be BCRP/ ABCG2 [86]. The tissue distribution of BCRP overlaps with P-gp expression in normal, noncancerous tissues. ABCG2/BCRP is widely expressed in the placenta, blood brain barrier, gastrointestinal tract, liver, kidney, testis, and lactating breast [87]. BCRP also appears to play a protective role against xenobiotics and their metabolites entering vital organs in the human body. BCRP expressed in the gut is thought to restrict the bioavailability of orally administered drugs and to facilitate biliary and renal elimination of drugs and xenobiotics in the liver and kidney [88].

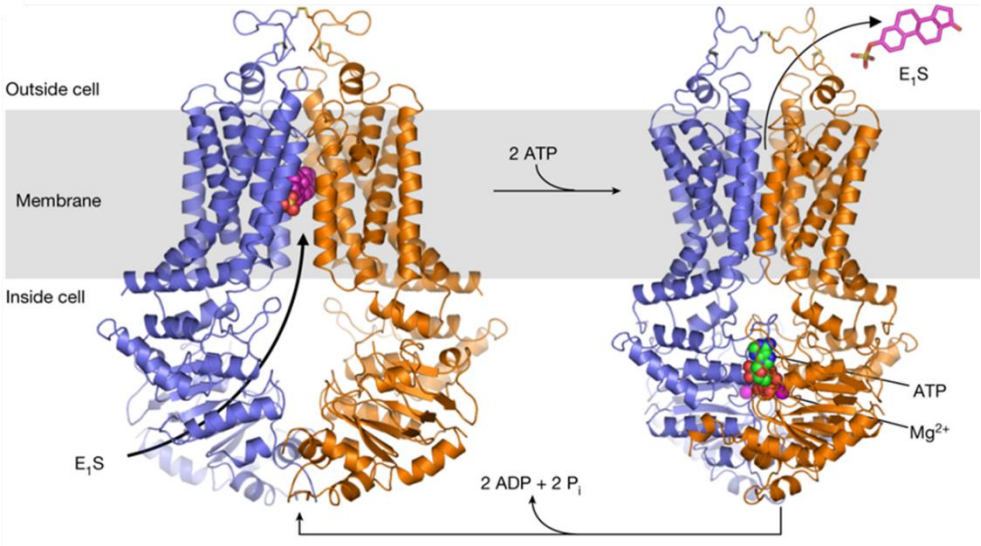

Figure 1.2 **- 3-Dimensional structure of BCRP**
Cartoon representation of BCRP bound to BCRP substrate estrone-3-sulfate (E_1S) in left and BCRP bound with ATP while releasing E_1S in right. Each monomer of BCRP is colored in blue and orange. NBDs are exposed to the inside of the cell and the TMDs span through the membrane. Image modified from Manolaridis *et al*. [84].

1.3.2 Role of BCRP in MDR cancers

As noted above, BCRP was initially discovered in a breast cancer cell line selected for an MDR phenotype by using doxorubicin and verapamil [73]. Cancer cell lines with numerous tissue origins exposed to mitoxantrone also were observed to exhibit BCRP-mediated MDR [89]. Other than traditional cytotoxic anti-cancer drugs such as doxorubicin, daunorubicin [90], mitoxantrone [74] and methotrexate [91], BCRP substrates include relatively novel chemotherapeutics such as topotecan [92], SN-38 [93] and clofarabine [94]. Topotecan and SN-38 are topoisomerase I inhibitors [95] and clofarabine is a nucleoside analogue [96]. Another class of BCRP substrates are oncogenic tyrosine kinase inhibitors. Imatinib, nilotinib and gefitinib are a few of the clinically used kinase inhibitors which are reported to interact with BCRP, lowering the efficacy of these chemotherapeutic treatments [90]. Photosensitizers used in photodynamic therapy are a class of molecules with the ability to generate reactive oxygen species after absorption of light of a specific wavelength. These agents can induce apoptosis and necrosis in treated tissues [97]. Both i*n vitro* and *in vivo* experiments have indicated that BCRP can significantly reduce the intracellular accumulation of photosensitizers and thereby reduce the effectiveness of photodynamic therapies [98]. Surprisingly, overexpression of BCRP has also been reported to promote a stem cell-like phenotype in prostate cells which are less responsive to hormone based therapies [99], and a stem cell-like cell population has been reported to escape from radiotherapy with higher mRNA expression of *ABCG2* [100].

The overexpression of BCRP in cancers has mainly been reported in hematologic cancers [77]. Numerous studies demonstrated the overexpression of BCRP in acute myelogenous leukemia (AML) samples compared to the healthy bone marrow cells. Higher mRNA levels in AML are correlated with relapse or refractory samples compared to the samples collected before

the treatments [101]–[103]. Acute lymphoblastic leukemia (ALL) and chronic myelogenous leukemia (CML) are two more hematological cancers with reported higher BCRP expression, although more studies are required to understand the functionality of BCRP in those cancers [104]–[106]. Other than blood related cancers, BCRP overexpression has been correlated with poor clinical outcomes of solid tumors, breast cancers, digestive tract tumors, melanomas, and non-small-cell lung carcinoma (NSCLC) [107]. In addition, recent studies suggest that BCRP can be used as a marker to identify cancer stem cells (CSCs) [108]. According to a novel theory, only CSCs in a tumor have the potential to self-renew and differentiate to maintain malignancy and these cells facilitate tumor relapse and tumor chemotherapy resistance [109], [110].Other studies also implicate BCRP in the chemotherapy resistance in relapsing tumors [111].

1.4 Physiological role of P-gp and BCRP in blood brain barrier

The blood brain barrier (BBB) is a structural and functional barrier between the blood and the brain / central nervous system which acts as a gate-keeper for molecules entering the CNS. The BBB prevents or limits the entrance of foreign materials (molecules or even cells) and function as a protective tissue barrier for the brain. The BBB is composed of endothelial cells, pericytes, immune cells, astrocytes, and the basement membrane. There are pores among the endothelial cells of blood capillaries in most of the peripheral tissues allowing small molecules to freely diffuse into the extracellular space around cells of the peripheral tissues. In contrast, the endothelial cells in brain capillaries have adherence and tight junctions sealing the capillaries. Further, pericytes and astrocytes also closely interact with these endothelial cells to support the barrier function. So physically these cells prevent the entrance of relatively large molecules allowing only the gas and small lipid soluble molecules to leave the capillaries and enter the brain [112]–[117]. Significantly, the molecules that can diffuse through cell membranes are also

limited in their ability to enter the CNS by the transporters that are expressed in the endothelial membranes of the BBB [118]. ABC transporters therefore play an important active role in BBB, and P-gp and BCRP are the two most important ABC transporters present in the BBB which limit xenobiotic entrance to the brain [119], [120].

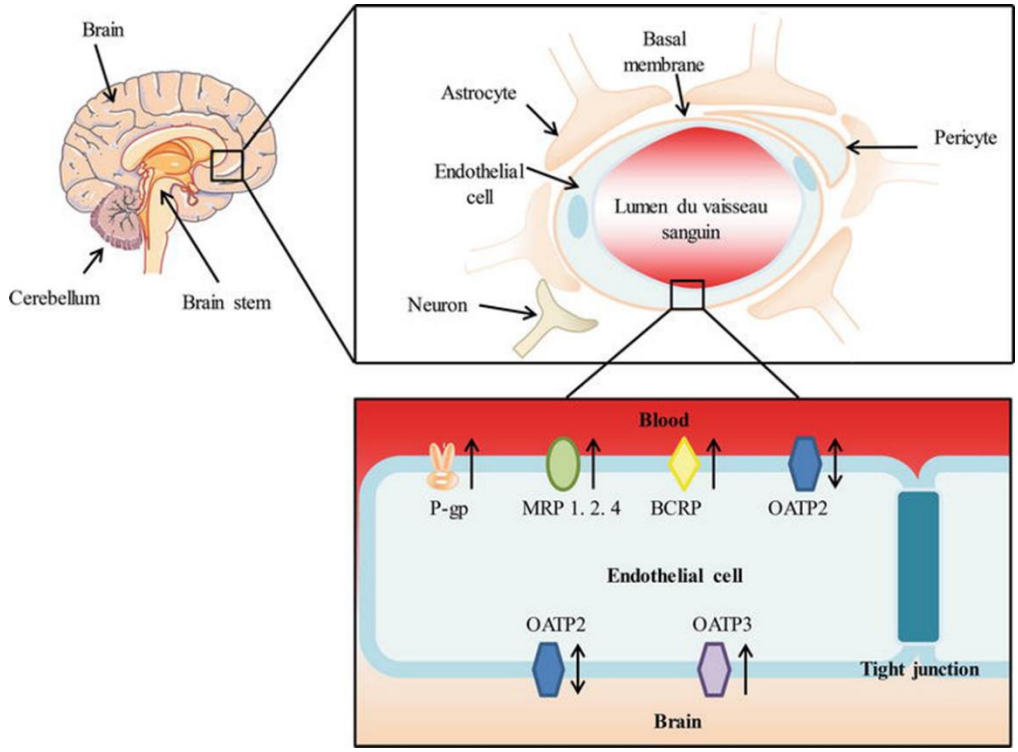

Figure 1.3 - **Structure and the location of the blood brain barrier**
Endothelial cells, astrocytes, pericytes and basal membrane together form the blood brain barrier. P-gp, BCRP and several other transporters in endothelial cells limit the entrance of xenobiotics from blood by extruding those back. Image modified from Helm *et al.* [121].

The BBB provides a massive pharmacological challenge to getting medications to reach targets in the brain. In fact, it has been estimated that 98% of the potential drugs targeted for central nervous system are unable to reach their target because of the BBB [122]. A considerable number of these drugs are among those that can be extruded by the P-gp and BCRP expressed in the BBB [123]. Imatinib and gefitinib are two tyrosine kinase inhibitors used to treat glioblastomas and brain metastases of cancers. These compounds, as mentioned above, are also

P-gp and BCRP substrates. The P-gp and BCRP present in the BBB thus lower the accumulation of these inhibitors in the brain [124], [125]. Furthermore, the accumulation in the brain of conventional chemotherapeutics like doxorubicin are also limited by P-gp and BCRP activities in the BBB [123]. P-gp is involved in reducing brain accumulation of taxanes such as paclitaxel [126] and BCRP can reduce the concentration of topoisomerase inhibitors such as mitoxantrone and topotecan [123]. P-gp also limits the entrance of HIV medications [127], [128], antihistamines [129], antidepressants [122] anti-epileptic [130] and antibiotics [131] through BBB into the brain where desired drug targets can be located. Because of the complications that arise from P-gp and BCRP activities in the BBB, the idea of transiently inhibiting P-pg and BCRP by the use of co-therapeutic inhibitors has also gained considerable attention for possible ways to successfully delivery therapeutic concentrations of drugs to the brain as much as for MDR reversal [132].

1.5 Inhibitors of P-gp and BCRP

1.5.1 P-gp inhibitors

Tsuruo *et al.* in the 1980s reported the use of verapamil, a good transport substrate of P-gp, as an MDR reversal agent in experiments performed both *in vitro* and *in vivo* [133]–[135]. Since that time, small, drug-like molecules that can compete with or interfere with the transport activity of P-gp (often termed modulators and inhibitors, respectively) have been extensively studied for the purpose of reversing MDR. P-gp inhibitors are classified into three generations based on their specificity, affinity, and toxicity[136].

The first generation inhibitors of P-gp are drugs which were used for other specific treatments, but that have the side effect of interacting with P-gp. Like verapamil, an antihypertensive agent, these first generation inhibitors were actually transport substrates for P-

gp and, hence, could compete with the extrusion of compounds that needed to be accumulated inside cells [11]. This generation of inhibitors consisted of numerous pharmaceuticals which were used for different purposes such as cardiac agents [137], antibiotics [138], immunosuppressants [139] , and antiviral agents [140]. But these drugs also could interact with other transporters and proteins causing unpredictable pharmacokinetics interactions. Furthermore, some these compounds had a low affinity for P-gp and thus required high serum concentrations to modulate P-gp activity which increases the likelihood of off-target drug interactions [12], [141].

Second generation inhibitors were derivatives of first generation such as dexverapamil [142] and analogues of cyclosporin A (PSC833) [139]. These compounds were modified to try to avoid the undesirable pharmacokinetics which the first generation drugs possessed. Although some of these compounds acted better than first generation inhibitors, they still retained properties which limited using them as P-gp inhibitors clinically. Some of the compounds from second generation were not specific for P-gp and increased chemotherapy related toxicities [11].

The third generation of P-gp inhibitors like tariquidar [143] were developed to overcome the limitations of the second generation with higher specificity and affinity towards P-gp to lower the observed toxicities. These P-gp inhibitors had been developed by using quantitative structure-activity relationships (QSAR) and combinatorial chemistry approaches. [2]. Some of these third generation inhibitors are still under clinical development to improve efficacy and specificity. Inhibitors like zosuquidar and laniquidar were reported to be non substrates for P-gp [143]. A third generation P-gp inhibitor, tariquidar has the ability to inhibit ATPase activity of P-gp thus suggested to bind with NBD or to an allosteric location [144]. However, the word

"modulator" has been used in literature for both P-gp inhibitors such as tariquidar or P-gp pump substrate competitive inhibitors like verapamil [145], [146].

1.5.2 BCRP inhibitors

Many studies have been performed that demonstrated the reversal of BCRP-mediated MDR by the use of BCRP inhibitors which are non substrates for BCRP or substrates which are competitive inhibitors of drug transport *in vitro* [90], [147]. Like the first generation of P-gp modulators, BCRP substrates have been studied as competitive inhibitors of transport to reverse the MDR phenotype. The majority of the compounds tested were tyrosine kinase inhibitors which were also substrates of P-gp [148], [149]. Fumitremorgin C is a well-studied agent which interfered with BCRP activity, but nevertheless showed significant neurotoxicity when the experiments were performed *in vivo* [150], [151]. The fumitremorgin C analogue, Ko143, has been reported to inhibit BCRP specifically and has exhibited promising data *in vivo* with less toxicity than the parent drug [151]. The proton pump inhibitor, pantoprazole, a drug used for the treatment of peptic ulcers, has also been used as a BCRP inhibitor in preclinical studies but showed uncertain results [152].

1.5.3 Clinical trials of P-gp and BCRP inhibitors

P-gp inhibitors have gained only a limited success clinically, although they have been repeatedly successful in reversing MDR in *in vitro* and *in vivo* studies [11]. A P-gp inhibitor of first generation, verapamil, has been clinically tested in combination with adriamycin to treat ovarian cancers and lymphomas. These clinical trials failed due to increased prevalence of side effects such as cardiac dysfunctions including heart failures [153]–[155]. The majority of these first generation inhibitors failed in clinical trials due to either high toxicities or lack of efficacy in human trials [11]. In contrast, however, the use of the P-gp modulators, tetrandrine, tesmilifene

[11] and cyclosporin A, for AML have been shown to improve clinical outcomes [156]. Specially, cyclosporin A inclusion with chemotherapy resulted in significant gains in relapse-free and overall survival, once again raising hopes for a strategy of using P-gp inhibitors as co-therapeutics during chemotherapies [156].

Only a handful of studies among many clinical trials have reported enhanced treatment outcomes for third generation P-gp inhibitors. The majority of the clinical trials focused on third generation inhibitors failed to improve chemotherapy efficacy. A study focused on dofequidar fumarate (MS-209), a P-gp and MRP-1 inhibitor, exhibited prolonged progression-free survival of breast cancer patients without prior treatments when used in combination with the chemotherapeutics, cyclophosphamide, doxorubicin, and fluorouracil [157]. Another study which was focused on the use of the P-gp inhibitor, tariquidar, in combination with vinorelbine, reduced the clearance of vinorelbine and increased its concentration in tumor masses[158].

According to a review published in 2011, there have only been five clinical trials, concentrating solely in BCRP inhibitors and the reversal of MDR in advanced solid tumors. These studies utilized tyrosine kinase inhibitors which are BCRP substrate as chemosensitizers in combination with chemotherapy. Although tolerable levels of inhibitor doses were achieved, clinical benefits were not observed [159]. Additionally, a phase III clinical trial for colorectal cancers treated with the tyrosine kinase inhibitor, sorafenib, combined with chemotherapeutics did not improve the outcomes for the treatment group compared to the chemotherapy only treatment [160].

Development of compounds that inhibit both P-gp and BCRP may open BBB and increase oral availability of therapeutics due to the overlapped expression of P-gp and BCRP at the BBB and the epithelial of gut respectively [132], [134]. Pilot studies have reported the ability of

enhancing blood brain permeability to drugs safely using tariquidar [161], [162]. Furthermore, the use of elacridar, a dual inhibitor of P-gp and BCRP, was reported to significantly increased the oral bioavailability of the chemotherapeutic, topotecan, in cancer patients [163].

Except for several inhibitors which have shown some promising data in clinical trials, the requirement of clinically approved P-gp and BCRP inhibitors remains as a significant, unmet medical need. Further studies are required to identify novel inhibitors of these transporters with lower side effects for the purpose of reversing MDR in cancers, increasing BBB permeability of drugs, as well as increasing the oral availability of important therapeutics.

1.6 Rationale

After three decades of extensive studies on reversing transporter mediated MDR in cancers, the requirement of having a clinically approved inhibitors for P-gp and BCRP remains unfulfilled. The demonstrated successes of P-gp inhibitors in a few clinical studies indicate the requirement of identifying and optimizing novel inhibitors that have high specificity for the transporters and which are intrinsically less toxic [11]. A major focus of our group is to identify inhibitors of P-gp or BCRP which are not transport substrates for the relevant transporters. Using high-throughput computational screenings, our group has identified many different P-gp inhibitors (including compounds **29**, **34** and **45**) which reversed the paclitaxel resistance shown in the P-gp overexpressing DU145TXR prostate cancer cell line [164], [165].

The scopes of this study are continuation of analyzing potential P-gp inhibitors **29**, **34** and **45**, lead optimization of **29** to improve P-gp inhibition efficacy and the identification of novel BCRP inhibitors. Follit *at el*. reported the reversal of paclitaxel mediated resistance in prostate cancer cells *in vitro* [165] using **29**, **34** or **45.** We hypothesize that these inhibitors should be applicable with other P-gp overexpressing cancer cell lines and chemotherapeutics other than

paclitaxel if P-gp is the accurate target of **29**, **34** or **45**. If these compounds are inhibiting P-gp that will lead to a higher intracellular accumulation of P-gp substrates/ chemotherapeutics. Higher accumulation of chemotherapeutics in cancer cells due to P-gp inhibition should then impact the viability, apoptosis, cell migration and colony formation ability of cancer cells. Also, our computational approach is to find P-gp inhibitors which are non P-gp substrates. Hence, we hypothesized that intracellular accumulation of **29**, **34** and **45** would not be affected by P-gp inhibition with known P-gp inhibitors. Furthermore, if we are successful in lead optimization of compound **29** in either conventional or computer based methods, we should be able to observe improved efficacy in lead optimized variants of P-gp inhibitor **29** under *in vitro* conditions. Finally, we expect to identify BCRP inhibitors using *in vitro* assays from an in house library of small molecules which has accumulated over the time in laboratory which were initially targeted for either BCRP, P-gp or bacterial transporter proteins.

CHAPTER 2: TARGETED INHIBITORS OF P- GLYCOPROTEIN 29, 34 AND 45 INCREASE CHEMOTHERAPEUTIC-INDUCED MORTALITY OF MULTIDRUG RESISTANT TUMOR CELLS

2.1 Introduction

Multidrug resistance (MDR) remains a major obstacle despite all the advances in chemotherapy [4], [5], [65], [166]. P-gp is one of the most studied proteins regarding the reversal of MDR in cancer [167]. The ability of P-gp to efflux a broad range of chemotherapeutics out of the cancer cells enables the MDR in cancers [168]. Although inhibition of efflux by P-gp has been the center of many studies of P-gp as a drug target, no clinically approved P-gp inhibitors are available yet [11]. The majority of previous inhibitors of P-gp are indeed transport substrates for P-gp and showed only a limited success in clinical trials, likely because of side effects resulting from high concentrations required to inhibit P-gp [11].

Computational approaches are a rapid and economical strategy for drug discovery [169]. Research from our lab has utilized molecular dynamics and docking approaches to screen for inhibitors of P-gp using computational homology models of P-gp [43]. A previous study by Brewer *et al*. [164] employed high-throughput, parallel computational screens of a database of drug-like structures [170], [171] to a homology model of P-gp [43]. This study [164] mainly focused on identifying P-gp inhibitors targeting the nucleotide binding domains (NBD) of the P-gp protein without being substrates to the drug binding domains (DBD). After screening millions of drugs like molecules from data bases, the study yielded four inhibitors that specifically

targeted the NBDs of P-gp while avoiding interactions with the DBD. These four inhibitors (compounds **19**, **29**, **34** and **45**) significantly inhibited the ATPase activity of P-gp, while three of these inhibitors (compounds **19**,**34** and **45**) directly affected the nucleotide binding to the P-gp. These predicted inhibitors were studied by Follit *et al*. [165] in the P-gp overexpressing DU145 TXR prostate cancer cell line [172]. This study revealed that **29**, **34** and **45** reversed the P-gp mediated paclitaxel resistance in DU145 TXR prostate cancer cells [165]. SMU-19 did not reverse this drug resistance, probably due to the negative charge carried by the molecule which likely made it cell impenetrable [165]. These inhibitors had only a modest cytotoxicity by themselves on cancer cells as well as HFL1 non-cancerous cells [173] when these cells were treated with inhibitor concentrations that corresponded to those used for the reversal of paclitaxel resistance in DU145 TXR prostate cancer cells.

In the following study we further analyzed these three inhibitors. Here we show that these three inhibitors can be used to reverse MDR in the P-gp over-expressing ovarian cancer cell line A2780 ADR. We demonstrated the ability of these P-gp inhibitors to reverse P-gp mediated paclitaxel and vinblastine resistance, thus reducing the viability, cell migration and colony formation, while also increasing cell apoptosis. These inhibitors also increased the P-gp substrate accumulation in cells as tested with daunorubicin and calcein-AM. Additionally, in this study we introduced a novel cellular assay to identify P-gp transport substrates to confirm that the novel inhibitors we report here are not P-gp substrates.

2.2 Results

2.2.1 Overexpression of P-glycoprotein leads to multidrug resistance in the ovarian cancer cell line, A2780ADR

Follit *et al*. [165] showed the ability of compounds **29**, **34**, or **45** to reverse MDR in a prostate cancer cell line that over-expresses P-gp [172]. In the present study, we expanded our work to a drug resistant ovarian cancer cell line. Figure 2.1A shows the characterization of paired ovarian cancer cell lines, A2780 [174], and the highly drug resistant line derived from it, A2780ADR [137]. Western blot analyses using a P-gp-specific primary antibody showed that while the A2780ADR cells expressed significant amounts of P-gp (Figure 2.1A, left lane), no P-gp was detectable in the parental A2780 cells (Figure 2.1A, right lane). Also consistent with earlier work using prostate cancer cells [137], the results using the ovarian A2780ADR cells showed much higher resistance than the parental A2780 cell line to the vinca alkaloid, vinblastine, when tested using a resazurin-based cell viability assay [175], [176] (Figure 2.1B). High levels of resistance to paclitaxel by A2780ADR cells were also observed when exposing the cells to increasing concentrations of the taxane, paclitaxel (Figure 2.1C). Inclusion of 60 µM novobiocin, a relatively specific inhibitor of BCRP [177], or 250 µM probenecid, an inhibitor of the multidrug resistance associated protein 1 (ABCC1, MRP-1)[178], together with vinblastine had no effect on the sensitivity of A2780ADR cells to the chemotherapeutic (Figure 2.1B). These results strongly suggest that the A2780ADR ovarian cancer cell line was phenotypically multidrug resistant and that this MDR phenotype was correlated to overexpression of P-glycoprotein and not BCRP or MRP-1.

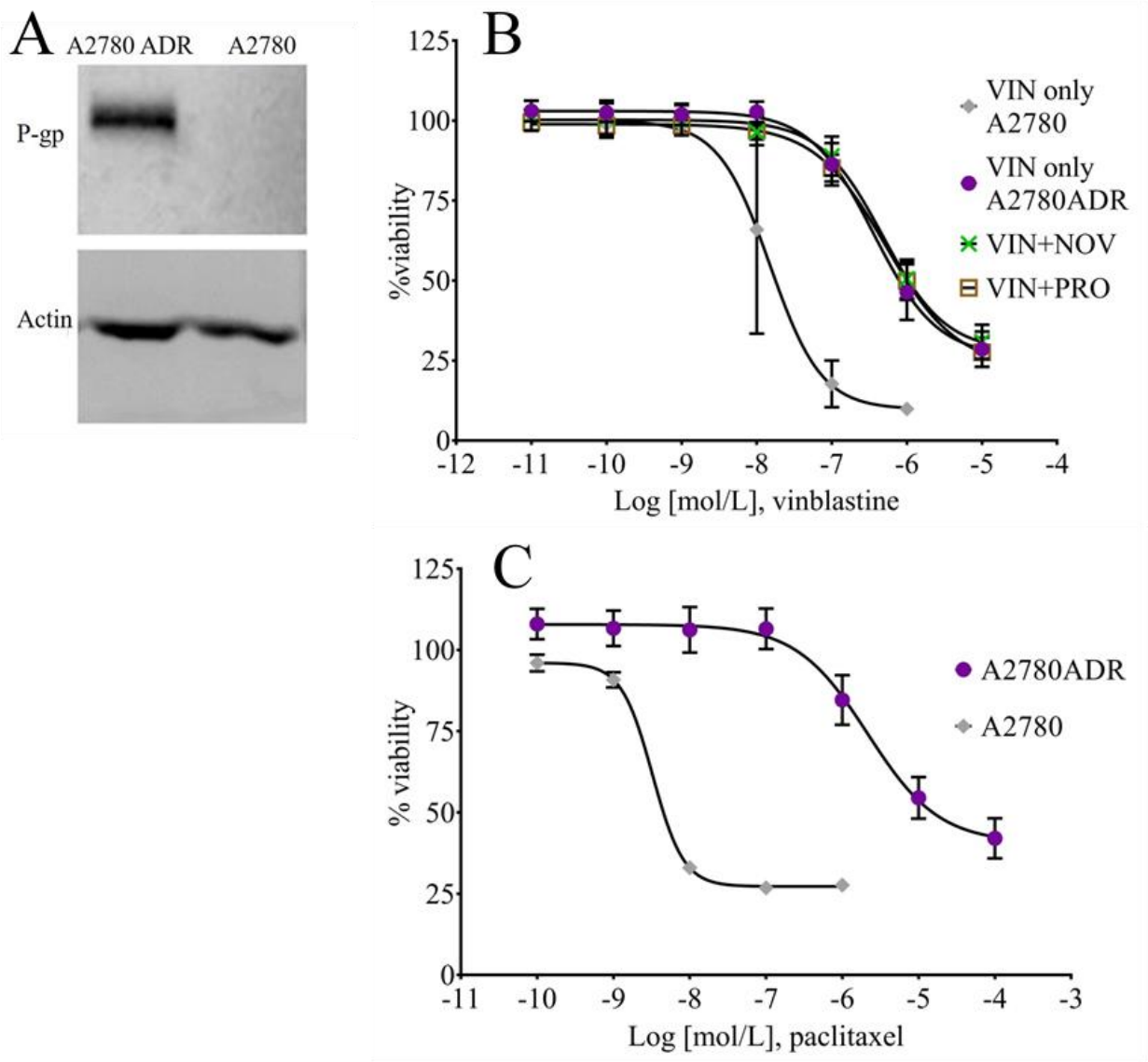

Figure 2.1- **The multidrug resistance phenotype of an ovarian cancer cell line.**
A - Western blot analyses of A2780ADR (left lane) and A2780 (right lane) were performed using anti-P-gp and anti-actin antibodies. **B** - Cell viability was determined using the resazurin assay to analyze the resistance to vinblastine; *diamonds*, chemotherapeutic-sensitive cell line A2780; *circles*, chemotherapy-resistant cell line A2780ADR; *open squares*, addition of 250μM of the MRP1-specific inhibitor, probenecid; *crosses*, addition of 60μM of the BCRP-specific inhibitor, novobiocin. **C** - Cell viability assays as in Panel B, but in the presence of paclitaxel; *diamonds*, chemo-sensitive cell line A2780; *circles*, chemotherapy-resistance cell line A2780ADR. Data represents the mean ± SD of 12 replicates from two independent experiments. Some error bars are too small to be visible outside of the data points. PTX, paclitaxel; VIN, vinblastine; NOV, novobiocin; PRO, probenecid.

2.2.2 Inhibitors of P-glycoprotein reverse MDR phenotype of the ovarian cancer cell-line, A2780ADR

Figure 2.2 shows the relative viability of A2780ADR cells as reported by the resazurin assay when incubated with increasing concentrations of paclitaxel (Figure 2.2A) or vinblastine (Figure 2.2B) with or without addition of P-gp inhibitors 29, 34, 45, or verapamil. The structures of the compounds 29, 34 and 45 are shown in Figure 2.2C. It can be seen from Figure 2.2A and B that the sensitivity of the MDR cell line to chemotherapeutics was increased by several orders of magnitude in the presence of the P-gp inhibitors. Inclusion of the BCRP inhibitor, novobiocin, or the MRP-1-inhibitor, probenecid, had no discernable effect on these cells (Table **2**.**1**), suggesting that neither BCRP nor MRP-1 contributed to the MDR phenotype of the cells. Table **2**.**1** compares the calculated IC50 values for the chemotherapeutics paclitaxel or vinblastine in the presence or absence of P-gp inhibitors for the two ovarian cancer cell lines. No sensitization of the non-MDR parental cell line A2780 was observed. These results suggest that the ovarian cell line A2780ADR is multidrug resistant because of overexpression of P-gp and that its MDR phenotype can be reversed by the inhibitors of P-gp ATPase activity, compounds **29**, **34** and **45** [164], [165], as well as the P-gp transport substrate and competitive transport inhibitor, verapamil.

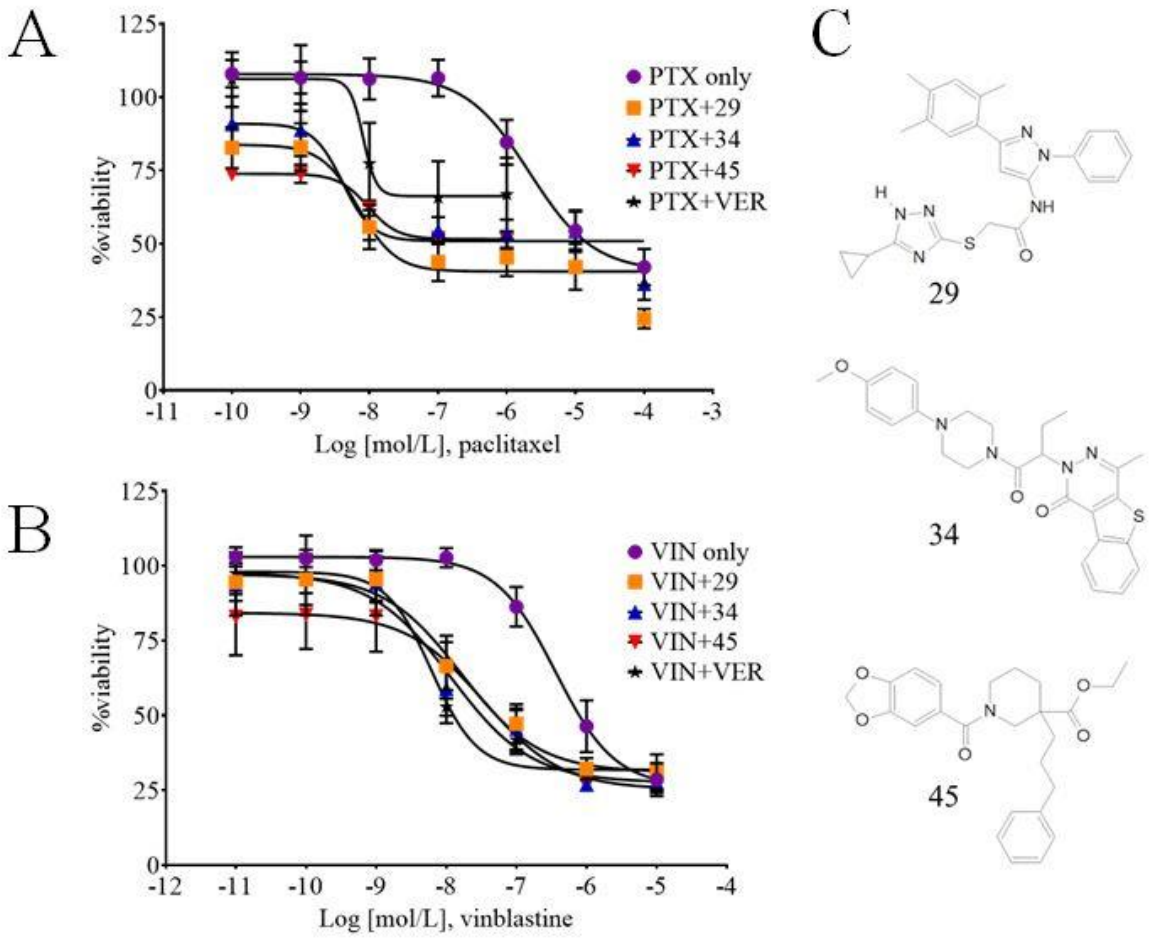

Figure 2.2 - **Reversal of paclitaxel or vinblastine resistances by novel inhibitors of P-glycoprotein using metabolic viability assays.**

A2780ADR cells were treated in the presence of compounds 29, 34, 45 or verapamil with the indicated concentrations of chemotherapeutic. **A** - circles, paclitaxel alone; squares, paclitaxel plus 25 µM compound 29; triangles, paclitaxel plus 25 µM compound 34; inverted triangles, paclitaxel plus 25 µM compound 45; stars, paclitaxel plus 25 µM P-gp substrate verapamil. **B** - circles, vinblastine alone; squares, vinblastine plus 10 µM compound 29; triangles, vinblastine plus 10 µM compound 34; inverted triangles, vinblastine plus 10 µM compound 45; stars, vinblastine plus 10 µM P-gp substrate verapamil. Data represents the mean ± SD of 12 replicates from two independent experiments. **C** - Chemical structures of novel P-gp inhibitors 29, 34 and 45. PTX, paclitaxel; VIN, vinblastine; VER, verapamil.

Table 2.1 – **In silico identified P-gp inhibitors reverse MDR phenotype of ovarian cancer cell line.**
IC_{50} concentrations of chemotherapeutics which resulted in 50% decrease in A2780ADR viability were calculated from data as shown in Figures 1, S3 and S4 using a nonlinear, four-parameter curve fitting procedure.

		paclitaxel IC_{50}(nmol/L)	Fold sensitization	vinblastine IC_{50} (nmol/L)	Fold sensitization
A2780ADR	paclitaxel/vinblastine only	2146		361	
	+ compound 29				
	5 μM	121	18	52	7
	10 μM	42	52	16	22
	25 μM	7	308		
	+ compound 34				
	5 μM	57	38	42	9
	10 μM	20	107	12	31
	25 μM	4	528		
	+ compound 45				
	5 μM	122	18	49	7
	10 μM	90	24	34	11
	25 μM	10	225		
	+ verapamil				
	5 μM	53	41	19	19
	10 μM	22	99	6	58
	25 μM	8	265		
	+ novobiocin				
	60 μM			475	1
	+ probenecid				
	250 μM			525	1
A2780	paclitaxel/vinblastine only	5		15	
	+ compound 29				
	10 μM	5	1	14	1
	+ compound 34				
	10 μM	5	1	14	1
	+ compound 45				
	10 μM	4	1	16	1
	+ verapamil				
	10 μM	5	1	13	1

2.2.3 Novel P-gp inhibitors increased apoptosis in MDR prostate cancer cells when co-treated with paclitaxel

Results of resazurin viability assays with the A2780ADR cells (Figure 2.1 and Figure 2.2) show unexpectedly high residual cell viabilities of between 25% with vinblastine and up to 60% when

paclitaxel was used. While the overall results were consistent with increased cytotoxicity of chemotherapeutics in the presence of P-gp inhibitors, these results did not directly demonstrate that co-administration with inhibitor led to increased cell mortality. To test for increased cell mortality, the adherent MDR prostate cancer cells (DU145TXR) [172] were used, since the semi-adherent properties of A2780ADR cells made cell imaging much less reliable. In experiments designed to assess the induction of apoptosis, DU145TXR cells were treated either with 1 μM paclitaxel alone, 10 μM P-gp inhibitors alone, or combinations of paclitaxel with inhibitors for 48 hours.

Analysis of these assays took advantage of the facts that acridine orange is taken up both by viable and non-viable cells, intercalates with double stranded DNA, and emits green fluorescence, while ethidium bromide is only taken up by non-viable cells and emits a strong red fluorescence after interchelating with DNA [179], [180]. As shown in Figure 2.3, cells treated with vehicle, paclitaxel or P-gp inhibitors alone showed green fluorescence with highly organized nuclear morphologies, suggesting no induced apoptosis. In Figure 2.3B, the blue arrow points out one such morphologically non-apoptotic nucleus. Upon combination treatment with chemotherapeutic and P-gp inhibitors, the number of cells with shrunken, rounded, and darker condensed cell morphologies increased (Figure 2.3A, bright field panels). The number of cells that demonstrated obvious chromatin fragmentation also increased (Figure 2.3B, white arrows). The number of dead cells, as indicated by ethidium bromide fluorescence also increased after co-treatments with chemotherapeutic and P-gp inhibitors (Figure 2.3B, yellow arrows) compared to

paclitaxel only treated cells. These results indicated that paclitaxel induced apoptosis in DU145TXR cancer cells when P-gp activity was blocked by the P-gp targeted inhibitors.

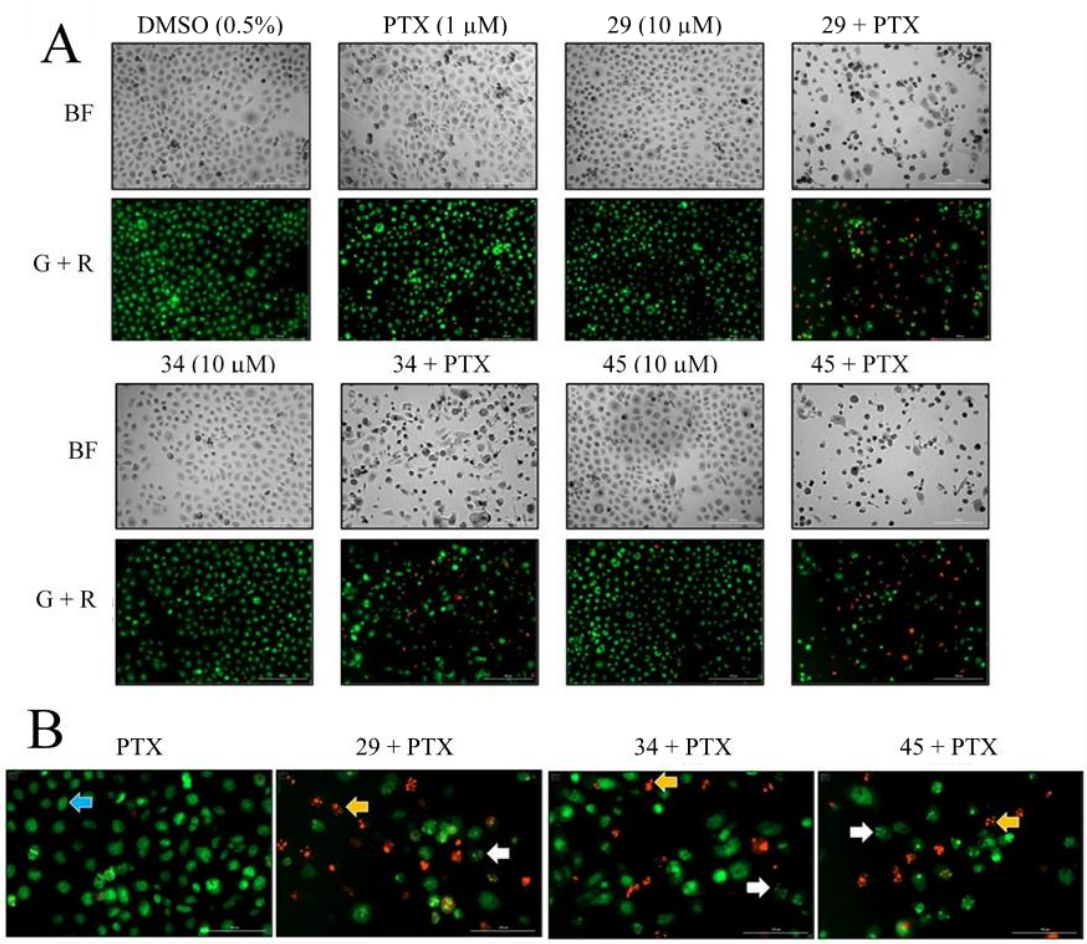

Figure 2.3 - **Reversal of paclitaxel resistance by novel P-gp inhibitors induces apoptosis in MDR prostate cancer cells.**
A - DU145TXR cells were treated either with 1 μM paclitaxel alone, 10 μM of novel P-gp inhibitors alone, or combinations of paclitaxel with P-gp inhibitors for 48 hours, followed by staining with acridine orange and ethidium bromide. Top panels show the bright field images while lower panels show the merged images obtained using GFP and Texas red fluorescence filters. Both were recorded with 10X objectives. **B** - Enlarged images of the merged images obtained in panel A with the treatments shown. The blue arrow represents a nucleus that is not affected by paclitaxel. Cells in early stages of apoptosis with visible nuclear fragmentation are indicated with white arrows, and apoptotic cells, stained red with ethidium bromide are indicated by yellow arrows. PTX, paclitaxel; BF, bright field photomicrograph; G + R, green plus red fluorescence composite images.

2.2.4 Reversal of MDR by added P-gp inhibitors results in inhibition of cell proliferation upon exposure to previously sub-lethal concentrations of chemotherapeutics

To experimentally test the hypothesis that cells which had residual metabolic activity after co-treatment with chemotherapeutic and P-gp inhibitors were either dying or lost proliferation ability, colony formation experiments [181] were performed. Figure 2.4A shows the results of qualitative colony formation experiments, where A2780ADR cells were treated for 48 hours with either vehicle alone, 0.1 μM vinblastine or 1 μM paclitaxel, 10 μM P-gp inhibitor alone, or combinations of chemotherapeutic and P-gp inhibitor. Time of exposure to chemotherapeutic and or inhibitor were the same as in Figure 2.2. The cells were then washed with media that did not contain chemotherapeutic or inhibitors and were allowed to recover for 96 hours after which the presence of cell colonies was assessed by crystal violet staining. In the presence of inhibitor in combination with paclitaxel or vinblastine, no cell colonies were observed (Figure 2.4A). In contrast, exposure to paclitaxel, vinblastine, or the inhibitors alone, resulted in very dense, viable cell colonies which were qualitatively equivalent to the DMSO control (Figure 2.4A).

To more quantitatively assess cell viability and colony formation and to test a different multidrug resistant cancer cell line, similar experiments were performed using the MDR prostate cancer cell line, DU145TXR [172]. The conditions for these experiments were chosen to represent the lowest exposure time and inhibitor concentration that resulted in significant differences in the number of colonies formed. Cells were treated for 24 hours with 0.5 μM paclitaxel alone, 5 μM inhibitor alone, or combinations of inhibitor and chemotherapeutic. Afterwards, the media containing inhibitor and/or chemotherapeutic were removed and the cells were allowed to recover for 120 h in the absence of chemotherapeutic or P-gp inhibitor. The cells were fixed and stained as described above. Figure 2.4B, top panel, shows images of the crystal

violet stained colonies visible to the unaided eye. Figure 2.4B bottom, shows the statistical analyses of two such independent experiments. The number of colonies formed in the presence of paclitaxel and P-gp inhibitors was found to be significantly lower than when cells were grown with inhibitor or chemotherapeutic alone. These results support the hypothesis that the residual metabolic activities reported by the resazurin viability assays in Figure 2.1and Figure 2.2 were due to the residual metabolic activities of cells that were dying, but not yet dead.

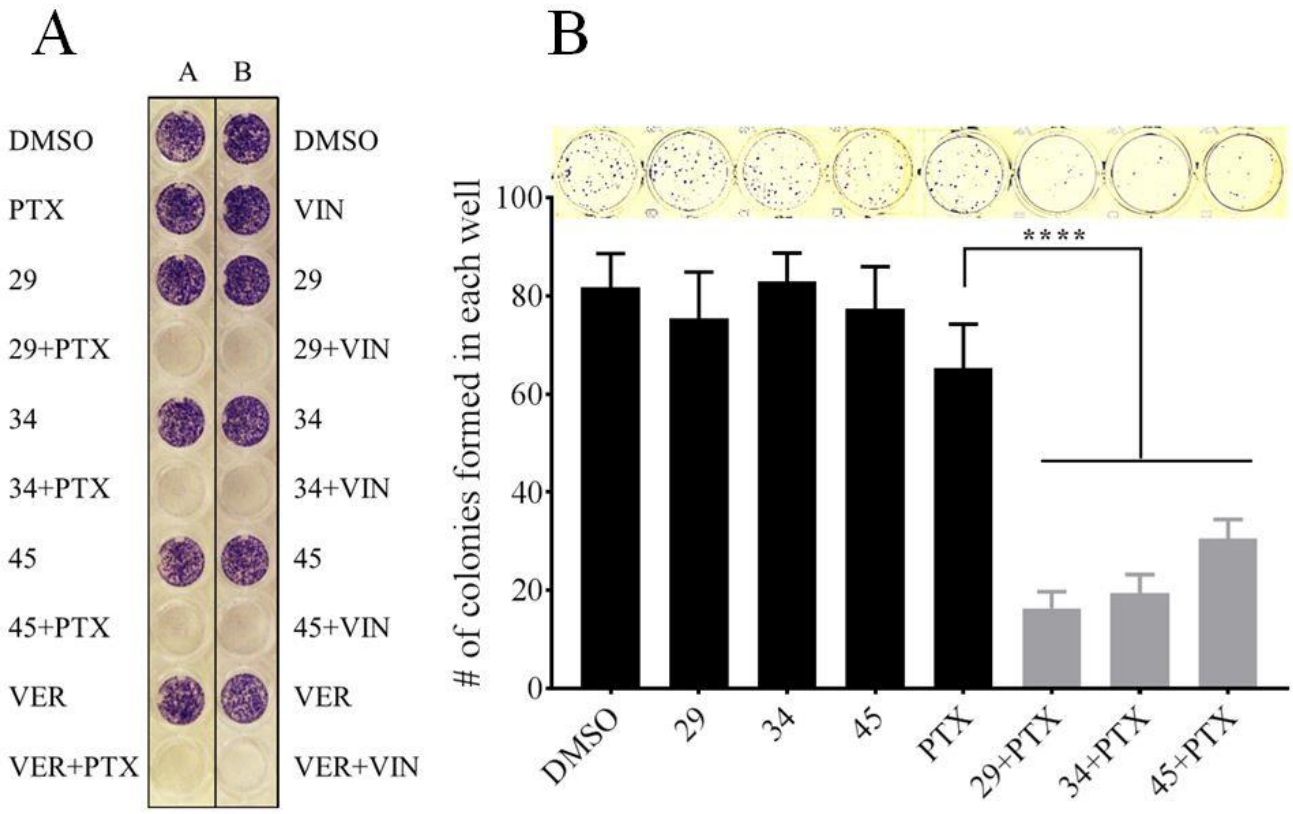

Figure 2.4 - **Reversal of chemotherapy resistances by novel inhibitors of P-glycoprotein.** **A** - Qualitative colony formation analyses using multidrug resistant ovarian cancer cells. A2780ADR cells were treated with chemotherapeutics and/or inhibitors as indicated in the figure for 48 hrs, washed and subsequently cultured for an additional 96 hours. Remaining cell colonies were stained with crystal violet. Left column from top to bottom: vehicle (DMSO); vinblastine (VIN) alone; compound **29** alone; vinblastine and compound **29**; compound **34** alone; vinblastine and compound **34**; compound **45** alone; vinblastine and compound **45**; verapamil (VER) alone; vinblastine and verapamil. Right column from top to bottom: vehicle (DMSO); paclitaxel (PTX) alone; compound **29** alone; paclitaxel and compound **29**; compound **34** alone; paclitaxel and compound **34**; compound **45** only; paclitaxel and compound **45**; verapamil (VER) alone; paclitaxel and verapamil. The concentrations used were 0.1 µM vinblastine, 1 µM paclitaxel, 10 µM of inhibitors **29**, **34**, **45** or verapamil. **B** - Quantitative colony formation analyses using multidrug resistant prostate cancer cells. The experiments were performed as above, except that DU145TXR cells were seeded and grown to lower densities than in A, and exposure to chemotherapeutic and inhibitors was for 24 hours at lower inhibitor concentrations. Top: Images of a representative experiment showing stained colonies after 5 days of recovery. Treatments were performed with 5 µM of P-gp inhibitors **29**, **34** or **45** alone, 0.5 µM paclitaxel (PTX) alone, or in combination. Bottom: Quantitative analysis of colonies formed in B. Each histogram represents the average ± S.D. (n=6, three replicates from two individual experiments; **** $P < 0.0001$).

2.2.5 P-glycoprotein inhibitors prevent multidrug resistant cancer cells from migrating when exposed to chemotherapeutics that interrupt microtubule dynamics

To assess whether the P-gp inhibitors affect cancer cell migration in the presence of chemotherapeutics, wound healing assays [182]–[184] were performed with the MDR prostate cancer cell line [172]. Figure 2.5 shows the results of these wound healing assays under conditions of limited cell proliferation in the absence or presence of 0.1μM vinblastine and 5μM inhibitor **29**, **34**, or **45**. Controls with the P-gp inhibitors alone (no chemotherapeutic present) are also shown. Figure 2.5A shows micrographs typical of the scratch zones immediately after the injury (zero time) and after 14 hours of incubation in low serum media. These experiments were performed in media containing 1% serum to have a minimum effect from cell growth on wound closure. Figure 2.5B presents the averages of the relative wound closures normalized to wound closure in the presence of vehicle only (DMSO). Addition of vinblastine or the P-gp inhibitors by themselves resulted in reduction of the width of the scratch wound similar to vehicle controls, indicating that the MDR cancer cells were able to migrate into the wound site and close the scratch gap under these non-proliferative conditions. When either of the three P-gp inhibitors were used in combination with vinblastine, significant inhibition of wound healing was observed, suggesting that cancer cell migration was strongly inhibited. The closing of scratch area was limited to between 41% (vinblastine with **29** or **45**) and 32% (vinblastine with **34**) of those of the vehicle only controls. There was no significant difference when 2.5 or 5 μM of inhibitor was used in the presence of chemotherapeutic.

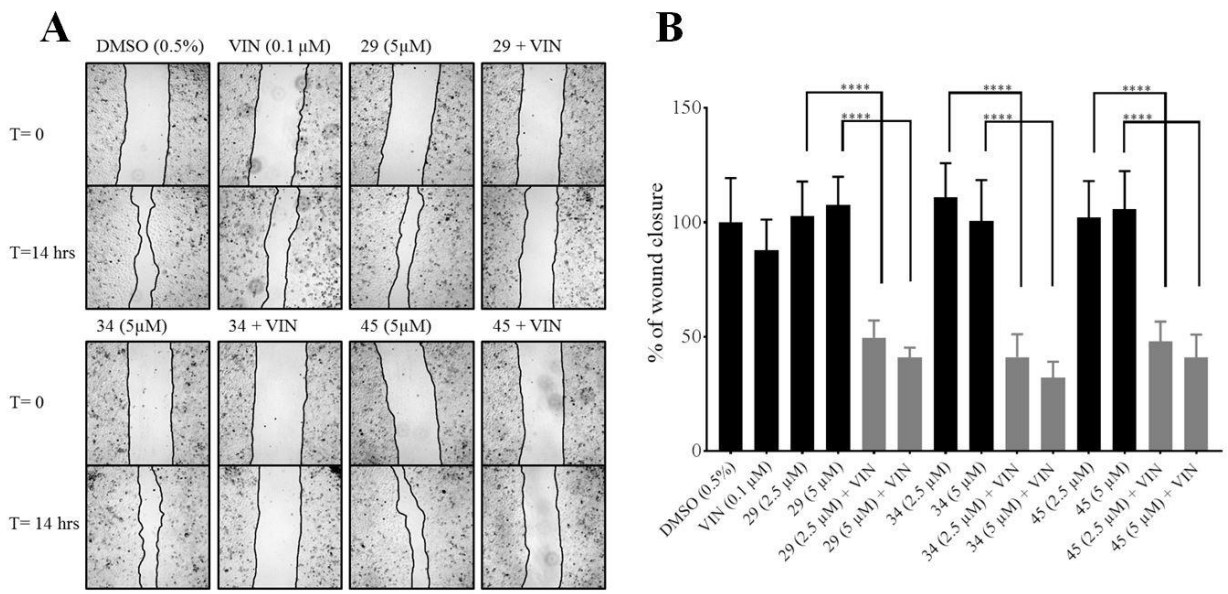

Figure 2.5 - **P-gp inhibitors prevent the migration of MDR cancer cells in the presence of chemotherapeutics that target microtubule dynamics.**
A - Wound healing assays. Confluent monolayers of the MDR prostate cancer cell line, DU145TXR, were manually scratched and subsequently cultured for 14 hours under conditions that inhibited cell proliferation. Representative 4x bright field micrographs of the scratch zones were recorded. Closure of the scratches was then evaluated in the presence of chemotherapeutic vinblastine (VIN) alone, P-gp inhibitors **29**, **34** or **45** alone, as well as in the indicated combinations. The edge of the wound is marked by a black line. **B** - Percentage wound closure. The average percentage of wound closure under different treatment conditions was compared to vehicle treated. Data are expressed as average ± S.D. of duplicate experiments (n = 12; **** $P < 0.0001$). DMSO, carrier vehicle only; VIN, 0.1 µM vinblastine; 29, 34, or 45 indicates added P-gp inhibitor at 2.5 or 5 µM.

2.2.6 The intracellular retention of transport substrates of P-glycoprotein is enhanced in the presence of P-gp inhibitors in MDR cancer cells over-expressing P-gp

The results presented in Figure 2.2 to Figure 2.5 suggested that P-glycoprotein inhibition leads to enhanced therapeutic efficacies. To determine whether the P-gp inhibitors caused increased cellular retention of P-gp transport substrates, we assessed the accumulation of a known P-gp substrate, calcein AM. Calcein AM is an uncharged, acetoxymethyl derivative of the anionic fluorescent dye calcein and is known to be a substrate for P-gp [185]. Cellular esterases

convert calcein AM to calcein, which is not transported by P-glycoprotein, making it a useful fluorescent probe for P-gp transport activity.

Figure 2.6A shows that inclusion of P-gp inhibitors **29**, **34**, or **45** in media containing calcein AM with the P-gp overexpressing ovarian cancer cell line, A2780ADR, resulted in significant increases in intracellular calcein as detected by its green fluorescence. Compound **19** had been identified in earlier studies as an inhibitor of P-gp ATPase activity in cell-free biochemical assays [164], but was shown to be ineffective in reversing multidrug resistance in cell-based assays [165]. This is likely due a negative charge of the molecule at neutral pH, making it unable to enter intact cells. Inclusion of the P-gp transport substrate verapamil also led to significant increases in intracellular fluorescence, suggesting that uninhibited P-glycoprotein activity in these cells was responsible for the low intracellular calcein accumulation observed in the absence of added P-gp inhibitors or substrates. Addition of the BCRP-specific inhibitor, novobiocin, or the MRP-1 specific inhibitor, probenecid, did not lead to increased intracellular fluorescence, suggesting that BCRP and MRP-1 were not responsible for removing calcein AM from these cells. Time courses for the changes in calcein fluorescence intensities in the presence of the different inhibitors are shown in Figure 2.6B. The data indicate that both increased rates of accumulation as well as increased overall intracellular concentrations of calcein were achieved when P-gp specific inhibitors were present.

It is worth noting that a number of cells in the uninhibited controls (Figure 2.6A and B) also showed a few isolated puncta of fluorescence. This is hypothesized to be a consequence of subpopulations of cells in the MDR cultures that are not over-expressing P-gp. Given the plasticity of cancer cell genetics, this observation may be expected. Inclusion of chemotherapeutics would be expected to decrease the number of these calcein positive cells in the uninhibited control experiments.

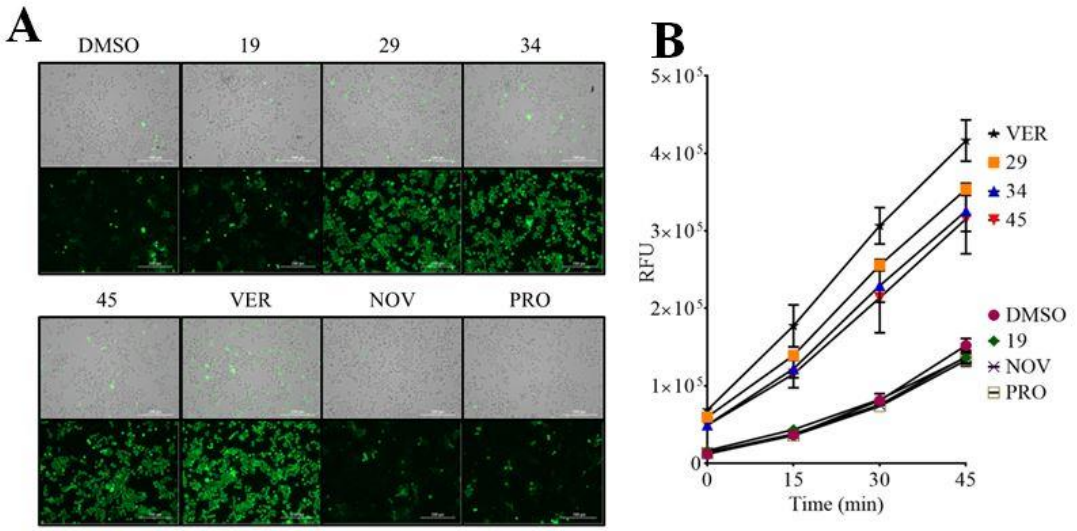

Figure 2.6 - **P-gp inhibitors restore calcein-AM or Daunorubicin accumulation in MDR ovarian cancer cells.**
A - Calcein-AM accumulation. Calcein AM accumulation upon P-gp inhibition was analyzed as described in methods using A2780ADR cells. All experiments had identical components except for the additions indicated. Additions were: DMSO, carrier vehicle at 0.5% final volume; compounds **19**, **29**, **34** or **45** at 10 μM; VER, 10 μM verapamil; NOV, 60 μM novobiocin; PRO, 250 μM probenecid. Scale bars are 200 μm. **B** - Time course of calcein accumulation. Fluorescence measurements were made on the entire wells during the imaging experiments described in panel A. The increase in relative fluorescence resulting from accumulated calcein is plotted versus the time of incubation. The indicated additions were as described in panel A. Each data point represents the average ± S.D.

2.2.7 Cellular retention of daunorubicin in A2780ADR cells is enhanced by the addition of P-gp inhibitors

The differential accumulation of the chemotherapeutic daunorubicin in the MDR ovarian cancer cells in the presence and absence of various multidrug resistance pump inhibitors was

assessed in the next set of experiments. Similar in design to the calcein AM accumulation experiments just described, these experiments took advantage of the intrinsic red fluorescence of daunorubicin. Figure 2.7A shows significant increases in intracellular daunorubicin fluorescence when the cells were treated with daunorubicin in combination with 10 μM inhibitor **29**, **34**, or **45**. Inclusion of BCRP- or MRP-1 specific inhibitors (60 μM and 250 μM, respectively) did not result in observable increases in intracellular daunorubicin fluorescence suggesting that these effects were dependent on the specific inhibition of P-glycoprotein. Figure 2.7B presents the quantification of daunorubicin accumulation as assayed in Figure 2.7A. The accumulation of daunorubicin in the presence of the experimental P-gp inhibitors was comparable to that observed for the non-MDR parental cell line, A2780 (Figure 2.7B).

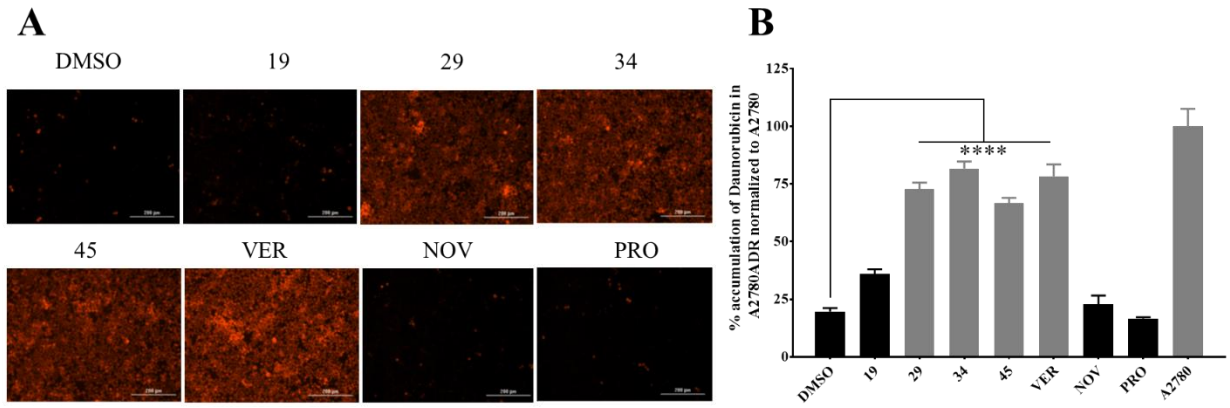

Figure 2.7- **P-gp inhibitors restore daunorubicin accumulation in MDR ovarian cancer cells.**
A - daunorubicin accumulation. Intracellular daunorubicin accumulation in A2780ADR cells was observed similarly to the accumulation of calcein (see panel A). After a 2 hour incubation with 10 µM daunorubicin, fluorescence images of the cells were obtained using a Texas Red filter. Additions were as indicated in panel A. **B** - Quantification of intracellular daunorubicin accumulation. A2780ADR cells were incubated as described for panel C. After the 2 hour incubation, cells were washed twice with cold RPMI to remove extracellular daunorubicin, and then lysed. The fluorescence of each well was measured at excitation 488/20 nm and emission 575/20 nm. Percent accumulation of daunorubicin in A2780ADR cells was normalized to the parental A2780 cells. Additions were as indicated in panel A. Each histogram represents the average ± S.D. from two independent experiments (n =6; **** $P < 0.0001$).

2.2.8 Increased accumulation and deep penetration of calcein in 3D tumor spheroids treated with P-gp inhibitors

To assess the ability of the targeted P-gp inhibitors to facilitate the penetration of P-gp substrates into cells in tumor-like structures, microtumor spheroid cultures of an MDR prostate cancer cell line [172] were produced. Incubation of the spheroids with calcein AM in the presence of either vehicle alone or P-gp inhibitor **29**, **34**, or **45** showed considerably increased calcein fluorescence (Figure 2.8A top row). The relative calcein fluorescence was visualized as 3D surface plots using the pixel intensities of the corresponding images (Figure 2.8A, lower panel). Calcein accumulation was higher in the interior regions of the microtumors in the presence of P-gp inhibitors than accumulation on the outside surfaces of the microtumors in the DMSO control. These experiments suggest that calcein penetrated deeper into the interior of the

microtumor in the presence of P-gp inhibitors. The time dependence of calcein AM uptake and calcein accumulation in the presence or absence of compound **29** is shown in Figure 2.8B.

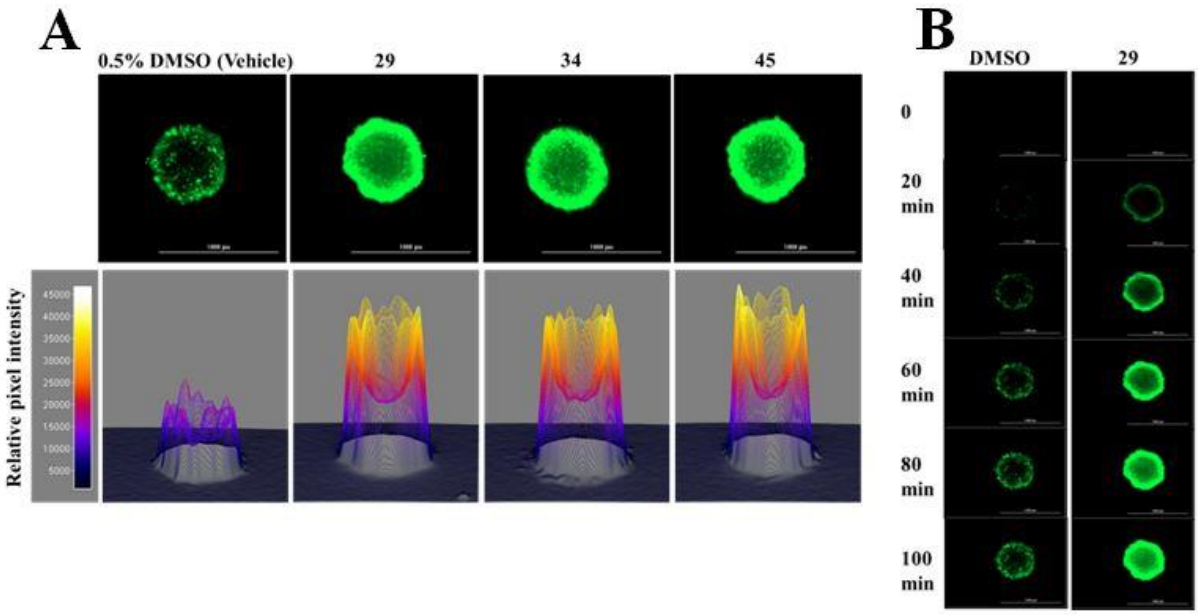

Figure 2.8 **- P-gp inhibitors increase the accumulation and penetration of calcein-AM in MDR prostate cancer spheroids.**
A - *Calcein accumulation in 3D-spheroids.* Upper panel – After 100 minutes of incubation with 2.5 µM of the P-gp substrate calcein-AM, fluorescence images of the spheroids were recorded. DMSO, 0.5% final volume; compounds **29**, **34** or **45** at 15 µM. Scale bar indicates 1000 µm. Lower panel – 3D surface plots representing the pixel intensities of the corresponding images from the experiments above. **B -** *Time course of calcein accumulation.* Fluorescence images of the spheroids treated with vehicle only or P-gp inhibitor 29 were obtained over 20 minute intervals using a GFP filter as described in panel A. Increases in calcein accumulation in the presence of compound **34** or **45** were observed to be similar to those shown with compound **29** (data not shown).

2.2.9 Increased cytotoxicity of daunorubicin in the presence of P-glycoprotein inhibitors in multidrug resistant prostate cancer microtumors

The experiments described in Figure 2.2 to Figure 2.5 showed that the cytotoxicity of chemotherapeutics like paclitaxel or vinblastine to MDR cancer cells in traditional 2D cell culture was increased in the presence of the P-gp inhibitors **29**, **34**, or **45**. It was of interest to test whether combination treatment of P-glycoprotein inhibitors with chemotherapeutic would

increase the cytotoxicity of chemotherapeutics in microtumors. To investigate this hypothesis, DU145TXR spheroids were treated for 48 hours with either vehicle alone, P-gp inhibitor **29** alone, daunorubicin alone, as well as in combination with two different concentrations of compound **29**. After the treatment, reagents were removed and the spheroids were incubated with fresh complete media for an additional 4 days. The growth of the spheroids under these conditions is shown in Figure 2.9A. The change in size of the microtumors was quantified as the total surface area of the spheroids. Growth of the tumors in the presence of 15 or 25 μM of **29** alone was similar to that in the presence of DMSO alone, demonstrating the low toxicity of **29**. In the presence of 1 μM daunorubicin, the tumor size did not change significantly over the course of the experiment, while combination with 15 or 25 μM of **29** led to a ~ 60% reduction in the size of the microtumors. Figure 2.9B shows a representative set of photomicrographs that correspond to the end-points of these experiments. The left panel shows bright field images of the microtumors after treatments indicated in the figure. The middle panel shows the red fluorescence of the same microtumors upon addition of ethidium bromide, which stains dead cells [179]. Merged images are shown in the right panel. The results indicate that the efficacy of cancer cell killing by the daunorubicin chemotherapy treatment of these microtumors was increased in the presence of the P-glycoprotein inhibitor **29**.

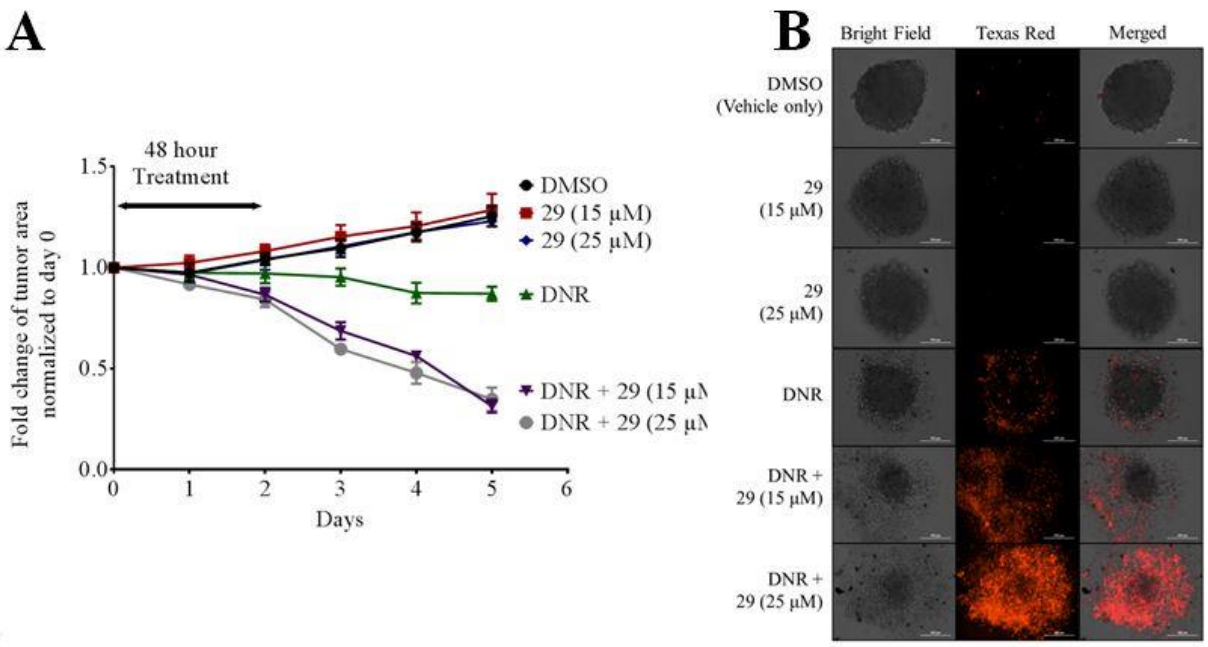

Figure 2.9 - **Inhibition of P-gp leads to increased daunorubicin-induced cell death in MDR spheroid microtumors.**
A - *Time course of changes in tumor area.* MDR DU145TXR spheroids were prepared and treated with P-gp inhibitory compound **29** with or without daunorubicin as described in methods. Areas of the spheroids were calculated at each day of the experiment and fold change plotted versus time. Values were normalized to the size of the tumor before addition of chemotherapeutic. Each point represents average ± S.D. (n=4) **B** - *Photomicrographs of spheroids at the end of the experiment.* At the end of the experiment, dead cells were illuminated by ethidium bromide staining and bright field and fluorescence (Texas Red channel) micrographs of typical spheroids were recorded. Treatments were as indicated in the panel labels. For each spheroid shown, bright field (left), Texas Red fluorescence (middle) and merged (right) images are shown. DNR, daunorubicin.

2.2.10 P-gp inhibitors 29, 34 and 45 do not affect P-gp protein expression levels

Previous studies have shown that reversal of multidrug resistances in cancers can sometimes be due to lowered expression of the protein and not to direct inhibition of P-gp transport by an experimental compound [186][187]. To test whether the inhibitors used in this study affected P-gp expression, Western blot analyses of the P-gp overexpressing prostate cancer cell line were performed after incubation for 48 hours with inhibitors **29**, **34**, or **45**. The conditions used in this experiment led to at least 17-fold sensitization of the DU145 TXR cells to

paclitaxel [165]. The results of the Western blot analyses are shown in **Figure 2.10**. No decreases in P-gp protein expression were observed.

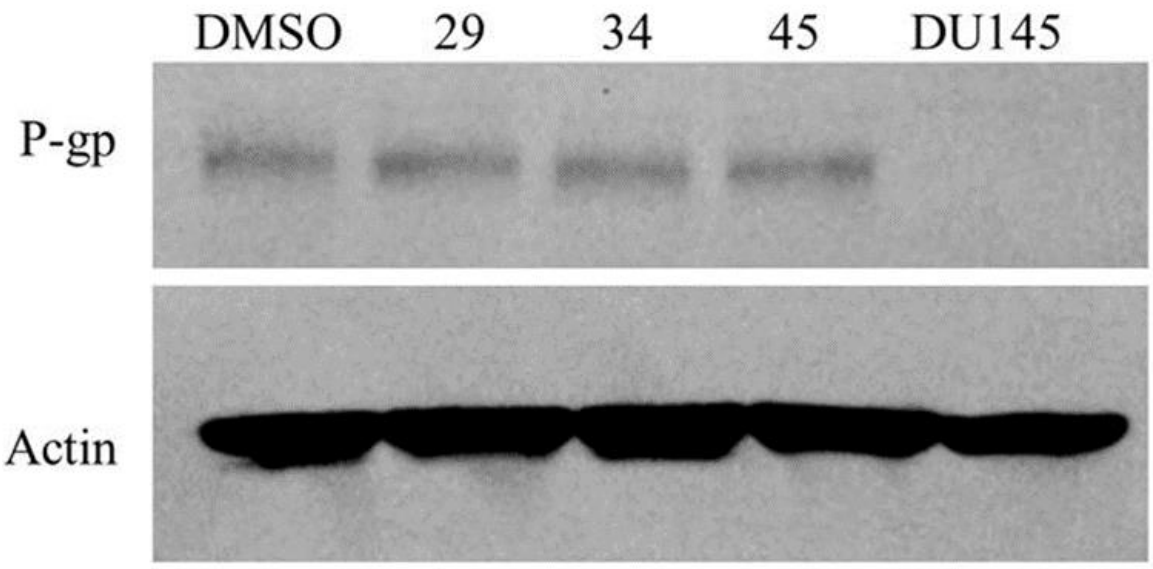

Figure 2.10 - **P-gp expression is unchanged by compound treatment in DU145 TXR prostate cancer cell line.**
Western blots of DU145 TXR cancer cells treated with 5 μM of compounds (**29**, **34** or **45**) and vehicle/DMSO were performed using anti-P-gp and anti-actin antibodies. 50 μg of cell lysates were loaded in each lane. Analyses were performed using anti-P-gp antibody C219 from Enzo Life Sciences, NY (top) and anti-β-actin antibody from Santa Cruz Biotechnology, CA (bottom) as described in Methods. P-gp was not detected in the parental drug sensitive DU145 prostate cancer cell line.

2.2.11 P-gp inhibitors 29, 34 and 45 are not transport substrates of P-gp

The original premise of our search for P-gp inhibitors was that compounds that are not transport substrates of the pump would make better lead compounds for future development for clinical use [164], [165]. To test whether compounds **29**, **34** and **45** were transport substrates, accumulation assays were performed where DU145TXR cells were incubated with 5 μM of **29**, **34** and **45** in the presence or absence of the known P-gp inhibitor tariquidar [188], [189]. A P-gp transport substrate, daunorubicin, was used as a positive control. After incubation for 2.5 hours, cells were washed with ice-cold buffer and counted. After cell lysis, the cell contents were

analyzed by LC-MS/MS. The results of these analyses are shown in Figure 2.11. These studies indicate that cellular accumulation of compounds **29**, **34** and **45** was not different in the presence or absence of tariquidar, while cellular accumulation of the P-gp substrate, daunorubicin, was significantly increased in the presence of tariquidar. These results support the hypothesis that compounds **29**, **34** and **45** are not P-gp transport substrates.

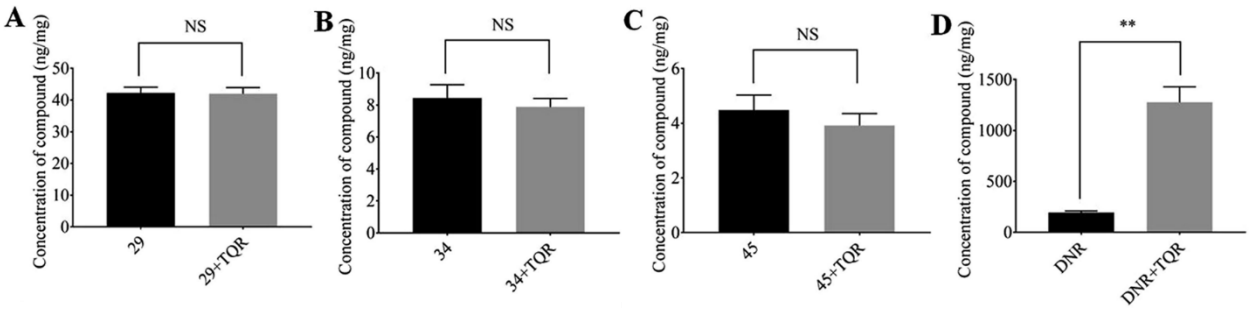

Figure 2.11 **- Compounds 29, 34 and 45 are catalytic inhibitors of P-gp and not transport substrates** Quantitative LC-MS/MS analysis of intracellular accumulation of **29** (panel **A**), **34** (panel **B**), **45** (panel **C**), or Daunorubicin (panel **D**) in DU145 TXR. Each histogram represents the average ± S.D. (n=3, two independent experiments); ** $P < 0.01$; NS – not significant). DNR, daunorubicin; TQR, tariquidar.

2.2.12 Inhibitors 34 and 45 are P-gp specific, while compound 29 also affects the breast cancer resistance protein

In order to assess whether the inhibitors were specific for P-gp or would also inhibit other ABC transporters, we created a BCRP-overexpressing breast cancer cell line, MCF-7 M100, which we derived from MCF-7 cells [190] by exposing the cells to increasing, sub-lethal concentrations of the BCRP pump substrate and chemotherapeutic, mitoxantrone [191]. Figure 2.12A shows the results of Western blot analyses of cell lysates of the MCF-7 and MCF-7 M100 cell lines indicating that the MCF-7 M100 derivative line overexpresses the BCRP protein.

Figure 2.12B shows the results of experiments that suggest that compounds **34** and **45** inhibit only P-gp, while compound **29** inhibits both P-gp and BCRP. In these experiments, the MCF-7

M100 cells were exposed to mitoxantrone (a BCRP substrate), verapamil (a P-gp substrate), novobiocin or Ko143 (BCRP inhibitors), and the P-gp inhibitors **29**, **34** and **45** as indicated in the figure. Cell viability was assessed using MTT assays [192], [193]. The results indicate that cellular viability of the MCF-7 M100 cell line was reduced when mitoxantrone was co-administered with the BCRP inhibitors, novobiocin and Ko143, but no effect was observed when the P-pg substrate, verapamil, was added. The addition of mitoxantrone or the inhibitors individually did not affect cell viability. Compounds **34** or **45** when co-administered with mitoxantrone did not significantly affect the viability of MCF-7 M100 cells. Compound **29**, however, in combination with mitoxantrone, caused statistically significant reduction in cell viability when compared to the viability of the cells in the presence of **29** alone. These results suggest that compounds 34 and 45 are P-gp specific, while compound **29** inhibits both P-gp and BCRP.

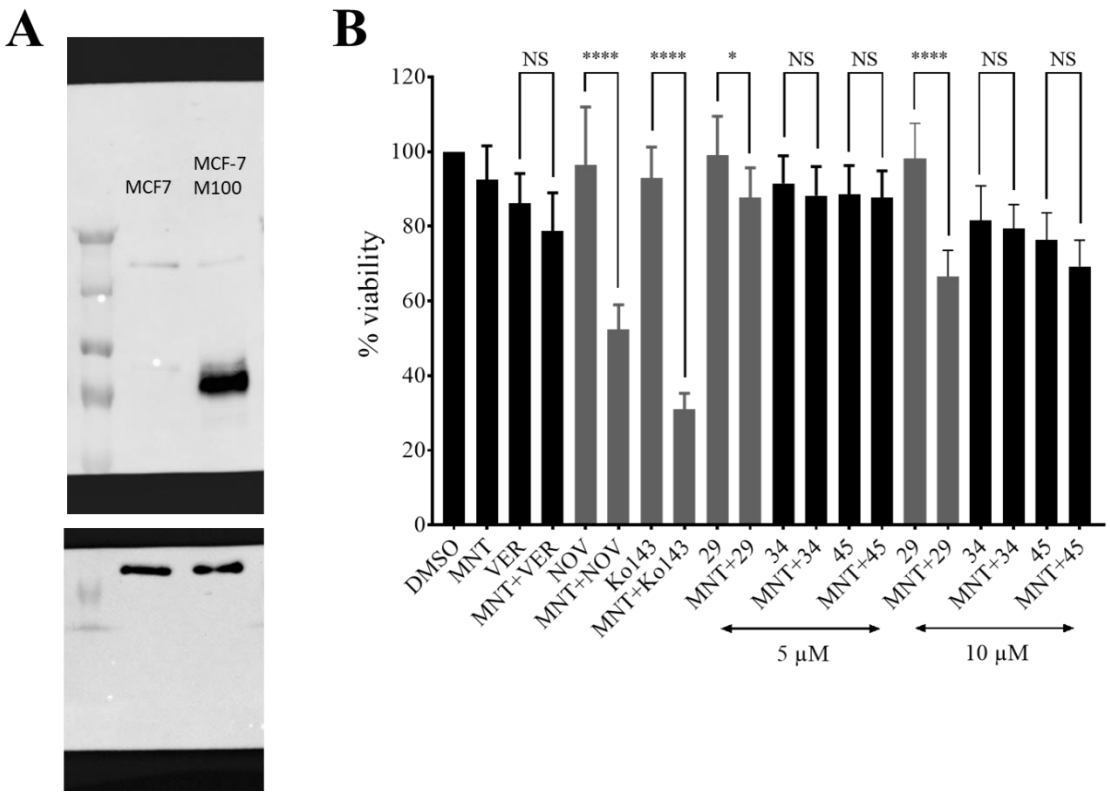

Figure 2.12 **- Inhibitors 34 and 45 are specific for P-gp specificity while compound 29 also inhibits BCRP.**

A - Western blot analysis of protein expression in cell lysates from breast cancer cell lines MCF-7 (drug sensitive) and MCF-7 M100 (multidrug resistant). A single SDS gel was run as described in Methods and then cut in two parts for probing with two different primary antibodies. Top: Western blot analysis of MCF-7 and MCF-7 M100 was performed using anti BCRP antibody B1 (from Santa Cruz Biotechnology, CA). Bottom: The lower half of the same gel was probed with β-actin monoclonal antibody C4 (from Santa Cruz Biotechnology, CA). The proteins loaded were of course identical in both top and bottom panels:
Lane #1 - Spectra™ Multicolor Broad Range Protein Ladder (catalog # 26623), Visible bands from top to bottom in the two panels represent 260, 140, 100, 70, 50, 40, 35 kDa, respectively.
Lane #2 – total cell extract from cell line MCF-7 (drug sensitive breast cancer cell line), 5 µg
Lane #3 – total cell extract from cell line MCF-7 M100 (multidrug resistant breast cancer cell line), 5 µg

B - MCF-7 M100 cells were treated with 50 nM of the chemotherapeutic mitoxantrone and either compound 29, 34, 45 at 5 or 10 µM, verapamil at 10 µM, novobiocin at 200 µM or Ko143 at 1 µM as indicated in the figure. Each histogram presents the average ± S.D. of the determinations (n=8, Replicates from two individual experiments; **** $P < 0.0001$; * $P < 0.1$). MNT, mitoxantrone; VER, verapamil; NOV, novobiocin

2.3 Methods and Materials

2.3.1 Cell lines and cell culture

The chemotherapeutic sensitive DU145 human prostate cancer cells [194] as well as the multidrug resistant sub-line, DU145TXR [172] were generous gifts from Dr. Evan Keller (University of Michigan, Ann Arbor, MI). The MDR DU145TXR was maintained under positive selection pressure by supplementing complete medium with 10 nM paclitaxel (Acros Organics, NJ). The above mentioned cell lines as well as the chemotherapeutic sensitive A2780 ovarian cancer cells (93112519, Sigma) and the multidrug resistant A2780ADR (93112520, Sigma) [137], [195] were maintained in complete media consisting of RPMI-1640 with L-glutamine, 10% fetal bovine serum (FBS; BioWest, Logan, UT), 100 U/mL penicillin and 100 µg/mL streptomycin in a humidified incubator at 37 °C and 5% CO_2. The drug-resistant line A2780ADR was maintained under positive selection pressure by supplementing complete medium with 100 nM doxorubicin (Fisher Scientific, NJ). Cell culture materials were purchased from Corning Inc. (Corning, NY) unless otherwise stated. A BCRP over-expressing breast cancer cell line (MCF-7 M100) was established by us according to a previously described method [191]. The drug sensitive MCF-7 (ATCC) [190] breast cancer cell line was exposed to increasing concentrations of the chemotherapeutic, mitoxantrone, over 60 passages. The mitoxantrone resistant MCF-7 M100 cell line was maintained under positive selection pressure by supplementing complete medium with 100 nM mitoxantrone (Santa Cruz Biotechnology, CA).

2.3.2 Western blot analyses

Whole cell lysates were prepared using approximately five million cells from each cell line. Cells were lysed in 500 µL of SDS buffer (125 mM Tris HCl pH 6.8, 20% v/v glycerol,

4% w/v SDS and 2% v/v β-mercaptoethanol) containing 5 μL of protease inhibitor cocktail (P8340, Sigma). The lysates were filtered through a spin column (QIAprep ®) by centrifugation at 5000 rpm for 5 minutes and used for Western blot analysis. The lysate proteins were resolved by denaturing SDS-PAGE [196] for 100 minutes at 110 V and subsequently transferred to a PVDF membrane (Bio-Rad, CA) using a Mini Transblot cell (Bio-Rad) for 70 minutes at 110 V. The transfer buffer contained 192 mM glycine, 25 mM Tris, and 10% methanol. The membrane was blocked overnight at 4 °C with 4% powdered skimmed milk in TBS-T (12 mM Tris–HCl pH 7.5, 0.5 M NaCl, 0.05% Tween 20). Washed membranes were incubated with the P-gp mouse monoclonal antibody C219 (Enzo Life Sciences, NY), the BCRP-specific monoclonal antibody B1 (from Santa Cruz Biotechnology, CA), or the β-actin monoclonal antibody C4 (Santa Cruz Biotechnology, CA), diluted to between 1:500 and 1:2000 in TBS-T and 4% powdered skimmed milk for 2 hours at room temperature. Washed membranes were subsequently incubated for 1 hour at room temperature with alkaline horseradish peroxidase-conjugated goat anti-mouse secondary antibody sc-2005 (Santa Cruz Biotechnology, CA) diluted to 1:10000 in TBS-T containing 4% milk powder. Membranes were washed in TBS-T and P-gp, BCRP, or β-actin were visualized using enhanced chemiluminescence detection (ECL kit, Thermo Scientific, IL). To evaluate P-gp protein expression levels of cells after inhibitor treatment, DU145TXR cells were treated with 5 μM of P-gp inhibitors **29**, **34** or **45** for 48 hours after which cell lysates were prepared and Western blot analyses were performed as described above.

2.3.3 Resazurin cell viability assay

The resazurin assay is a well-established cell viability assay [197] which relies on the reduction of the blue, water soluble resazurin to highly fluorescent resafurin [197] under the

reducing environment in the cell. The fluorescence of resafurin is directly proportional to the number of viable cells and can be measured by excitation at 530 nm and emission at 590 nm [197]. The assay was performed as follows: Cells were trypsinized from monolayers and seeded with 4000 cells in 150 µL of complete medium in a 96 well plate. After 24 hours, cells were treated with chemotherapeutics and / or P-gp inhibitory compounds dissolved in DMSO, or DMSO controls diluted in complete medium for 48 hours. The chemotherapeutics, paclitaxel and vinblastine, were purchased from Acros Organics, NJ, and MP Biomedicals, France, respectively. Upon 42 hours of treatment, resazurin assays were performed as described in [175] using 440 µM of resazurin (Acros Organics, NJ) solution prepared in PBS (137 mM NaCl, 2.7 mM KCl, 10 mM Na_2HPO_4, 1.8 mM KH_2PO_4, pH 7.4). After 6 hours of incubation with resazurin, the resulting fluorescence was measured by excitation at 530 nm and emission at 590 nm using a Bio-Tek Synergy 2 multi-mode plate reader (Bio-Tek, Winooski, VT). DMSO was used as the vehicle, 250 µM probenecid and 60 µM novobiocin (both from Alfar Aesar, MA) were used as negative controls, and verapamil (MP Biomedicals, France) was used as a positive control for P-gp inhibition. Percent viability was calculated using DMSO treated cells as representative for 100% viability. Background fluorescence was determined using resazurin and complete medium without cells.

$$\% \text{ Viability} = \frac{\text{Fluorescence of experimental cells - Background fluorescence}}{\text{Fluorescence of DMSO treated cells - Background fluorescence}}$$

The results were plotted as the mean with standard deviation (SD) of twelve replicates per concentration from at least two independent experiments. The graphical representations and IC_{50} values were determined using four parameter variable slope non-linear regression, using the following equation: Y=bottom + (top-bottom)/(1 + 10^((logIC50-X)*Hill

Slope(GraphPad Prism™, La Jolla California, USA, Version 6.05). The reported "fold sensitization" was calculated as follows.

$$\text{Fold sensitization} = \frac{IC_{50} \text{ value of A2780ADR cells treated with chemotherapeutic only}}{IC_{50} \text{ value of A2780ADR or A2780 cells treated with chemotherapeutic and P-gp inhibitory compound}}$$

2.3.4 MTT cell viability assay for BCRP over-expressing MCF-7 M100 breast cancer cell line

MCF-7 M100 cells were trypsinized from monolayers and seeded with 2500 cells in 150 µL of complete medium in a 96 well plate. After 24 hours, cells were treated with mitoxantrone (50 nM, Santa Cruz Biotechnology, CA) and / or P-gp inhibitory compounds dissolved in DMSO, or DMSO controls diluted in complete medium for 96 hours. After 96 hours of treatment, MTT assays were performed as described in [198] using 5 mg/mL of MTT (Acros Organics, NJ) solution prepared in PBS (137 mM NaCl, 2.7 mM KCl, 10 mM Na_2HPO_4, 1.8 mM KH_2PO_4, pH 7.4). After 4 hours of incubation with MTT, the media was removed, and the formazan crystals were dissolved in 100 µL of DMSO. The absorbance at 570 nm was then measured using a BioTek Cytation 5 imaging multi-mode reader (Bio-Tek, Winooski, VT). Data were obtained from two independent experiments. DMSO was used as the vehicle, 200 µM of novobiocin (Alfar Aesar, MA) and 1 µM of Ko143 (Sigma) were used as positive controls, and verapamil (MP Biomedicals, France) was used as a negative control for BCRP inhibition. Percent viability was calculated using DMSO treated cells as representative for 100% viability.

2.3.5 Colony formation assay

Colony formation assays were performed similar to those described in [181] with slight modifications. A2780ADR cells were seeded at 4000 cells per well in 96 well plates for

24 hours and incubated for 48 hours with chemotherapeutics vinblastine (0.1 μM) or paclitaxel (1 μM) alone, as well as 10 μM inhibitors, compounds **29**, **34**, **45** or verapamil alone, or combinations of chemotherapeutics and inhibitors at the concentrations given above. After 48 hours, the media were replaced with drug free media and cells were allowed to grow for an additional 96 hours. To visualize cells that had grown during that period, media were removed from the wells of 96 well plates and cells were fixed with a mixture of methanol and acetic acid 3:1 (v/v) solution. After 5 minutes, the fixation solution was removed and the cells were stained with 0.5% w/v crystal violet (Alfar Aesar, MA) in 25% methanol for 30 minutes. Finally, crystal violet was removed and the plates were washed with running water to remove excess crystal violet. Cells that had continued to grow over the 96 hour incubation time were visible as blue dots in nearly confluent cell colonies. No growth was observed where P-gp inhibitors and chemotherapeutic were co-administered during the initial 48 hr incubation.

In a more quantitative colony formation assay similar to [181], DU145 TXR cells were seeded in 24 well plates with 200 cells per well. After 24 hours, cells were treated with 500 nM paclitaxel or 5 μM inhibitors alone, as well as combinations of inhibitors and chemotherapeutics for 48 hours. The media was then removed and cells were allowed to form colonies for 5 days in drug-free complete media. Cells were fixed and stained as described above. Colonies visible to the naked eye were counted and recorded by persons blinded to all experimental conditions. The experiment was repeated two times.

2.3.6 Scratch assay

Scratch assays were performed as outlined previously [183] with minor modifications. Cells were trypsinized from monolayers and diluted in complete culture medium to a density of 25,000 cells in 300 μL cell suspension per well in 48-well plates and cultured until

confluent. The monolayers of cells were scratched using a 200 µL pipette tip. Media was removed and the cells were washed with PBS to remove any floating cells. Low serum (1%) containing media was then added to the wells together with 0.1 µM vinblastine with or without 2.5 or 5 µM P-gp inhibitory compounds, or 0.5% DMSO as a drug-carrier vehicle control. Immediately after the scratching and media additions, the wounds were imaged using a BioTek Cytation 5 imaging multi-mode reader (Bio-Tek, Winooski, VT). After 14 hours, the remaining wounds were imaged again and the areas of the wounds before and after treatment were quantified using ImageJ software [199]. The percentage of wound closures in each test were calculated compared to vehicle treated experiments. Each individual experiment was performed in triplicate and 2 images were obtained for each well. The whole experiment was repeated at least once, and n = 12 was used for the statistical analysis.

2.3.7 Calcein AM assay

To assess inhibition of P-gp-catalyzed transport of the P-gp pump substrate, calcein AM, A2780ADR cells were seeded at 40,000 cells per well in 96 wells plates and allowed to grow in complete medium for 48 hours. Medium was removed and cells were treated with or without 10 µM P-gp inhibitory compounds and 2.5 µM calcein AM (Life Technologies, OR) and diluted into phenol red free RPMI 1640 media. The cells were imaged over 45 minutes in 15 minute intervals using both GFP fluorescence and bright field filters. Fluorescence was measured by excitation at 485 nm with a 20 nm gate and at emission at 535 nm with a 20 nm gate using a BioTek Cytation 5 imaging multi-mode reader (Bio-Tek, Winooski, VT). DMSO was used as the vehicle, 10 µM experimental compound **19** (which does not penetrate intact cells) [164], 250 µM probenecid and 60 µM novobiocin were used as negative controls, and verapamil was used as a positive control for competitive inhibition of P-gp transport. Results

were plotted as the mean with standard deviation (SD) of three replicates per concentration and are representative of at least two independent experiments.

2.3.8 Daunorubicin accumulation experiments

A2780ADR cells were seeded in 96 wells plates at 150,000 cells per well in complete media and allowed to grow overnight. Medium was then removed and cells were treated with or without 15 μM P-gp inhibitory compounds and in the presence of 10 μM daunorubicin (MP Biomedicals, France) diluted in complete medium. After 2.5 hours of incubation, media were removed and cells were washed once with PBS containing DMSO 5% and once with 2% DMSO and imaged using a Texas Red fluorescence filter and a BioTek Cytation 5 imaging multi-mode reader.

To quantify the accumulation of daunorubicin in cells, assays were carried out as above, but cells were lysed in 100 μL of PBS containing 0.5% SDS and 0.5% Triton X100 immediately after the washing step. The fluorescence of daunorubicin was measured using excitation at 488 nm with a 20 nm gate and emission at 575 nm with a 20 nm gate using the BioTek Cytation 5 imaging multi-mode reader.

2.3.9 Calcein AM uptake in spheroids

Spheroids of the multidrug resistant prostate cancer cell line, DU145TXR, were produced as described [200] with the following modifications. Cells were trypsinized from monolayers and diluted in complete culture medium to a density of 15000 cells in a 200 μL cell suspension per well in 96-well plates. Prior to the experiment, all wells used for the assay had been coated with 2.5% low melting agarose in RPMI. After seeding, the 96-well plates were centrifuged at 600 rpm for 20 minutes. Centrifugation was repeated after 24 hours to obtain more tightly packed spheroids. Spheroids that had formed six days after seeding were

used for experiments. Spheroids were pretreated with 15 μM of P-gp inhibitors **29**, **34** or **45** for 3 hours and then incubated with 2.5 μM of calcein-AM. Fluorescence images were obtained every 20 minutes for a total of 100 minutes using a GFP filter. The resulting TIFF image files were analyzed using ImageJ software and interactive 3D surface plot plugging was used to obtain 3D graphs based on the pixel intensities of images. Each experiment was carried out in triplicate and the whole experiment was duplicated.

2.3.10 Spheroid growth and spheroid area reduction assay

Spheroid cultures were prepared as described above except that the growth was initiated with only 2000 cells per spheroid. Prepared plates were incubated at 37 °C for 72 hours in a humidified incubator with 5% CO_2 for spheroid formation. The spheroids were treated with daunorubicin at the concentrations indicated, with or without compound 29 that had been diluted in 50 μL of complete medium. Half of the medium was replaced after every 48 hours of incubation. The spheroids were imaged every 24 hours using a BioTek Cytation 5 imaging multi-mode reader and the areas of the spheroids were determined using the BioTek Gen5 software. The fold change of tumor spheroid area was determined each day by comparing the area of each spheroid to that of day one. Dead cells in the spheroid culture on day six were visualized and imaged after staining with 10 μL of a 0.01% ethidium bromide (Fisher Scientific, NJ) solution diluted into PBS.

2.3.11 Fluorescence microscopic analysis of cell apoptosis

Double staining with acridine orange/ ethidium bromide (AO/EB) is a reliable method to detect apoptosis and was carried out as described in [179] with slight modifications. Briefly, 16000 cells were seeded in 48 well plates in 300 μL of complete media and incubated for 24 hours. After 24 hours, cells were treated with 1 μM paclitaxel and 10 μM P-gp inhibitory

compounds in DMSO or DMSO controls for 48 hours. Then dual stain containing solution AO/EB (100 µg/ml each) was added to each well and images were acquired using a BioTek Cytation 5 imaging multi-mode reader with GFP (for green fluorescence from acridine orange), Texas Red fluorescence (for red fluorescence from ethidium bromide) and bright field filters.

2.3.12 Cellular Accumulation Assays for Experimental P-gp Inhibitors

DU145TXR cells were seeded in 6 well plates with ~350,000 cells per well. After 48 hours, the media was replaced with fresh media and cells were treated with 5 µM of compounds (**29**, **34**, or **45**) and daunorubicin with or without 500 nM of tariquidar (MedKoo Biosciences, Chapel Hill, NC, U.S.A.) Experiments were performed in triplicate. After 2.5 hours of incubation with compounds, cells were washed with Hank's Balanced Salt Solution (HBSS, Corning Inc. NY), harvested using trypsin, and counted. Each sample was then washed with 2 mL of ice-cold HBSS and diluted in cold HBSS at a final concentration of 1 million cells/mL. All samples were frozen with liquid nitrogen and stored at −80 °C until analysis. The samples were submitted to the preclinical pharmacology core laboratory in University of Texas Southwestern for LC-MS/MS analyses. LC-MS/MS analyses were performed in there essentially as described in [201]. 250 µl of treated or untreated cell lysate was aliquoted into Eppendorf tubes. Blank lysates were spiked with varying concentrations of each compound to create a standard curve. Each sample was mixed with 0.5 ml of a solution containing 0.15% formic acid and 120 ng/ml n-benzylbenzamide internal standard in methanol, vortexed 15 sec, incubated 10 min at RT and then centrifuged twice at 16,100 × g. The supernatant was then analyzed by LC-MS/MS using a Sciex 4000QTRAP mass spectrometer coupled to a Shimadzu Prominence LC. Chromatography conditions were as

follows. Buffer A consisted of water + 0.1% formic acid and Buffer B consisted of methanol + 0.1% formic acid for compound 29, 34, and 45 and acetonitrile + 0.1% formic acid for daunorubicin. The column flow rate was 1.5 ml/min using an Agilent C18 XDB, 5 micron packing 50 × 4.6 mm column. The gradient conditions for compounds 29, 34, and 45 were 0–1.0 min 3% B, 1.0–2.0 min gradient to 95% B, 2.0–3.5 min 95% B, 3.5–3.6 min gradient to 3% B. 3.6–4.5 min 3% B. Gradient conditions for daunorubicin were 0–2.0 min 5% B, 2.0–3.5 min gradient to 60% B, 3.5–5.0 min 60% B, 5.0–5.1 min gradient to 5% B, 5.1–7.5 min 5% B. Compounds were detected in MRM mode after optimization of machine parameters by detection of the following parent/daughter ions: 459.1/278.1 for 29, 477.1/285.1 for 34, 424.1/149.0 for 45, and 528.1/321.0 for daunorubicin. N-benzyl benzamide (212.1/91.1) was used as the internal standard. A value 3-fold above the signal obtained from blank lysate was designated as the limit of detection (LOD). The limit of quantitation (LOQ) was defined as the lowest concentration of standard at which back calculation yielded a concentration within 20% of theoretical and above the LOD. The LOQ for all analytes was between 0.1–0.5 ng/ml. The protein pellet remaining after addition of organic solvent was resuspended in 25 µl of 0.1 M NaOH, boiled for 5 min, and 5 µl was mixed with 200 µl of 1:50 B:A reagent (Thermofisher BCA Kit) in order to determine the protein concentration. A BSA standard curve was prepared in H_2O and mixed in the same ratio. The samples were incubated 30 min at 37 °C and read at 562 nM. Compound concentrations in the lysates were then normalized to protein content for each sample.

2.4 Discussion

In the above study, we obtained further evidence that the P-gp inhibitors **29**, **34** and **45** originally reported by Brewer *et al*. and Follit *et al*. reverse MDR by specifically inhibiting P-gp,

in both 2-dimensional cultures of prostate and ovarian cancer cells and 3-dimensional cultures of prostate cancer cells. We showed that the reversal of MDR is caused by specific inhibition of P-gp and that this inhibition led to increased accumulation of P-gp substrates. The decreased P-gp transport activity was also shown not to be the result of downregulation of P-gp expression. We showed in addition that these inhibitors are not transport substrates of P-gp. Compounds **34** and **45** were shown to be specific for P-gp, whereas compound **29** modulated the activity of the breast cancer resistance protein and P-glycoprotein.

Worldwide in 2018, nearly 4% of cancer related deaths are due to ovarian cancer in females and 7% of cancer related deaths are due to prostate cancer in males [202]. Chemotherapy has been regarded as standard therapy for advanced epithelial ovarian cancer while chemotherapy has shown to prolong life in patients with metastatic castration-resistant prostate cancer [203], [204]. Nevertheless, MDR in chemotherapy related to P-gp is still a major challenge to ovarian cancer treatments and castration-resistant prostate cancer [205], [206]. We have demonstrated our findings using P-gp overexpressing ovarian cancer cell line, A2780 ADR and the prostate cancer cell line DU145 TXR, which has been extensively used for P-gp inhibition in earlier studies [207]–[212]. In this study we selected chemotherapeutics which are used in clinical settings. Paclitaxel and vinblastine have been used clinically against both ovarian and prostate cancers [213]–[216]. The P-gp substrate daunorubicin has been clinically evaluated against acute myeloid leukemia [217]–[219] which is a cancer in blood cells known for acquiring MDR through P-gp overexpression [220]–[222].

One of the major issues of using viability assays can be these assay values may not directly correlated to cell proliferation or give an idea about cell death [223]–[225]. We have used well-known resazurin (Alamar Blue) [226] or tetrazolium salts like MTT [193] assays for viability

determination of cancer cells. Both of these assays are based on reduction ability of metabolically active mitochondria of viable cells which can be used to calculate IC50 values. According to Figure 2.2 approximately 50% viability was observed for the A2780ADR line at paclitaxel concentration from 100 nM to 10 µM range treated with inhibitors. Such high viability could be due to the residual activity of mitochondria of non-proliferating cells or cells are in apoptosis. We wanted to evaluate whether an ovarian cancer cell underwent that kind of a treatment can survive and start to proliferate again. According to Figure 2.4A ovarian cancer cells treated with 1 µM of paclitaxel and 10 µM of P-gp inhibitors for 48 hours, a similar condition to viability assay mentioned earlier failed to generate any colonies up to 96 hours after the treatment in drug free media. This indicated that cells treated with a concentration from 100 nM to 10 µM range of paclitaxel with P-gp inhibitors may have lost proliferation capability although metabolic activity was still relatively high as seen in the Figure 2.2 .

The inability of drugs to penetrate solid tumors is a major barrier in drug delivery [227]. We used a liquid overlay on agar method [200] to generate 3D spheroids with multidrug resistant DU145TXR prostate cancer cells. Results of experiments using these microtumors treated with P-gp inhibitors showed stronger accumulation of calcein AM even in internal parts of the spheroid (Figure 2.8). In time course experiments, nearly complete tumor penetration of the fluorescent dye was observed after about 100 minutes of incubation, suggesting that the P-gp inhibitors affected cells inside the tumor. Increased cytotoxicity of daunorubicin in the presence of inhibitor **29** indicated that the inclusion of the P-gp inhibitor resulted in significantly increased cell mortality and destruction of these microtumors (Figure 2.9). Our attempts to create spheroids from the MDR ovarian cancer cell line, A2780ADR failed due to the lack of tight association

among cells which is required for spheroid formation. This could be as a result of low expression of claudin 4 which is required for spheroid formation [228].

Our focus was to avoid P-gp pump substrates and identify P-gp inhibitors that were not pump substrates like for example verapamil, which had limited or no success in clinical trials as they were required in high systemic concentrations leading to toxicity [11]. Protein-based assays as described in Brewer *et al.* [164] suggested that P-gp inhibitors **29**, **34** and **45** were not P-gp substrates. In this study we wanted to confirm that **29**, **34** and **45** are not P-gp substrates in cellular assays as well. The cellular assays based on Caco-2 cells using transwell plates that are frequently used for recognizing P-gp substrates are laborious and expensive [229]. Here we describe a relatively simple assay utilizing the ability of P-gp overexpressing cancer cells to pump out P-gp substrates efficiently and accumulate those substrates upon inhibition of P-gp. We demonstrated this using the known P-gp substrate, daunorubicin as the positive control and tariquidar as the P-gp inhibitor. Tariquidar treatment significantly increased the daunorubicin accumulation while such impact was not observed with compounds **29**, **34** and **45** concluding those are not P-gp substrates, suggesting that the identified inhibitors are indeed not transported to a significant degree by P-gp.

According to Hanahan and Weinberg, the complexity of a cancer cell compared to a normal cell can be reduced to six principles called "hallmarks" [230]. They describe that a cancer cell is different from a normal cell, because cancer cells stimulate their own growth, are insensitive to growth inhibitory signals, resist apoptosis, proliferate indefinitely, and sustain angiogenesis and metastasis [230]. Chemotherapy is designed to exploit these “hallmarks”, however, over-expression of transporters of xenobiotics like P-gp allow cancer cells to survive in the presence of chemotherapeutics [4], [231]–[234]. Combining chemotherapy with our P-gp inhibitors, we

have shown that chemotherapy can exploit those “hallmarks” again by reducing the viability, reducing colony formation, cell migration and increasing apoptosis in MDR cancer cells.

CHAPTER 3: PROLONGED INHIBITION OF P-GLYCOPROTEIN AFTER EXPOSURE TO CHEMOTHERAPEUTICS INCREASES CELL MORTALITY IN MULTIDRUG RESISTANT CULTURED CANCER CELLS

3.1 Introduction

The efficacy of the various P-gp inhibitors was proven to be a success in P-gp overexpressing cell culture models and some *in vivo* experiments[165], [235]–[237]. Nevertheless P-gp inhibitors had shown only a limited success in clinical settings to date. Due to this, there are no clinically approved P-gp inhibitors to treat P-gp overexpressing MDR cancers[11], [238]. The minimal positive outcome of the clinical trials was mainly due to inhibitor toxicities, drug-interactions, and clinical trial design problems. While, many of these initial inhibitors were P-gp transport substrates requiring relatively high systemic concentrations for efficacy, others lacked specificity for P-gp and led to drug interactions [11]. This highlights the requirement for novel P-gp inhibitors and novel treatment strategies to battle against P-gp overexpressing MDR cancers.

In the previous study we had shown three P-gp inhibitors (**29**, **34** and **45**) that reversed the MDR in ovarian and prostate cancer cell lines. The inhibition of P-gp resulted in a higher accumulation of P-gp substrates such as the chemotherapeutic daunorubicin. These inhibitors retained 3 to 4 fold daunorubicin concentration in ovarian cells compared untreated cells [235]. In this study we show that the accumulated chemotherapeutics can be retained in P-gp overexpressing cancer cells by P-gp inhibitor **29** after an initial brief exposure to chemotherapeutics. This prolonged retention of the chemotherapeutics by P-gp inhibitor **29** significantly increases the efficacy of

treatment in prostate cell culture model. Although this study utilized *in vitro* methodologies, this strategy should be further explored in *in vivo* and clinical settings.

3.2 Results

3.2.1 The presence of P-gp inhibitor 29 results in cellular retention of previously accumulated daunorubicin in multidrug resistant prostate cancer cells

In experiments aimed at investigating whether the rate of release of chemotherapeutic drugs from multidrug resistant human prostate cancer cells was affected by the continued presence of the P-gp inhibitor, compound **29** [164], [165] (Figure 3.1D), we first exposed DU145TXR cells [172] to daunorubicin in the presence of compound **29** to enable the cells to significantly accumulate the chemotherapeutic. The media containing daunorubicin and compound **29** were then removed and replaced with fresh media with or without addition of **29**. The relative rates of release of daunorubicin from the cells were observed using the intrinsic fluorescence of the chemotherapeutic. Figure 3.1A shows a time-course of release of daunorubicin over 105 minutes in the absence and presence of added P-gp inhibitor. The figure clearly shows that daunorubicin release was significantly slower in the presence of **29** than it was in its absence. Figure 3.1B shows the relative amounts of daunorubicin retained by these cells at the end of the 105 min time-course. After washing the cells in cold PBS at the 105 minute time point of the daunorubicin release assay, these cells were lysed as described in Methods. The total relative fluorescence of each well was measured using the Cytation 5 to quantify the intracellular daunorubicin accumulation. It is clear that the MDR prostate cancer cells retained significantly more daunorubicin when incubated in the presence of inhibitor **29** than cells incubated without P-gp inhibitor for the same period of time (Figure 3.1B, compare black bar to light gray bar). When DU145TXR cells were incubated with daunorubicin in the presence of **29** followed by a

release period in the absence of **29**, the overall retention of daunorubicin was comparable to experiments where cells were incubated with daunorubicin alone (Figure 3.1B, compare light gray to dark gray bars). This indicates that the cells that were loaded with daunorubicin in the presence of **29** released all of the daunorubicin accumulated due to P-gp inhibition within a relatively short time period (~105 min) when P-gp inhibition was not maintained. The data also suggest that the intracellular steady state concentration of chemotherapeutic reached in the presence of P-gp inhibitor far exceeded the intracellular steady state concentration of therapeutic when P-gp was not inhibited. The fluorescence micrographs presented in Figure 3.1C of cells preloaded with daunorubicin plus **29** followed by 105 min of daunorubicin release in the presence (right panel) or absence (left panel) of P-gp inhibitor **29** demonstrate qualitatively the higher retention of daunorubicin observed in these MDR prostate cancer cells when P-gp inhibition was maintained after chemotherapeutic treatment ended.

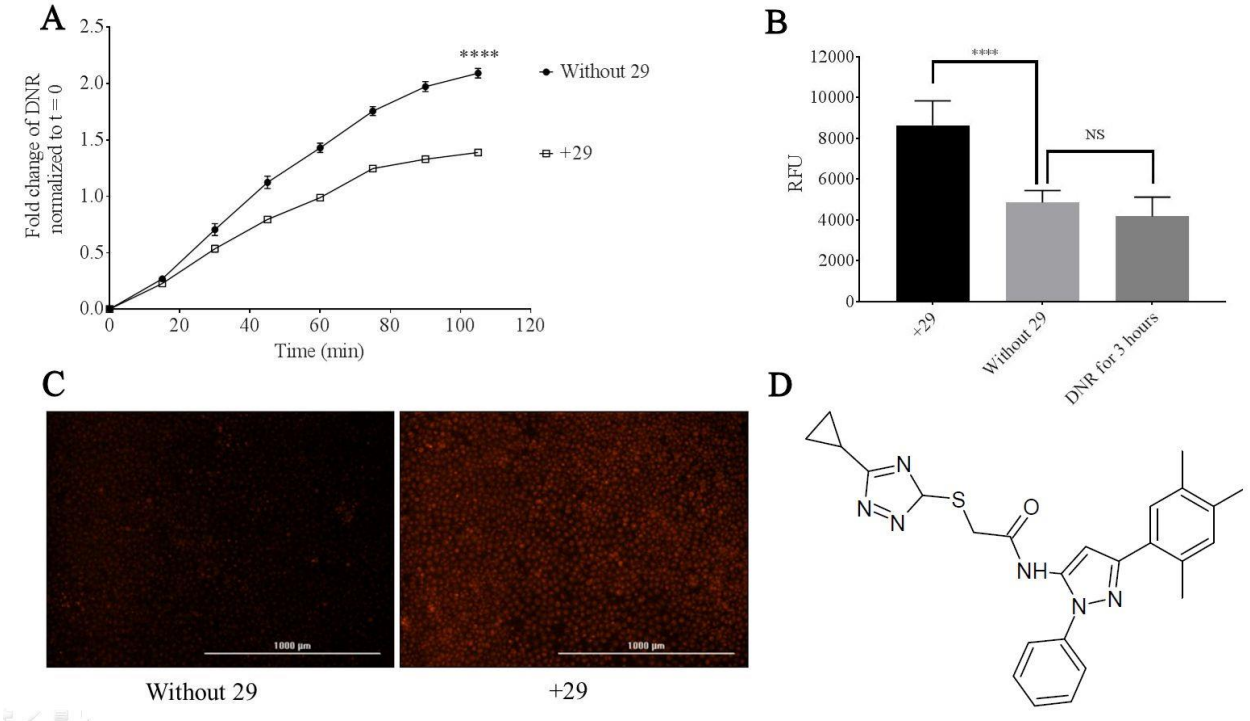

Figure 3.1 **- Effects of P-gp inhibition on the retention of daunorubicin in the multidrug resistant prostate cancer cell line, DU145TXR.**

A – Fluorescence of daunorubicin released from the cells in the presence or absence of P-gp inhibitor **29** was measured over time and results were normalized to t = 0. In these experiments, cells were preloaded with daunorubicin by incubation in the presence of the P-gp inhibitor **29** as described in Methods. After the preloading, cells were washed and media were replaced with complete media with or without **29**. Results indicate that the presence of P-gp inhibitor in the medium decreased the relative rate of daunorubicin release. Data are expressed as average ± S.D. of duplicate experiments (n = 12; **** $P < 0.0001$). **B** – The total fluorescence of daunorubicin accumulated in the cells was measured at the 105 min time point as indicated in **A** after washing and complete lysis of the cells as described in Methods. A significant amount of daunorubicin was retained in the cells in the presence of P-gp inhibitor **29** as opposed to those cells maintained in its absence. The right most bar graph shows the quantity of daunorubicin accumulated in cells that were exposed to daunorubicin for the entire time-course in the absence of P-gp inhibitor. The figure indicates significantly decreased steady state accumulation of chemotherapeutic in the absence P-gp inhibition compared to that observed in the continued presence of inhibitor. Data are expressed as average ± S.D. of duplicate experiments (n = 12; **** $P < 0.0001$; "NS" = no significant difference). **C** – Fluorescence images of daunorubicin retention in the DU145TXR cells at the 105 min time point. After washing the cells with cold PBS as described in Methods, fluorescence micrographs were obtained using a Cytation 5 imager and a Texas Red filter. The concentration of compound **29** was 25 µM and daunorubicin was 10 µM. **D** – Structure of compound **29**.

3.2.2 The viability of multidrug resistant, P-gp overexpressing prostate cancer cells is reduced by extended exposure to P-gp inhibitor 29 after exposure to chemotherapeutics

As shown in Figure 3.1, increased amounts of chemotherapeutics were retained in P-gp-overexpressing cells when the cells were continuously exposed to P-gp inhibitor **29** after removal of chemotherapeutic from media. In order to determine if this increased retention of chemotherapeutics in the cells in the extended presence of **29** resulted in decreased cell viabilities, we carried out a series of resazurin viability experiments [175] as modified in [235]. In these assays, we first exposed DU145TXR cells to paclitaxel (Figure 3.2A) or vinblastine (Figure 3.2B) in the presence of P-gp inhibitor **29** and allowed the cells to accumulate the chemotherapeutics as described for daunorubicin in Figure 3.1. After a 2-hour pre-incubation in the presence of inhibitor and chemotherapeutic, the media containing chemotherapeutic and inhibitor were removed and replaced by complete media with or without P-gp inhibitor **29**. This was followed by a 22 hour incubation period, resulting in total incubation times of 24 hours. Control groups were maintained with drug free complete media (0.5 % DMSO). It can be seen in Figure 3.2 that treatment with the P-gp inhibitor alone for 24 hours did not significantly affect cell viability as judged by the resazurin assay. Addition of paclitaxel (Figure 3.2A) or vinblastine (Figure 3.2B) alone for 2 hours, or paclitaxel or vinblastine plus inhibitor **29** for two hours also did not significantly decrease viability of these MDR prostate cancer cells when compared to the DMSO-vehicle controls. In stark contrast, the treatment of the cells with either paclitaxel or vinblastine in the presence of P-gp inhibitor **29** for two hours, followed by an extended P-gp inhibitor exposure for 22 hours after washing the cells free from non-internalized chemotherapeutic. This extended inhibitor treatment resulted in significant reduction in cell

viability for both paclitaxel and vinblastine (gray bars in Figure 3.2A and B). The decreased viability of the MDR cancer cells upon "extended P-gp inhibitor" treatment was not significantly different than 24 hour continuous exposures to either paclitaxel or vinblastine alone with or without P-gp inhibitors present (Figure 3.2A and B, rightmost three bars). These results indicate that 2 hour exposures to chemotherapeutics combined with a 24 hour total exposure to P-gp inhibitors decreased the viability of these MDR cancer cells equally well as compared to a continuous 24 hour treatment with chemotherapeutic.

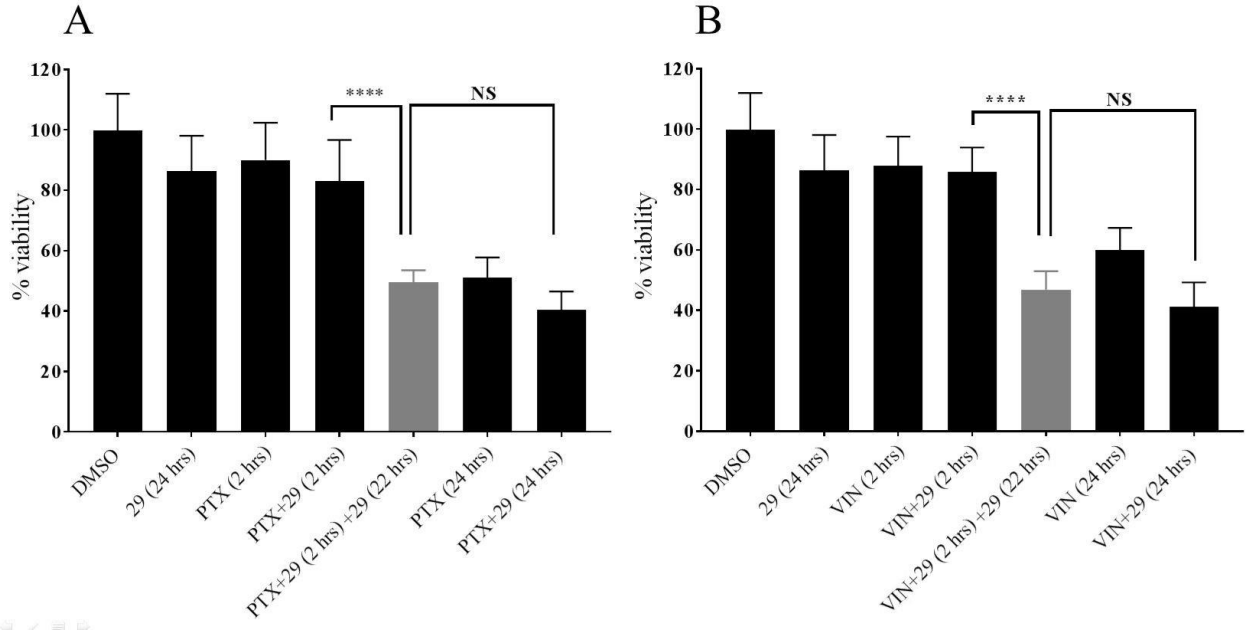

Figure 3.2 **- The increased chemotherapeutic retention in MDR cells treated for extended times with P-glycoprotein inhibitor 29 decreased viabilities of DU145TXR cells.**

In these experiments, DU145TXR cells were preloaded with either paclitaxel (**A**) or vinblastine (**B**) in the presence of P-gp inhibitor **29** unless indicated in the figure. After the preloading incubation, cells were washed and media were replaced with complete media with the indicated additions. Control experiments included exposure of the cells to DMSO alone (0.5% final concentration), P-gp inhibitor **29** alone (25 μM), paclitaxel (PTX, 10 μM), vinblastine (VIN, 10 μM) or the combinations and times indicated. The percentage of viable cells present at the end of the experiment is expressed as percentages of the DMSO-vehicle control experiments. Data are expressed as averages +/- S.D. of duplicate experiments (n = 8; **** $p < 0.0001$). "NS" = not significantly different. Measurements were made as described in Methods using a Cytation 5

3.2.3 Survival of P-gp overexpressing MDR prostate cancer cells is reduced by extended exposure to P-gp inhibitor 29 after exposure to chemotherapeutics

Figure 3.2 demonstrated that increased retention of chemotherapeutics due to extended P-gp inhibitor treatment led to decreased cellular viabilities. Although the resazurin assay is known to respond to mitochondrial metabolism, and this in turn is correlated with cellular viability [224], [226], it was of interest to assess whether these extended P-gp inhibitor treatments after short chemotherapy exposures actually decreased cancer cell survival. With this aim, we performed colony formation experiments in a manner similar to the viability experiments shown above. In these experiments, the cells were treated with the indicated compounds (chemotherapeutic and/ or P-gp inhibitor), were then washed and subsequently incubated for five days in the absence of added chemotherapeutic and P-gp-inhibitor **29**. At the end of the five-day period, cells were fixed and stained, and the colonies were counted by individuals with no knowledge of the experimental details to avoid any obvious biases. Figure 3.3A shows representative images of crystal violet stained colonies visible to the naked eye at the end of the experiment. Figure 3.3B shows that the observed colony numbers as shown as a percentage of the DMSO-only control were similar to the results reported in the viability assays in Figure 3.2. No significant difference in cell survival was observed when the cells were exposed to P-gp inhibitor **29** for 24 hours, or 2 hour exposure to paclitaxel, or 2 hour exposure to paclitaxel and inhibitor **29**. In contrast, and similar to the viability results presented in Figure 3.2, co-treatment of these MDR cancer cells for 2 hours with paclitaxel and P-gp inhibitor **29**, followed by extended treatment for 22 hours with only compound **29** resulted in a very significant decrease in

cellular survival, which was only slightly surpassed by a 24 hour continuous exposure of the cells to paclitaxel (Figure 3.3B, rightmost three bars).

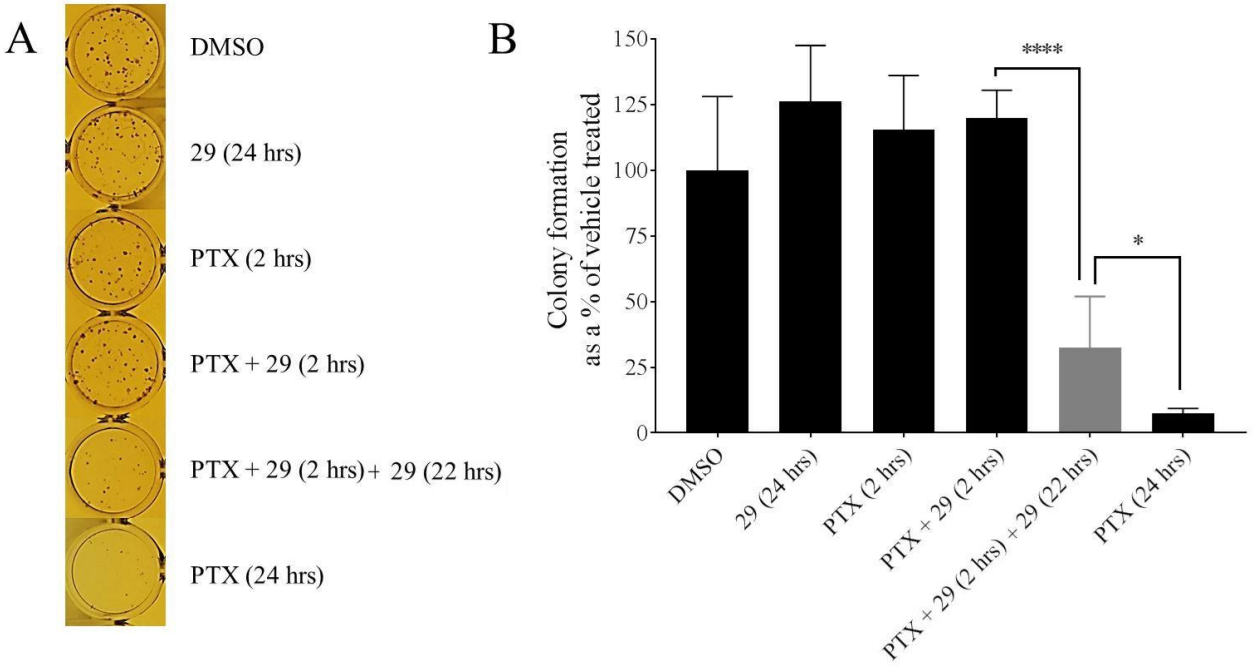

Figure 3.3 - **The increased chemotherapeutic retention in MDR cells treated for extended times with P-glycoprotein inhibitor 29 decreased cell survival as assessed by colony formation assays.**
Experiments were performed similarly to those reported in Figure 3.2 except that treatments with chemotherapeutic and / or inhibitor **29** were followed by a five day recovery period in complete media without addition of chemotherapeutics or P-gp inhibitor. The chemotherapeutic in these experiments was paclitaxel (PTX). At the end of the five day incubation, cells were fixed and stained. Colony formation was assessed as described in Methods. **A -** Representative images of the crystal violet stained colonies that were counted for the quantification shown in panel B. **B** – Quantification of the number of colonies observed after treatments with the indicated compounds and times. The data were normalized to the DMSO only control experiments and are expressed as average ± S.D. of duplicate experiments (n = 6; **** $P < 0.0001$; * < 0.1). The concentration of **29** and paclitaxel was 10 µM.

3.2.4 Increased retention of chemotherapeutic in MDR cancer cells treated for extended times with P-gp inhibitor 29 reduced cell migration

Wound healing assays [182]–[184], [235] have been used to detect and quantify the ability of cells to migrate from confluent to non-confluent growth areas. These assays use media

containing low concentrations of serum to inhibit cellular proliferation, but these suboptimal growth conditions do not inhibit the abilities of cells to migrate into non-confluent areas on a culture plate. In addition, relatively short treatment times of maximally 14 hours were used to ensure that cellular proliferation was limited. To assess whether the increased retention of chemotherapeutics during extended treatment of MDR cancer cells with P-gp inhibitor **29** would affect cancer cell migration, wound healing assays were performed as described in Methods using DU145TXR. The results shown in Figure 3.4A and B suggest that 14 hour treatments with inhibitor **29** alone or paclitaxel alone did not affect cancer cell migration relative to the vehicle-only DMSO control. A one-hour treatment of the cells with a combination of paclitaxel and P-gp inhibitor **29** likewise did not affect cell migration**.** In contrast, a short 1-hour co-treatment with chemotherapeutic and compound **29**, followed by a 13-hour exposure to P-gp inhibitor **29** reduced cell migration by nearly 50 %. Similar to the results shown in Figure 3.2 and Figure 3.3, the experiments shown in Figure 3.4 also clearly demonstrated that extended exposure to the P-gp inhibitor after relatively short exposures to chemotherapeutics dramatically enhanced the effects of the drugs on the cancer cells. In the case of the migration assays, it should be noted that the main mode of action of paclitaxel is blocking microtubule disassembly processes which are required for the cytoskeletal remodeling necessary for effective cell mobility. Decreased cell mobility is therefore consistent with continued presence of paclitaxel in the cells during treatment with the P-gp inhibitor.

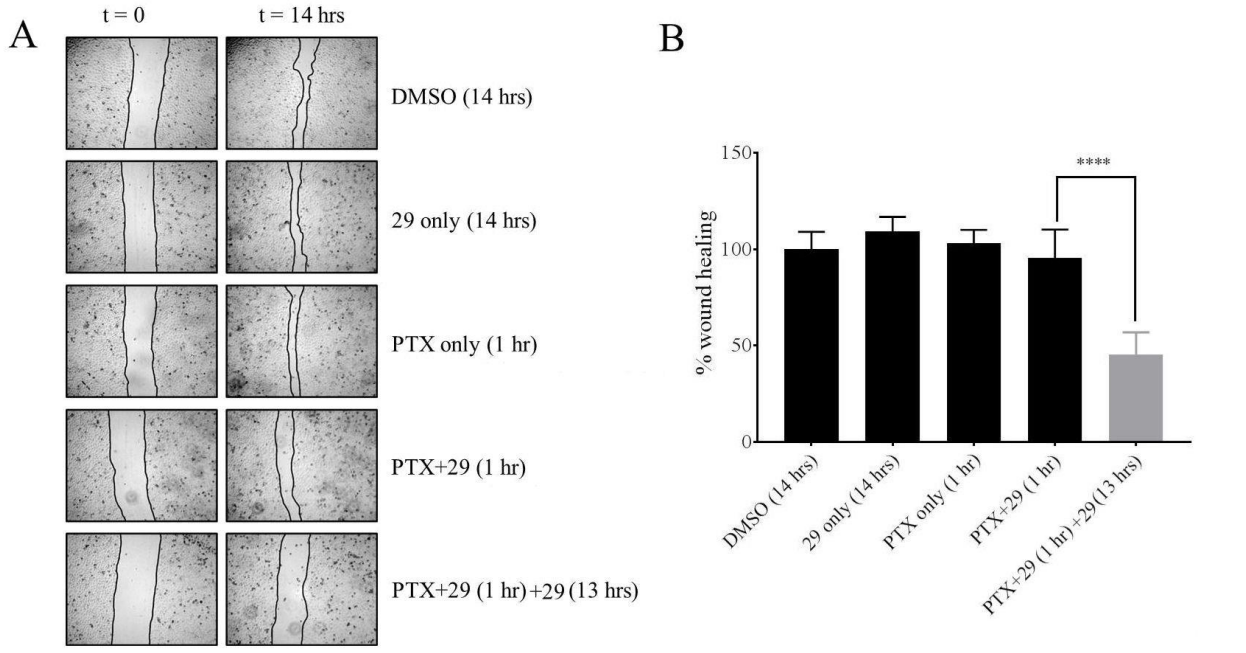

Figure 3.4 **- Increased retention of chemotherapeutics in MDR cells treated for extended times with P-glycoprotein inhibitor decreases cell motility as determined by wound healing assays.**

The treatments of cells with chemotherapeutic and P-gp inhibitor **29** (as indicated) were performed similarly to those reported in Figure 3.2 and Figure 3.3 except that these assays were designed to detect cellular migration independent of proliferation. **A -** Typical bright field images at zero time and after 14 hours for the chemotherapeutic and P-gp inhibitor treatments as indicated in the figure. Microscopy was as described in Methods using a Cytation 5 imager at 4 x magnification. The concentration of **29** was 15 µM for the initial treatment with 0.5 µM paclitaxel as indicated. Extended treatment of P-gp inhibitor **29** was carried out in at 7.5 µM for 13 hours. **B** – Results of wound healing assays are reported as a percentage of closure of the wound after 14 hours relative to the DMSO vehicle-only controls. Cells were treated with P-gp inhibitor **29** and paclitaxel for the times indicated. Data are expressed as average ± S.D. of duplicate experiments (n = 12; **** $P < 0.0001$).

3.2.5 Cellular retention of chemotherapeutics during extended exposure to inhibitor 29 increases apoptosis in P-gp over-expressing DU145TXR cells

Although Figure 3.2 indicated that increased and prolonged retention of chemotherapeutics in the presence of P-gp inhibitor **29** reduced metabolic activity and although the results of colony formation assays in Figure 3.3 indicated a significant decrease in the survival of cancer cells after

such extended inhibitor treatments, these results did not directly demonstrate increased cell mortality *via* apoptotic mechanisms. To assess cell death mechanism, the cancer cells were exposed to both acridine orange and ethidium bromide to attempt to discern early and late morphological changes to cells undergoing apoptosis after treating the cells with chemotherapeutic and / or inhibitor **29** for the times indicated in Figure 3.5. Acridine orange has been shown to be taken up by both viable and non-viable cells and to intercalate into double stranded DNA and emit green fluorescence. Ethidium bromide, also a DNA intercalating agent, is normally taken up only by non-viable cells and emits a red fluorescence upon binding to DNA [179], [180]. Use of these dyes allows detection of the nuclear morphology of the cells. Figure 3.5 shows that exposure of DU145TXR cells to 15 μM P-gp inhibitor **29** for 24 hours, or 10 μM paclitaxel for 1 hour did not result in any observable signs of apoptosis, *i.e.* chromosomal and/or cellular fragmentation. Under these conditions, no non-viable cells were detected by ethidium bromide red fluorescence when compared to the DMSO-vehicle only controls (Figure 3.5, top three panels). The blue arrows point to examples of cells possessing highly organized nuclear morphologies typical of viable, non-apoptotic cells. Treatment of cells for 1 hour with the same concentration of paclitaxel in the presence of P-gp inhibitor **29** also did not appreciably increase the occurrence of cells displaying typical apoptotic morphologies (Figure 3.5, bottom left panel). In contrast however, relatively short 1-hour exposures to paclitaxel followed by treatment with P-gp inhibitor **29** for 23 hour dramatically increased the number of cells showing chromatin fragmentation (white arrows, bottom center panel) and non-viable dead cells with fragmented nuclei (yellow arrows, bottom center panel). The data strongly suggest that extended exposure of P-gp inhibitor **29** to the cancer cells after initial paclitaxel treatment resulted in much higher incidences of induced apoptosis. The extent of the induced apoptosis under the prolonged P-gp

inhibitor treatments appeared to approach that resulting from a full 24 hour continuous exposure to paclitaxel.

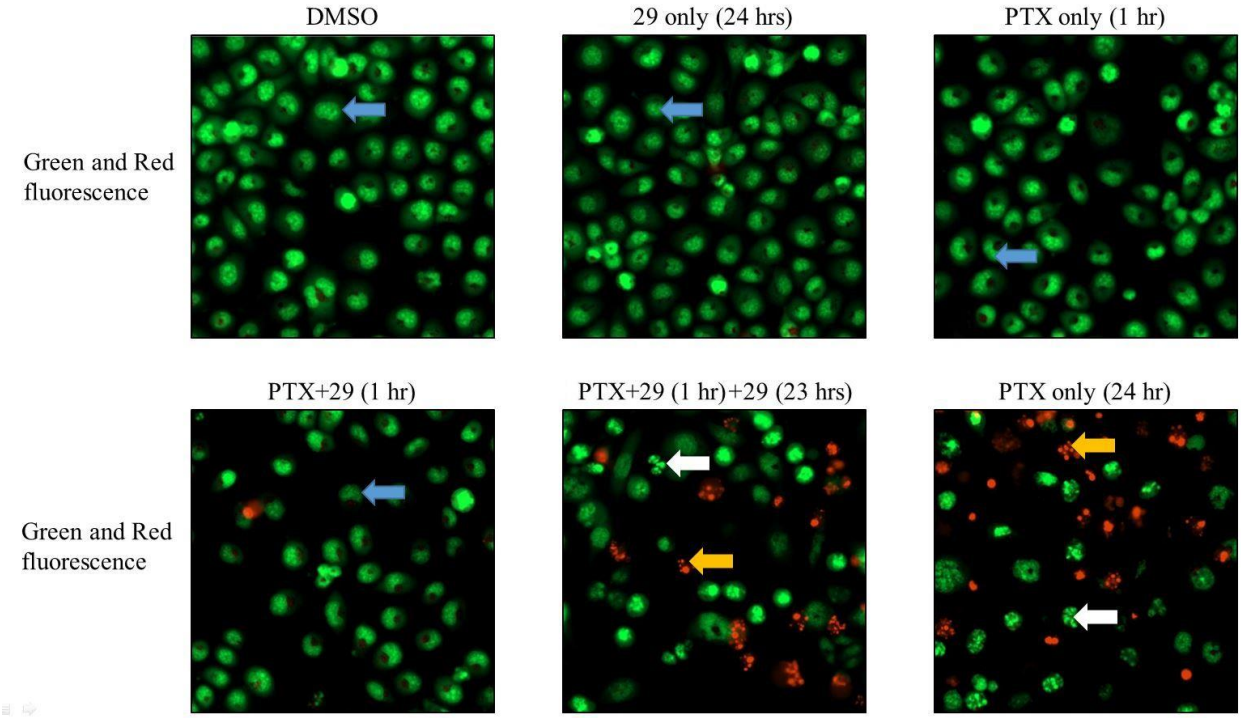

Figure 3.5 - **Increased apoptosis in P-gp over-expressing cancer cells after chemotherapeutic exposure when followed by extended P-gp inhibitor treatment**
P-gp over-expressing prostate cancer cells, DU145TXR, were exposed to 10 µM paclitaxel with or without 15 µM P-gp inhibitor **29** for 1 hour with or without extended P-gp inhibitor **29** treatment for another 23 hours as indicated in the figure. Cells were exposed to both acridine orange and ethidium bromide after the treatments were concluded. Blue arrows identify cells with highly organized nuclear morphologies typical of non-apoptotic cells. White arrows show cells with nuclear – chromatin fragmentation typical of apoptotic cells. Yellow arrows show dead cells with fragmented nuclei. Fluorescent images were obtained as described in Methods using a Cytation 5 imager.

3.2.6 Cells that do not over-express P-gp are not significantly affected by extended treatment with P-gp inhibitor 29

For further evaluation of the new inhibitor for potential future development for clinical use it was of interest to determine whether the extended P-gp inhibitor **29** treatment after exposure to chemotherapeutics might increase cytotoxicity of the chemotherapeutics in cells that do not over-express P-gp. To this aim, experiments identical to those reported in Figure 3.2 were performed

with the prostate cancer cell line, DU145 [194], that does not over-express P-glycoprotein [172] (Figure 3.6A) and with a relatively normal human lung fibroblast cell line, HFL-1 [173] (Figure 3.6B), which also does not over-express P-gp. Cells were incubated with the either inhibitor **29** or paclitaxel alone with or without an extended P-gp inhibitor treatment in the combinations indicated in the figure. No significant differences in cell viabilities with either the DU145 or the HFL-1 cell lines were observed between paclitaxel plus inhibitor **29** treatments for 2 hours or the identical treatments followed by 22 hours of exposure to P-gp inhibitor **29** (Figure 3.6A and B). These experiments demonstrated that the extended P-gp inhibitor treatment did not increase the toxicity of chemotherapy treatment to non-P-gp overexpressing cells.

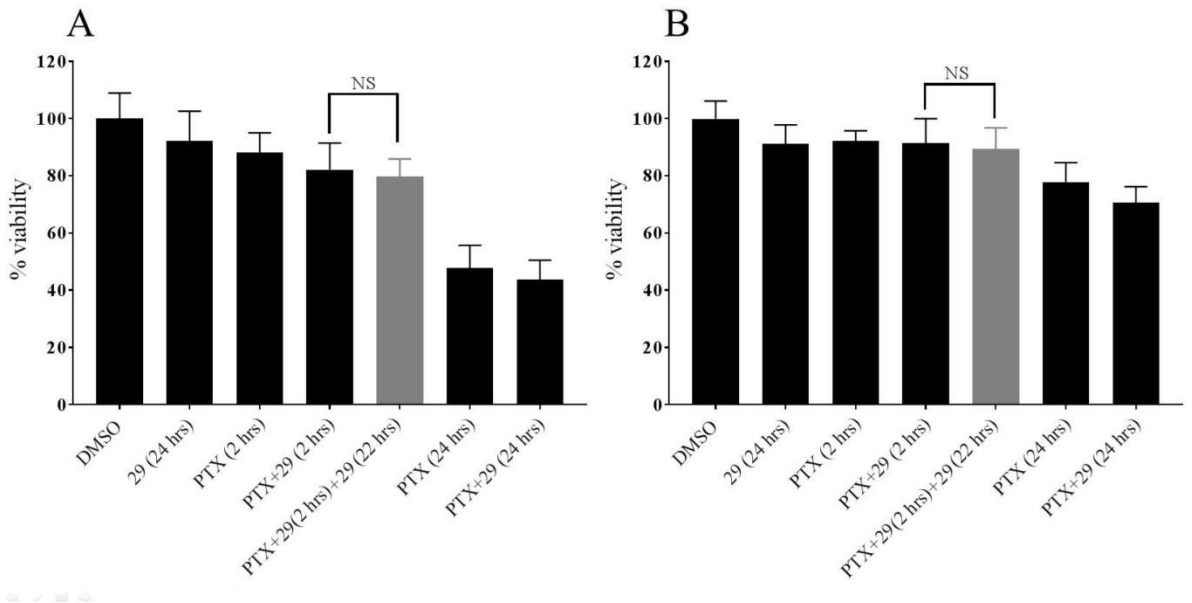

Figure 3.6 **- Extended treatments with P-glycoprotein inhibitor do not affect cells that do not over-express P-gp.**

In these experiments, cell viability was assessed with resazurin as described for Figure 3.2. **A** – DU145 cells were preloaded with paclitaxel (PTX) by incubation in the presence of 25 µM of P-gp inhibitor **29** unless otherwise indicated in the figure. After the preloading, cells were washed and media was replaced with complete media with the indicated additions. Control experiments included exposure of the cells to DMSO alone (0.5% final concentration), P-gp inhibitor **29** alone, paclitaxel alone, or in combinations and times indicated. Extended treatment with P-gp inhibitor **29** was carried out for 22 hours. **B** – Experimental protocols as in **A**, but using human lung fibroblast HFL-1 cells. For this experiment, the concentration of paclitaxel was 0.1 µM and that of compound **29** was 25 µM as indicated. The percentage of viable cells present at the end of the experiments were expressed as percentages of the DMSO- vehicle only control experiments. Data are expressed as averages +/- S.D. of duplicate experiments. "NS" = not significantly different. Measurements were made as described in Methods using a Cytation 5 imager.

3.3 Materials and methods

3.3.1 Cell lines and cell culture

The drug sensitive DU145 human prostate cancer cells [194] as well as the multidrug resistant sub-line, DU145TXR [172] were generous gifts from Dr. Evan Keller (University of Michigan, Ann Arbor, MI). The MDR DU145TXR cell line was maintained under positive selection pressure by supplementing complete medium with 10 nM paclitaxel (Acros Organics, NJ). The cell lines were maintained in complete media consisting of RPMI-1640 with L-

glutamine, 10% fetal bovine serum (FBS; BioWest, Logan, UT or Corning, NY), 100 U/mL penicillin and 100 μg/mL streptomycin in a humidified incubator at 37°C and 5% CO_2. Cell culture materials were purchased from Corning Inc. (Corning, NY) unless otherwise stated. The chemotherapeutics paclitaxel and vinblastine were purchased from Acros Organics, NJ, and MP Biomedicals, France, respectively. Human lung fibroblast cells, HFL-1 cells [173], were maintained in complete medium consisting of F12K with L-glutamine, 10% fetal bovine serum, 100 U/mL penicillin and 100 μg/mL streptomycin in a humidified incubator at 37°C and 5% CO_2.

3.3.2 Daunorubicin accumulation and release

DU145TXR cells were seeded in 96 wells plates at 3000 cells per well in complete media and allowed to grow until confluence. After removal of medium, the cells were treated with 25 μM P-gp inhibitory compound **29** [164] (IUPAC: 2-[(5-cyclopropyl-4H-1,2,4-triazol-3-yl)sulfanyl]-N-[2-phenyl-5-(2,4,5-trimethylphenyl)-pyrazol-3-yl; SMILES: Cc5cc(c3cc(NC(=O)CSC1N=C(N=N1)C2CC2)n(n3)c4ccccc4)c(C)cc5C, Fig. 1D) and 10 μM daunorubicin (MP Biomedicals, France) diluted into complete medium. After 1.5 hours of incubation, medium was removed and cells were washed three times with 200 μL of cold PBS (137 mM NaCl, 2.7 mM KCl, 10 mM Na_2HPO_4, and 1.8 mM KH_2PO_4, pH 7.4). Half of the test wells were then incubated with 25 μM P-gp inhibitor **29** diluted into phenol red free RPMI-1640 and the other half of the test wells were supplemented with phenol red free RPMI-1640 containing 0.5 % DMSO (vehicle). The fluorescence of daunorubicin released from the cells was measured over 105 minutes in 15-minute intervals at excitation at 488/20 nm and emission at 575/20 nm using a Cytation 5 imaging multi-mode reader (BioTek, Winooski, VT).

After 105-minutes, the amount of daunorubicin remaining in the cells was measured qualitatively and quantitatively. To qualitatively observe the daunorubicin retained in the cells, medium was removed and the cells were fixed with 4% para-formaldehyde in PBS. The cells were imaged using a Cytation 5 imaging multi-mode reader with a Texas red fluorescence filter. To quantify the daunorubicin that had remained in the cells, medium was removed from each well and cells were lysed in 100 μL of PBS containing 0.5% SDS and 0.5% Triton X100. The fluorescence of daunorubicin was measured using the Cytation 5 imaging multi-mode reader.

3.3.3 Resazurin cell viability assay

Cells were trypsinized from monolayers and seeded into a 96 well plate with 3000 cells in 150 μL of complete media per well. After 48 hours of incubation, cells were treated for 2 hours with chemotherapeutics and / or P-gp inhibitor **29** dissolved in DMSO, and / or DMSO alone diluted into complete medium. At the times indicated, cells were washed with cold PBS that did not contain chemotherapeutic and treatment was continued for an additional 22 hours with compound **29** alone. At 18 hours of treatment, 440 μM of resazurin (Acros Organics, NJ) solution prepared in PBS was added for viability assays as described in [175]. The resulting resorufin fluorescence was measured after 6 hours of incubation of the cells with resazurin by excitation at 530 nm and emission at 590 nm using a Cytation 5. The percent viability was calculated using the DMSO treated cells as representative for 100% viability. Background fluorescence was determined using resazurin and complete medium without cells.

$$\% \text{ Viability} = \frac{\text{Fluorescence of experimental cells - Background fluorescence} \quad * 100}{\text{Fluorescence of DMSO treated cells - Background fluorescence}}$$

The results from these assays were plotted as the mean with standard deviation (SD) of at least eight replicates per treatment from two independent experiments using the program GraphPad Prism™ (La Jolla California, USA, Version 7).

3.3.4 Colony formation assay

Colony formation assays were performed similar to [181] with slight modifications. DU145 TXR cells were seeded in 24 well plates with 250 cells per well. After 24 hours, cells were treated for 2 hours with paclitaxel and / or P-gp inhibitor, compound **29**, dissolved in DMSO, or DMSO controls diluted in complete medium. The concentration of **29** and paclitaxel was 10 µM. The cells were then washed with cold PBS and exposed to compound **29** alone ("extended **29** treatment") for another 22 hours. The medium was then removed and cells were allowed to form colonies for 5 days in drug- and compound **29**-free complete media. To visualize the colonies, the medium was removed and cells were fixed with a mixture of methanol and acetic acid 3:1 (v/v) solution. After 5 minutes, the fixation solution was removed and the cells were stained with 0.5% w/v crystal violet (Alfar Aesar, MA) in 25% methanol for 30 minutes. After removal of crystal violet, the whole plates were washed with running water to remove excess dye. Colonies visible to the naked eye were counted and recorded by persons blinded to all experimental conditions. The number of colonies were normalized to vehicle-treated controls as percentages. The experiment was repeated two times with a total of three replicates each.

3.3.5 Scratch assays

Scratch assays were performed as outlined previously [183] with minor modifications. Cells were trypsinized from monolayers and diluted in complete culture medium to a density of 45,000 cells in 400 µL cell suspension per well in 48-well plates and cultured until fully confluent. The monolayers of cells were then scratched using a 200 µL pipette tip. The medium

was removed and the cells were washed with PBS to remove floating cells. Immediately after the scratching and media addition, the wounds were imaged using the Cytation 5. Complete medium with low serum content (1% v/v) was then added to the wells together with 0.5 μM paclitaxel with or without 15 μM P-gp inhibitor, compound **29**. In the no-treatment control only 0.5% final volume of DMSO was added in place of drugs and/or P-gp inhibitor. After 1 hour incubation, medium was removed from all the wells and the cells were washed with cold PBS. All test wells were incubated with 0.5% DMSO containing media with 1% FBS except for the wells that contained compound **29** only, and the wells with extended compound **29** exposure after co-treatment with paclitaxel and compound **29**. Extended treatment of P-gp inhibitor **29** was carried out in a concentration of 7.5 μM for 13 hours. The "wounds" in the confluent cell layers were then re-imaged and the area of the wounds before and after each treatment were quantified using ImageJ software [199]. The percentage of wound closure in each test was calculated compared to vehicle treated experiments. Each individual experiment was performed in triplicate and 2 images were obtained for each well. The whole experiment was repeated at least once, and n=12 was used for the statistical analysis.

3.3.6 Fluorescence microscopic analysis of cell apoptosis

Double staining with acridine orange/ ethidium bromide (AO/EB) is a reliable method to detect apoptosis and was carried out as described in [179] with slight modifications. 16,000 cells were seeded in 48 well plates in 300 μL of complete media and incubated for 48 hours. After 48 hours, cells were treated for 1 hour with 10 μM paclitaxel and 15 μM P-gp inhibitory compound **29** in DMSO or DMSO controls. Cells were then washed with cold PBS and an "extended treatment" with compound **29** alone was carried out as described above for another 23 hours. Cells not treated with compound **29** were treated with 0.5 % DMSO (vehicle). The AO/EB dual

stain containing solution (100 μg/ml each) was then added to each well and images were acquired using a Cytation 5 with GFP (for green fluorescence from acridine orange) and Texas red fluorescence (for red fluorescence from ethidium bromide).

3.4 Discussion

P-gp overexpressing cancer cells can limit the drug accumulation in the cancer cells and lower the effectiveness of the treatment [136]. Further, drug transporters such as P-gp can reduce the bioavailability of drugs by impacting pharmacokinetics parameters such as clearance and volume distribution [239]. Some experiments suggest that P-gp inhibitors can increase the bioavailability of drugs [240], [241]. Therefore P-gp inhibitors can be effective against MDR cancer, not only by increasing intracellular drug accumulation but also by increasing the bioavailability of chemotherapeutics [242].

Approximately 10%–20% of patients with prostate cancer develop metastatic castration-resistant prostate cancer (mCRPC) which is an advanced form of prostate cancer that develops following surgical castration [243]. Taxol based chemotherapy has been regarded as the first-line treatment for patients with mCRPC [244]–[246]. Nevertheless MDR related to P-gp is still a major challenge to castration-resistant prostate cancer treatments [206], [247]. In this study we have shown that P-gp inhibitor **29** can retain the chemotherapeutic daunorubicin inside DU145TXR [172], a P-gp overexpressing prostate cancer cell line (Figure 3.1) after a short exposure. Continuance of the P-gp inhibitor **29** treatment without the presence of chemotherapeutics, yielded a higher efficacy of the initial chemotherapeutic exposure (Figure 3.2 to Figure 3.5). We have demonstrated the increased efficacy of this experimental strategy of prolonged exposure to P-gp inhibitor by observing the reduced viability, colony formation, cell migration and increased apoptosis in MDR cancer cells. In all these assays, short term exposure

of chemotherapeutics had no or minimal impact on cancer cells. But we have clearly demonstrated that the retention of paclitaxel or vinblastine in cancer cells by P-gp inhibitor **29** is responsible for the improved outcome of these assays. Further, results of viability assays and apoptosis assays indicated that similar positive responses can be achieved by exposing the cells to chemotherapeutics in a short time period compared to exposing for a long time period by continuance of P-gp inhibitor **29** treatment. Clinically, the ability to reduce the exposure time of chemotherapy might be a significant advantage when chemotherapy related toxicity is a concern [248]–[250]. In support of this assertion is the fact that this strategy does not seem to affect the viability in cancer cells or non-cancerous cells that do not overexpress P-gp (Figure 3.6).

Although these studies were conducted *in vitro,* we believe this strategy can be explored *in vivo* and in clinical settings. Here we cite several clinical studies that administered P-gp inhibitors along with chemotherapeutics [72], [251]–[254]. In all these, the doses of P-gp inhibitors had been administered prior to or along with chemotherapeutics, without extended treatment of the P-gp inhibitor. These studies have mentioned that the doses of P-gp inhibitors were well tolerated by the patients but showed only a marginal increased efficacy of chemotherapy at best. However, based on our results in cell culture model, we hypothesize that addition of extra doses of P-gp inhibitor after the initial chemotherapy treatments would increase the intracellular retention of chemotherapeutics. This has the potential to make a positive impact on the outcome of chemotherapy in clinical trials influencing the bioavailability of the chemotherapeutics.

CHAPTER 4: EVALUATION OF LEAD OPTIMIZED VARIANTS OF P-GLYCOPROTEIN INHIBITOR 29 IN MULTIDRUG RESISTANT CELL CULTURE MODEL

4.1 Introduction

Computational methods have played a major role in drug design and discovery over three decades [255]. These methods contributed to the discovery of highly effective HIV medications (HIV protease inhibitors) like ritonavir, indinavir and saquinavir which have had a substantial impact on reducing AIDS related deaths [256]. Currently computational drug screenings are extensively utilized in identifying and modifying chemotherapeutics yielding experimental anticancer drugs such as Luminespib [257]–[261]. Lead optimization has become a primary focus in computational drug screenings [262]. High throughput computational screenings can yield small molecules as initial hit molecules and these can be optimized into lead molecules to increase their activity, reduce the off-target effects and improve overall pharmacology properties [263], [264]. Conventional lead optimization involves the synthesis of analogues of lead molecules and testing them in *in vitro* and *in vivo* assays which accounts for a considerable cost of developing a new drug [255], [265]. Computational lead optimization can reduce this cost by decreasing the number of molecules that have to be tested by increasing the proportion of new leads that have desired effects [255].

We have identified and studied three P-gp inhibitors (**29**,**34** and **45**) using high throughput computational studies and demonstrated their ability to successfully reverse MDR in P-gp

overexpressing prostate and ovarian cancer cell lines [164], [165], [235]. Inhibitor **29** is predicted to be an allosteric inhibitor with no effect on ATP binding on the NBD [164]. The following study shows *in vitro* testing results of several variants of P-gp inhibitor **29**. Three of these new variants (**216**, **227** and **231**) are the result from computational lead optimization using an in-lab produced software called ChemGen (Group 1). Five of the other variants (**238**, **255**, **278**, **280** and **286**) tested here were the result of conventional lead optimization (Group 2) which were

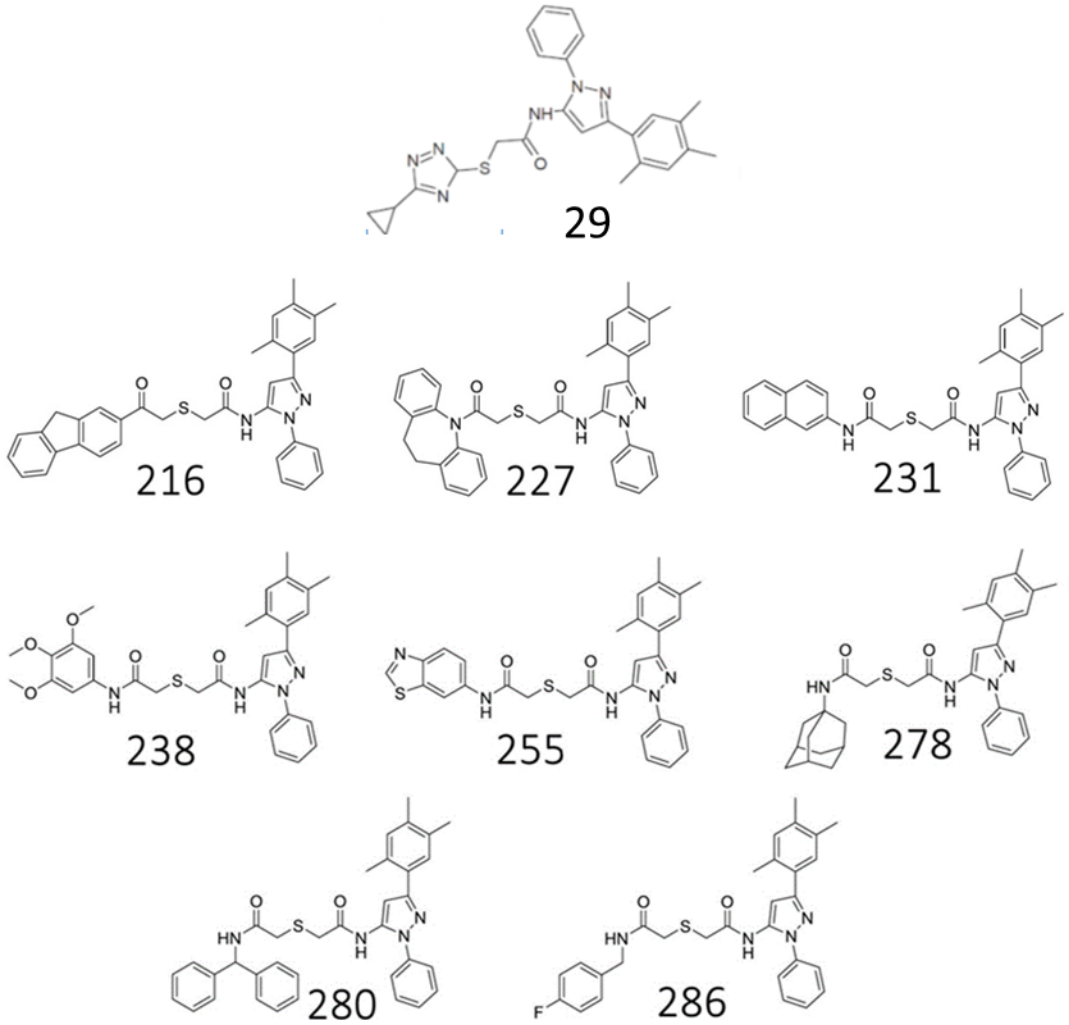

4.1 - **Structures of 29 variants.**
Parental P-gp inhibitor **29**, Group 1/ChemGen generated **29** variants (**216**, **227** and **231**), Group 2/Rationally synthesized **29** variants (**238**, **255**, **278**, **280** and **286**)
synthesized by Dr. Lippert's laboratory in the SMU Chemistry department.

4.2 Results

4.2.1 ChemGen/docking (Group 1) generated variants of P-gp inhibitor 29 resensitize a multidrug resistant, P-gp overexpressing prostate cancer cell line to paclitaxel

The mitochondrial reduction potential of cells is often used as an indicator for cell viability using MTT assays [192], [193], [266]. Using these assays we observed that the three Group 1 derivatives of **29** predicted through *ChemGen/*docking routine and synthesized here, **216**, **227** and **231**, re-sensitized the P-gp overexpressing prostate cancer cell line, DU145TXR [172], to the chemotherapeutic, paclitaxel. First, we analyzed the active range of the concentration of these variants of 29. **Figure 4.2** shows the viability of DU145TXR cells treated with P-gp inhibitor **29** variants **216**, **227** and **231** with or without 100 nM of paclitaxel (100 nM of paclitaxel can be tolerated by DU145TXR without any toxicity [165]). The inhibitory action of these derivatives can be observed from 3 µM onwards. **Figure 4.2** also shows that derivative 227 and 231 performed better than 29 combined with paclitaxel to lower the viability of cancer cells. Importantly, these derivatives did not show considerable cytotoxicity by themselves (in the absence of chemotherapeutic).

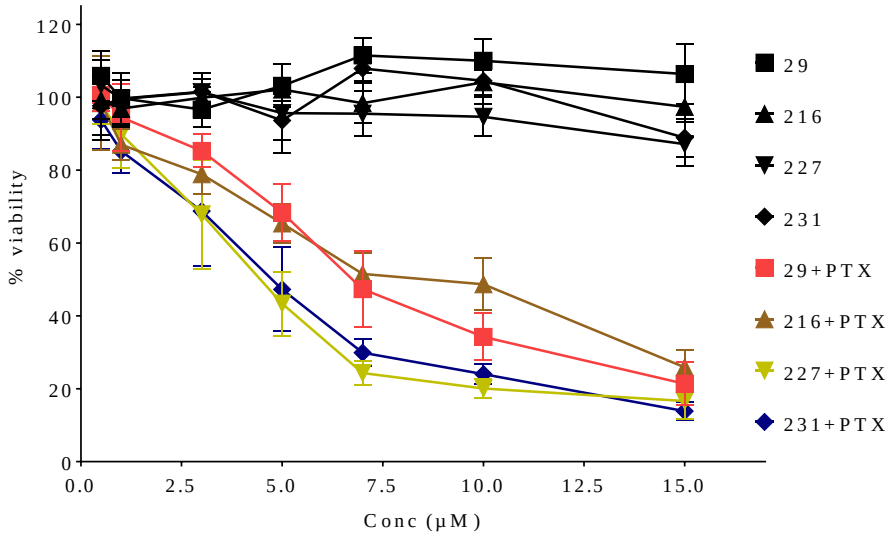

Figure 4.2 – **Reduction of viability to paclitaxel by ChemGen generated variants of the P-glycoprotein inhibitor, compound 29.**
The prostate cancer cell line, DU145TXR, that over-expresses P-glycoprotein was treated with inhibitors **216**, **227** and **231** (0.5, 1, 3, 5, 7, 10 or 15 µM) with or without 100 nM of paclitaxel (PTX). Metabolic activity assays using MTT were performed as described in Methods.

In order to calculate the IC_{50} values for reversing MDR in DU145TXR cells by these inhibitors, cells were treated with fixed concentrations of inhibitors and varying doses of paclitaxel (**Figure 4.3**). Analyses of the data (Table 4.1) revealed that in the presence of 3 µM inhibitor variant **216**, the observed IC_{50} value of paclitaxel was decreased by about 2.5 to 3-fold when compared to the presence of the parental compound **29** and about 8-fold when compared to paclitaxel alone. At increasing concentrations, the efficacy of variant **216** in increasing paclitaxel toxicity decreased when compared to the parental compound **29.** At the highest concentration tested (10 µM), the **216** variant was observed to be somewhat less effective than parental compound **29**. Unlike **216**, variants **227** and **231** were more effective than **29** at all concentrations tested, resulting in 4-fold decreased paclitaxel IC_{50} at 3 µM when compared to parental compound **29** and about 14-fold overall sensitization to paclitaxel when compared to paclitaxel alone. At higher concentrations (5 to 10 µM), addition of these variants resulted in

increased paclitaxel toxicity by up to 500 – 1000-fold at 10 µM, as compared to ~100-fold of the parental compound **29** at 10 µM. This data indicated that variants **227** and **231** were much better re-sensitizers of the multidrug resistant cells to paclitaxel than the original compound **29** at all concentrations tested, while variant **216** appeared to be marginally better than **29** at lower concentrations. These data support the hypothesis that the *ChemGen* generated optimized lead compounds and the docking analyses used to select Group 1 variants of compound **29** had increased affinity for P-gp resulting in improved efficacy for reversing chemotherapy resistance in a P-gp overexpressing cancer cell line than did the parental compound.

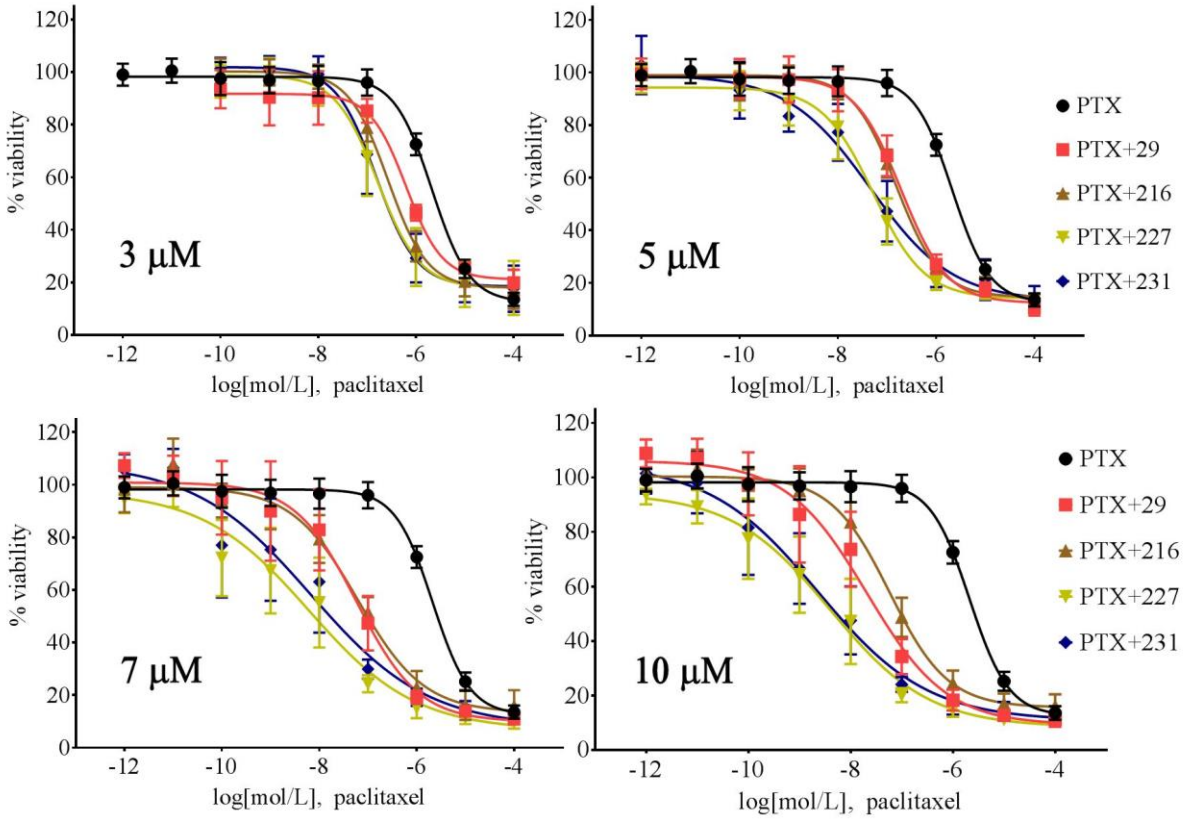

Figure 4.3 - **Reversal of paclitaxel resistance by ChemGen identified variants of the P-glycoprotein inhibitor, compound 29.**

The prostate cancer cell line, DU145TXR, that over-expresses P-glycoprotein was treated with either paclitaxel (PTX) or paclitaxel and either 3, 5, 7, or 10 µM of the P-gp inhibitors (upper left, upper right, lower left and lower right panels, respectively). Metabolic activity assays using MTT were performed as described in Methods. Calculated IC_{50} values for paclitaxel in the presence of the respective compounds calculated from this data are reported in Table 4.1.

Table 4.1 **- Increased toxicity of paclitaxel to DU145TXR in the presence of P-gp inhibitors identified by ChemGen/docking routine.**
Cytotoxicity of the chemotherapeutic, paclitaxel (PTX) to P-gp overexpressing prostate cancer cells, DU145TXR, was determined in the absence and presence of the *ChemGen* designed **29**-variants, **216, 227 and 231**. For each experimental compound IC_{50} values of PTX alone or in the presence of inhibitors, fold improvement of PTX sensitivity in the presence of inhibitor, and fold improvement of PTX sensitivity by variants compared to parental compound **29** are given.

PTX alone	**Inhibitor concentration**	**PTX+29**			**PTX+216**		
IC_{50} PTX (nM)		**IC_{50} PTX (nM)**	**Fold vs PTX**	**Fold vs PTX + 29**	**IC_{50} PTX (nM)**	**Fold vs PTX**	**Fold vs PTX + 29**
2120	3 µM	**629**	3	1	**266**	8.0	2.4
	5 µM	**194**	11	1	**154**	14	1.3
	7 µM	**59**	36	1	**62**	34	1
	10 µM	**21**	101	1	**57**	37	0.4
		PTX+227			**PTX+231**		
		IC_{50} PTX (nM)	**Fold vs PTX**	**Fold vs PTX + 29**	**IC_{50} PTX (nM)**	**Fold vs PTX**	**Fold vs PTX + 29**
	3 µM	**164**	13	3.8	**153**	14	4.1
	5 µM	**52**	41	3.7	**46**	46	4.2
	7 µM	**6**	353	10	**7**	303	8.4
	10 µM	**4**	530	5	**2**	1060	11

4.2.2 Accumulation and cellular retention of calcein AM in P-gp overexpressing prostate cancer cells upon incubation with Group 1 SMU-29 variants

Calcein AM accumulation assays have been used by us previously to evaluate P-gp-substrate accumulation in real time in the presence or absence of P-gp inhibitors [235]. For these assays, P-gp overexpressing DU145TXR cells were incubated with the respective inhibitors in

the presence of the P-gp substrate, calcein AM. Inhibition of P-gp leads to cellular accumulation of calcein AM and to cleavage of its acetoxymethyl ester groups by cellular esterases, resulting in the generation of the highly fluorescent compound, calcein. The anionic calcein is not a substrate of P-gp and remains in the cells. In these assays, the relative fluorescence of cellular calcein was measured over time and the results of these assays are shown in **Figure 4.4** (left panel). The data indicated that when these cells were treated with any of the three Group 1 **29** variants, the observed cellular accumulation of fluorescent calcein was lower than upon treatment with the parental compound **29**.

To test whether the lower accumulation of calcein in the presence of the Group 1 **29** variants was the result of retention of the compounds in the cellular membrane due to their increased logP values relative to **29** (estimated logP values for 29, 216, 227 and 231 are respectively 4.0, 6.6, 6.4 and 5.7. Values were obtained from Wise *et al.* unpublished), similar calcein accumulation assays were performed after a 6-hour pre-incubation with the **29**-variants and parental compound **29**, Figure 4.4 (right panel). We note for clarity that the preferential partitioning of variants in the hydrophobic part of the cell membrane would keep them more distant from the putative allosteric site on P-gp which is located adjacent to the membrane in the cytoplasm. The data of Figure 4.4 suggested that calcein accumulation in the presence of the variants was slightly improved by the 6 hrs preincubation for all Group 1 compounds compared

to the “no preincubation” experiments, but none of the variants showed better performance in these assays when compared to the parental compound **29**.

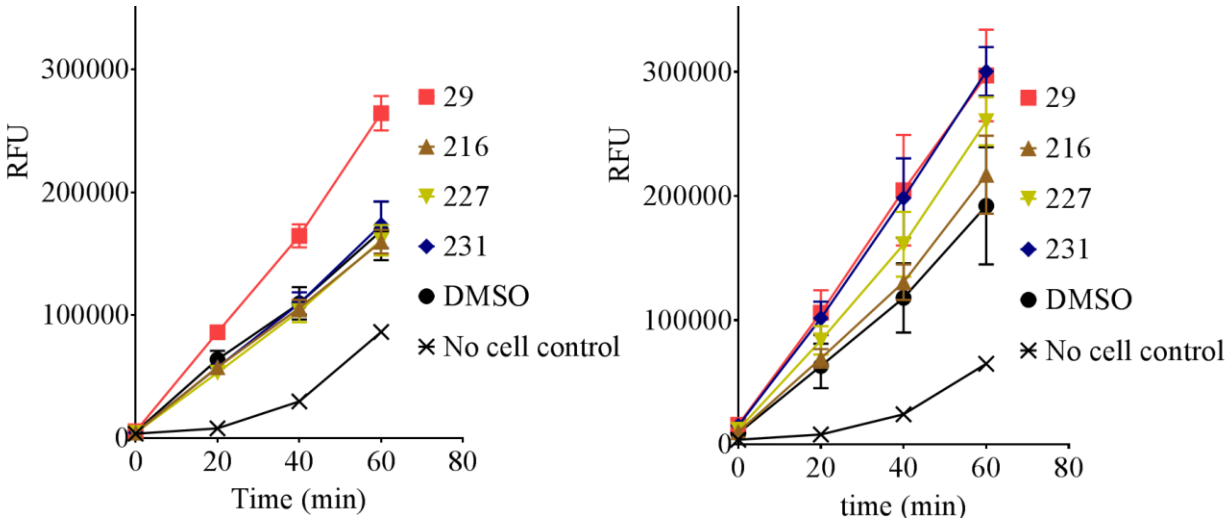

Figure 4.4 - **Cellular accumulation of the fluorescent dye, calcein, by inclusion of Group 1 variants of the P-glycoprotein inhibitor, compound 29, identified with ChemGen.**
The prostate cancer cell line, DU145TXR, that over-expresses P-glycoprotein was treated with calcein AM and without (**left**) or with (**right**) a 6-hr pre-incubation with 2 µM of the indicated P-gp inhibitors.

4.2.3 Effects of Group 2 variants on the paclitaxel sensitivity of P-glycoprotein overexpressing prostate cancer cells, DU145TXR

MTT assays were again used to assess the efficacy of the Group 2 **29-**variants on sensitizing the chemotherapy-resistant prostate cancer cell line, DU145TXR, to paclitaxel described before. Figure 4.5 shows the viability of DU145TXR cells treated with derivatives **238, 255, 278, 280** and **286** with or without 100 nM of paclitaxel. Again, inhibitory action of these variants can be observed at concentrations 3 µM and higher. All derivatives in Group 2 except for **286** performed better than original **29** when combined with paclitaxel to lower the viability of cancer cells. Variant **280** (Figure 4.5) exhibited a considerable level toxicity to cancer cells by itself even at 3 µM and **286** exhibited high toxicity at 15 µM concentration. To calculate the IC_{50} values for reversing MDR by these inhibitors, DU145TXR cells were treated with fixed

concentrations of inhibitors and varying doses of paclitaxel (**Figure 4.6**). The data for these tests is presented in Table 4.2 and suggest that the presence of all of the variants except for **286** increased the paclitaxel toxicities to these P-gp overexpressing cells compared to original inhibitor **29**. Compounds **238** and **255** increased paclitaxel toxicities to the greatest extents: At 5 μM concentration, compound **238** decreased the paclitaxel IC_{50} by about a thousand-fold, similar to compound **255** at 7 μM. Comparison with parental compound **29** showed that **238** improved sensitization of DU145TXR to paclitaxel by 3.4-fold at 3 μM, and by around 100-fold at 5 and 7 μM. At 10 μM, compound **238** resulted in a 300-fold decreased paclitaxel IC_{50} of DU145TXR compared to parental compound **29** at the same concentration. Compound **255** also showed substantial improvement in sensitization of DU145TXR to paclitaxel that was comparable to **238** at 3 μM, but the effect was not as pronounced at higher concentrations. The other three compounds, **278**, **280** and **286**, were similar or less effective than the Group 1 variants, **216**, **227** and **231**. In addition, compound **280** seemed to exhibit some toxicity to the multidrug resistant cancer cells as judged by the lowered cell viability at very low concentrations of paclitaxel in the presence of **280** (**Figure 4.6**).

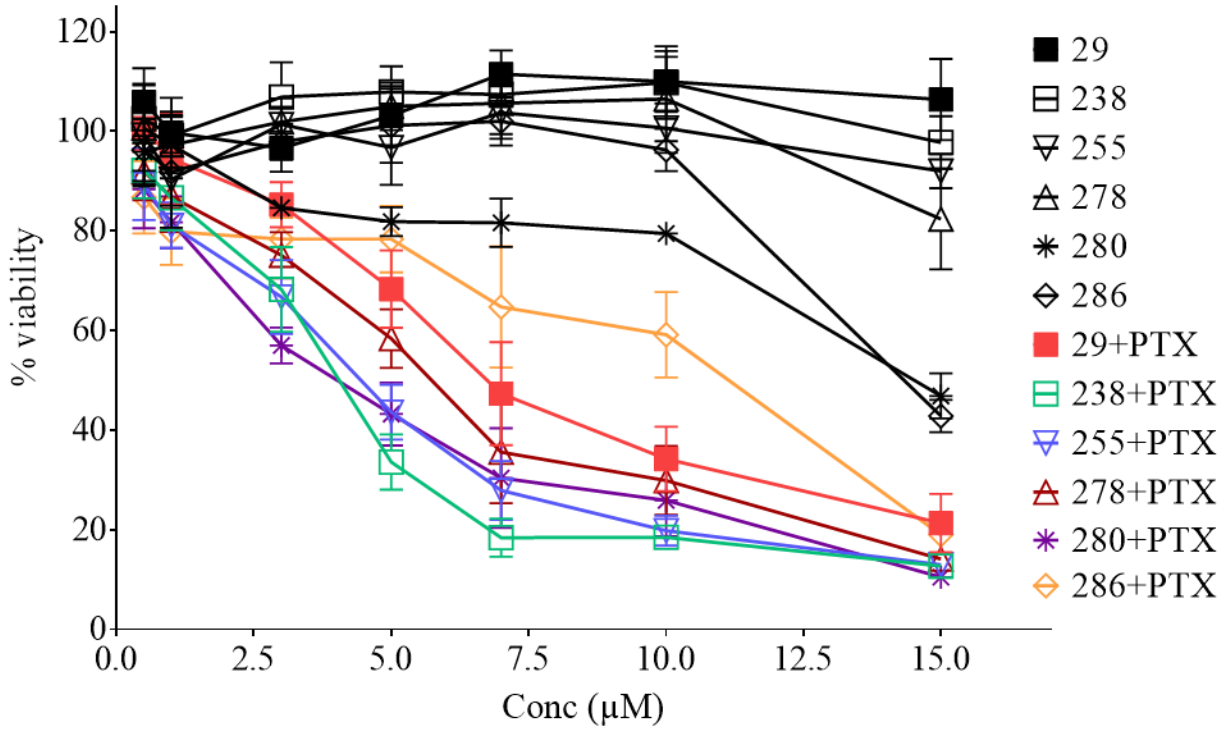

Figure 4.5 - **Reduction of viability to paclitaxel by Group 2 variants of the P-glycoprotein inhibitor, compound 29.**

The prostate cancer cell line, DU145TXR, that over-expresses P-glycoprotein was treated with inhibitors **238, 255, 278, 280** and **286** (0.5, 1, 3, 5, 7, 10 or 15 µM) with or without 100 nM of paclitaxel (PTX). Metabolic activity assays using MTT were performed as described in Methods.

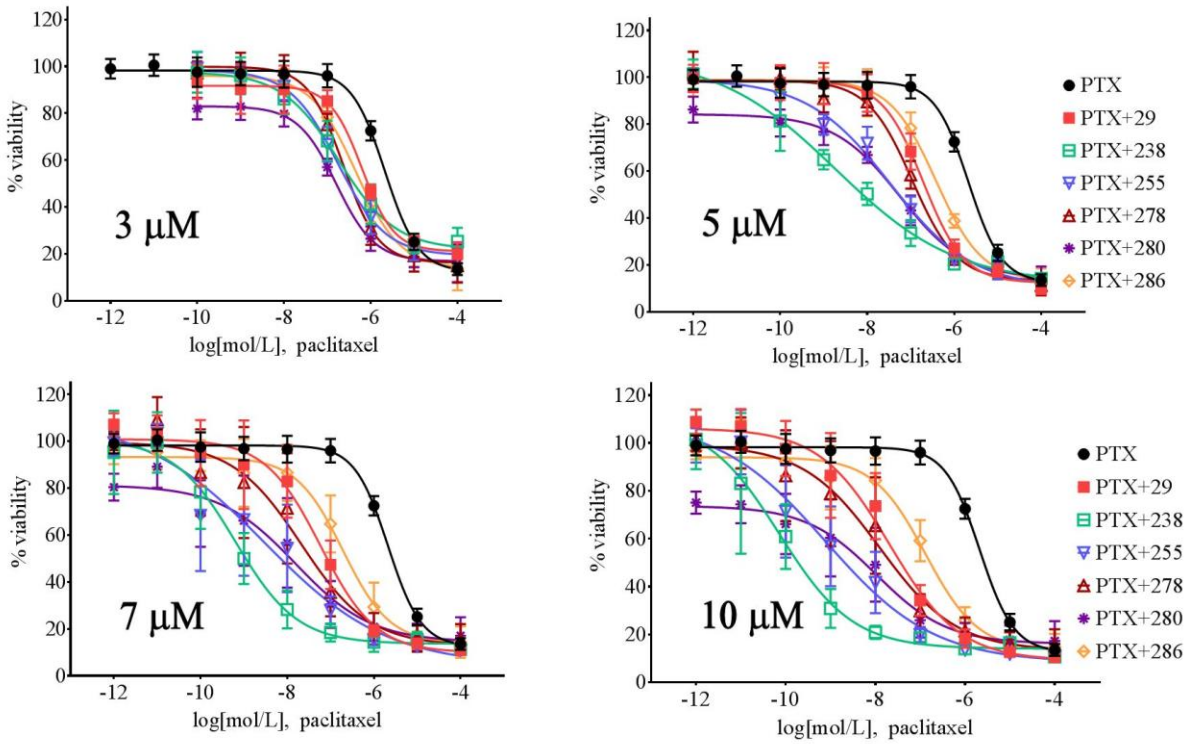

Figure 4.6 - **Reversal of paclitaxel resistance by rationally designed variants of the P-glycoprotein inhibitor, compound 29.**

The prostate cancer cell line, DU145TXR, that over-expresses P-glycoprotein was treated with either paclitaxel (PTX) or paclitaxel and either 3, 5, 7, or 10 µM of the P-gp inhibitors (upper left, upper right, lower left and lower right panels, respectively). Metabolic activity assays using MTT were performed as described in Methods. Calculated IC_{50} values for paclitaxel in the presence of the respective compounds calculated from this data are reported in Table 4.2.

Table 4.2 - **Increased toxicity of paclitaxel in the presence of rationally designed P-gp inhibitors.**
Cytotoxicity of the chemotherapeutic, paclitaxel (PTX) in P-gp overexpressing prostate cancer cells, DU145TXR, was determined in the absence and presence of the structural **29**-variants, **238, 255, 276, 280, and 286**. For each experimental compound, (a) IC 50 values of PTX alone or in the presence of inhibitors (in nM), (b) Fold improvement of PTX sensitivity in the presence of inhibitor, and (c) Fold improvement of PTX sensitivity by variants compared to parental compound **29** are given.

PTX alone	**Inhibitor concentration**	**PTX+29**			**PTX+238**		
IC_{50} PTX (nM)		**IC_{50} PTX (nM)**	**Fold vs PTX**	**Fold vs PTX + 29**	**IC_{50} PTX (nM)**	**Fold vs PTX**	**Fold vs PTX + 29**
2120	3 µM	**629**	3	1	**185**	11	3.4
	5 µM	**194**	11	1	**1.9**	1116	102
	7 µM	**59**	36	1	**0.64**	3312	92
	10 µM	**21**	101	1	**0.07**	30286	300
		PTX+255			**PTX+278**		
		IC_{50} PTX (nM)	**Fold vs PTX**	**Fold vs PTX + 29**	**IC_{50} PTX (nM)**	**Fold vs PTX**	**Fold vs PTX + 29**
	3 µM	**172**	12	3.7	**231**	9.2	2.7
	5 µM	**34**	372	5.7	**109**	19	1.8
	7 µM	**2.9**	731	20	**21**	101	2.8
	10 µM	**0.78**	2118	27	**13**	163	1.6
		PTX+280			**PTX+286**		
		IC_{50} PTX (nM)	**Fold vs PTX**	**Fold vs PTX + 29**	**IC_{50} PTX (nM)**	**Fold vs PTX**	**Fold vs PTX + 29**
	3 µM	**160**	13	3.9	**458**	4.6	1.4
	5 µM	**56**	38	3.5	**379**	5.6	0.5
	7 µM	**16**	133	3.7	**192**	11	0.3
	10 µM	**11**	193	1.9	**131**	16	0.2

4.2.4 Accumulation and cellular retention of calcein AM in DU145TXR in the presence of 29-variants from Group 2

Figure 4.7, left, shows that without pre-incubation, the presence of 5 µM of compounds **238** and **255** resulted in considerably increased calcein accumulation in DU145TXR cells when compared to **29**. The effect of compound **286** was comparable to **29**, while **278** and **280** caused less calcein accumulation than the parental compound. After a 6-hour pre-incubation (**Figure 4.7** – right panel), the effectiveness of inhibiting P-gp catalyzed transport of calcein AM remained strongest for the more polar **29** variants **238** and **255**, while that of the more hydrophobic variants **278**, **280** and **286** was comparable to **29**.

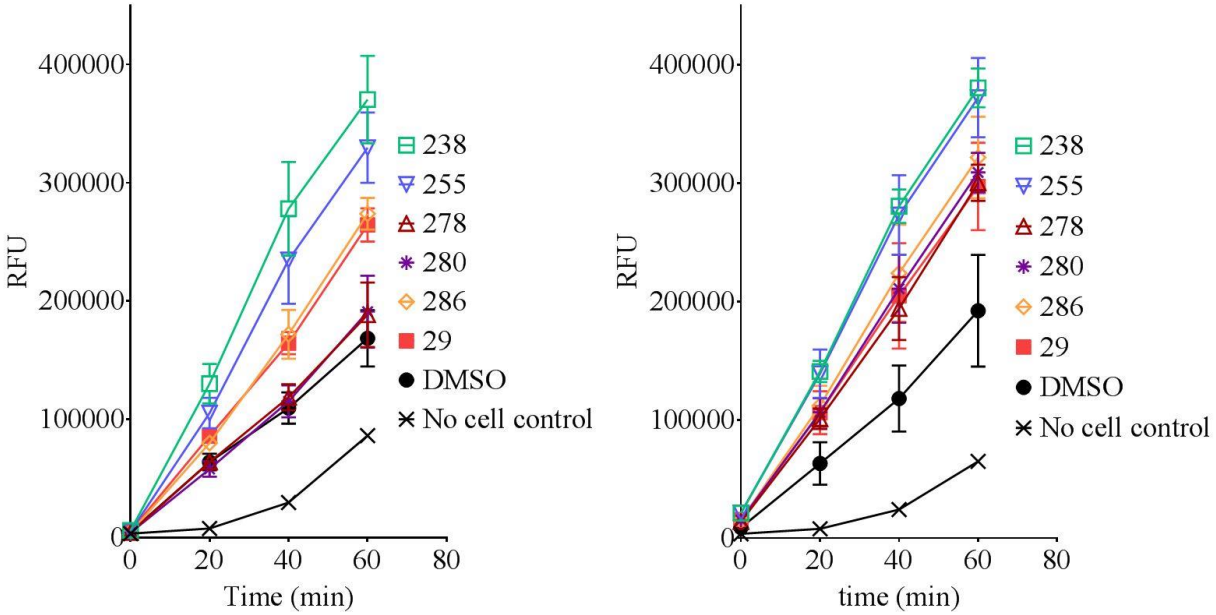

Figure 4.7 - **Cellular accumulation of the fluorescent dye, calcein, by inclusion of Group 2 variants of the P-glycoprotein inhibitor, compound 29.**
The prostate cancer cell line, DU145TXR, that over-expresses P-glycoprotein was treated with calcein AM and without (left) or with (right) a 6-hr pre-incubation with 2 µM of the indicated P-gp inhibitors.

4.2.5 Intracellular accumulation of compound 29 variants

Cell accumulation assays for each of the **29** variants were performed as in [235] to more directly assess whether the compounds were indeed transport substrates or not for P-gp. These

assays measured the intracellular accumulation of the experimental compounds using LC-MS/MS methods after incubation with the P-gp over-expressing cell line, DU145TXR, in the absence and presence of the strong P-gp inhibitor, tariquidar [267] (TQR). The concertation of **29** variants accumulated intracellularly normalized to cell lysate protein concertation is reported in Table **4**.**3**. Low levels of cellular accumulation of a compound in the absence of tariquidar accompanied by much higher levels of accumulation in the presence of tariquidar suggests that the compound in question may be a transport substrate of P-gp. In other words, if a compound is an effective transport substrate for P-gp, active P-glycoprotein in these cells would limit intracellular accumulation, while inhibited P-gp would result in higher intracellular concentrations. Daunorubicin (DNR) is an example of a good transport substrate for P-gp and showed very strong cellular accumulation in these assays when P-gp was inhibited by tariquidar, but much less accumulation in the cells when P-gp was not inhibited (**Figure 4.8**, DNR). If a compound is not a substrate of P-gp, no significant difference in intracellular accumulation of the compound with or without tariquidar is expected. **Figure 4.8** "**29**", shows that compound **29** is not a transport substrate for P-gp [235] and that no significant difference in cellular accumulation of **29** was observed with or without addition of tariquidar (TQR). **Figure 4.8** also presents the fold accumulation of each of the experimental **29**-variants in these assays normalized to the amount of compound found in the absence of TQR. This data is numerically presented in Table 5 as the ratio of observed accumulation in the presence of tariquidar divided by the accumulation observed in the absence of tariquidar for each of the experimental compounds. Ratios that are significantly greater than 1.0 indicate that a compound is very likely a transport substrate of P-gp.

None of the Group 1 molecules tested presented intracellular accumulations that were significantly different in the absence versus presence of TQR, similar to the parental compound **29** (**Figure 4.8**, **216**, **227** and **231**), indicating that the variants were not transport substrates of the pump. This data correlates with the observation that **216** and **227** did not activate basal ATPase activities by P-gp (data not shown; biochemical experiments were performed by Gang Chen Department of Biological Sciences, SMU). Compound **231** also showed no significant cellular accumulations in the presence of TQR (**Figure 4.8**) and only marginally activated basal ATPase activity of P-gp (data not shown). Taken together, these results suggest that none of the Group 1 compounds are good transport substrates for P-gp.

Of the Group 2 compounds, variant **238** showed a very large and significant increase in intracellular accumulation in the presence of TQR (**Figure 4.8**, **238**). Compounds **255** and **286** showed more modest, but statistically significant increases in intracellular accumulation when P-gp was inhibited in the presence of TQR. Compounds **278** and **280** did not show significantly different intracellular accumulations in the absence or presence of TQR. Based on the activation of basal ATPase activities (data not shown) by **238**, **255** and **286** and supported by their cellular accumulation data, these three Group 2 variants of **29** are very likely to be transport substrates of P-gp. Compound **280,** based on its activation of basal ATP hydrolysis, may also be a transport substrate of P-gp, but is not likely to be a good substrate. Group 2 compound **278** is very unlikely to be a transport substrate of P-gp, since it neither activates basal ATPase (data not shown) nor did it show significantly increased cellular accumulation in the presence of tariquidar (**Figure 4.8**, **278**).

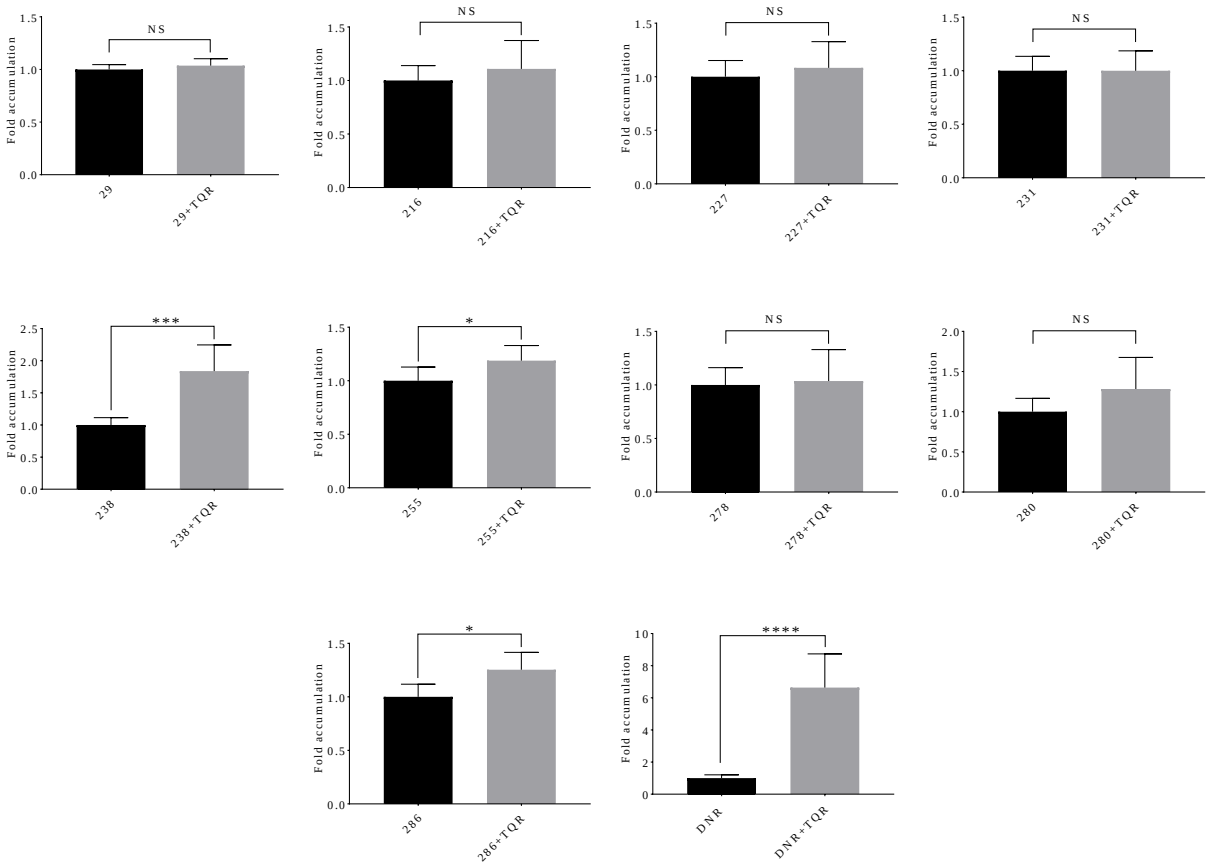

Figure 4.8 - **Cellular accumulation of 29 variants in the presence of absence of P-gp inhibitor tariquidar.**

Quantitative LC-MS/MS analysis as in of intracellular accumulation of compounds in the absence or presence of the potent P-gp inhibitor, tariquidar, in the P-gp overexpressing prostate cancer cell line, DU145 TXR. P-gp substrate daunorubicin was use as the positive control. For each compound data is normalized to accumulation of compound in the absence of tariquidar. Each histogram represents the average ± S.D. (n = 6, two independent experiments); *P < 0.05; ***P < 0.001; ****P < 0.0001; NS – not significant). DNR, daunorubicin; TQR, tariquidar.

Table 4.3 - **The intracellular accumulation of 29 variants.**
Quantitative LC-MS/MS analysis results of intracellular accumulation of compounds in the absence or presence of the potent P-gp inhibitor, tariquidar, in the P-gp overexpressing prostate cancer cell line, DU145 TXR. P-gp substrate daunorubicin (DNR) was use as the positive control. Data represents the average ± S.D. (n = 6, two independent experiments);

Compound	Average intracellular accumulation (ng/mL)	Average intracellular accumulation in presence of tariquidar (ng/mL)
29	29.83 ±13.84	30.60 ±12.81
216	1924.34 ±308.60	2101.66 ±365.00
227	1396.80 ±436.03	1492.98 ±526.57
231	2147.30 ±293.10	2150.02 ±420.12
238	244.67 ±31.60	454.38 ±125.31
255	264.45 ±67.90	320.60 ±105.64
278	833.72 ±173.42	863.10 ±244.26
280	2423.68 ±1034.07	2892.17 ±631.30
286	234.01 ±27.80	293.23 ±37.41
DNR	1312.70 ±346.36	7224.66 ±1960.72

4.2.6 Effects of Group 1 and Group 2 variants on the paclitaxel sensitivity of drug sensitive prostate cancer cells, DU145TXR and non-cancerous HFL-1 cells.

While **29**-variants showed reversal of paclitaxel resistance in cell viability assays in the P-gp overexpressing DU145TXR [172] cancer cells, similarly the effect on non P-pg overexpressing cells was evaluated using non P-gp overexpressing prostate cancer line, DU145 [194] and non-cancerous human lung fibroblast cells, HFL-1[173]. The toxicity of the chemotherapeutic, paclitaxel, was not increased in the presence of **29** or **29**-variants in cells that do not overexpress P-gp (**Figure 4.9**). These results indicate that increased lethality of paclitaxel

to the P-gp overexpressing cells was due to the inhibition of the pump and increased accumulation of paclitaxel to therapeutic levels within the cells.

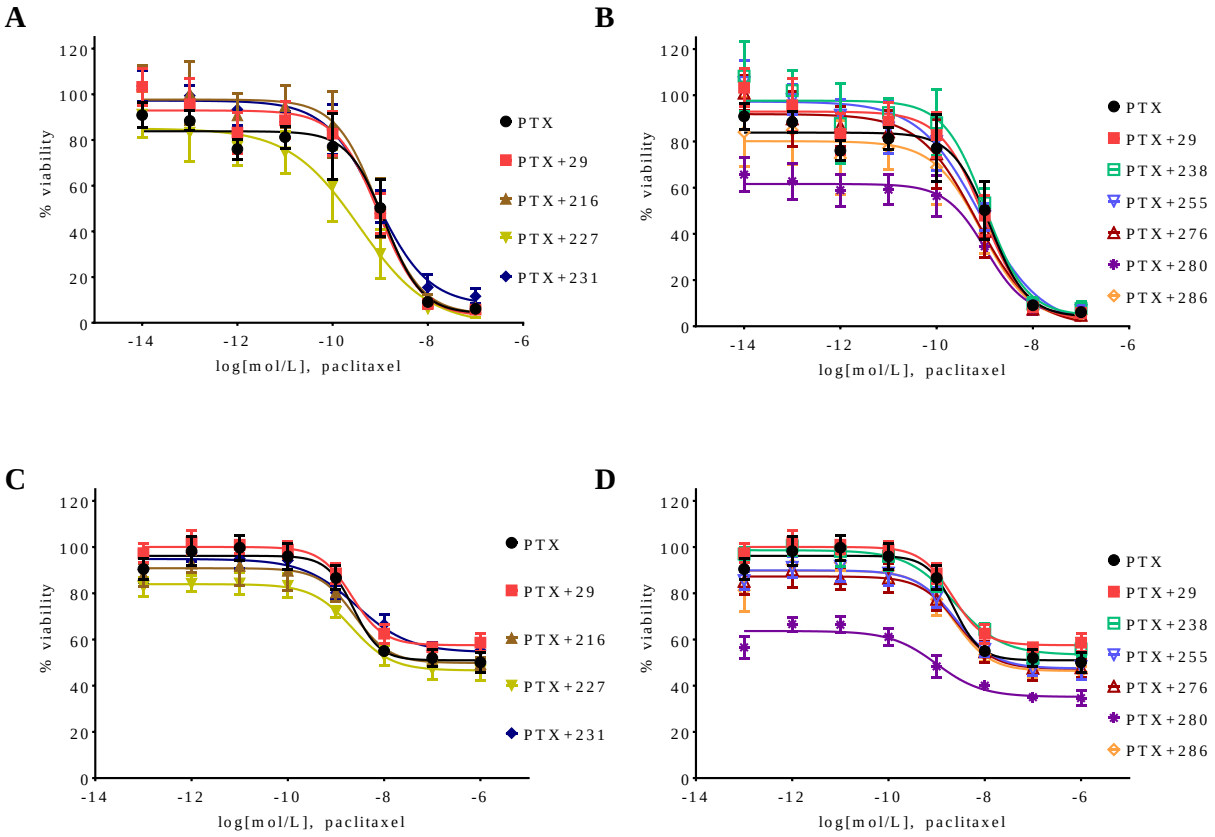

Figure 4.9 - **Variants from both Groups do not increase the paclitaxel toxicity in cells with no overexpression of P-gp.**
The prostate cancer cell line, DU145 with no overexpression of P-glycoprotein was treated with either paclitaxel (PTX) or paclitaxel and 10 μM of the P-gp inhibitors Group 1 (panel A) or Group 2 (panel B). Metabolic activity assays using MTT were performed as described in Methods.

4.3 Materials and methods

4.3.1 Cell lines and cell culture

The chemotherapeutic sensitive DU145 human prostate cancer cells [194] as well as the multidrug resistant sub-line, DU145TXR [172] were generous gifts from Dr. Evan Keller (University of Michigan, Ann Arbor, MI). The multidrug resistant DU145TXR was maintained under positive selection pressure by supplementing complete medium with 10 nM paclitaxel

(Acros Organics, NJ). Both cell lines were maintained in complete media consisting of RPMI-1640 with L-glutamine, 10% fetal bovine serum (FBS; BioWest, Logan, UT), 100 U/mL penicillin and 100 μg/mL streptomycin in a humidified incubator at 37°C and 5% CO_2. The noncancerous human fetal lung cell line, HFL1[173] was kindly provided by Dr. Robert Harrod (Southern Methodist University, Dallas, TX) and maintained in complete media consisting of F-12K with L-glutamine, 10% FBS (BioWest, Logan, UT), 100 U/mL penicillin, and 100 μg/mL streptomycin in a humidified incubator at 37°C and 5% CO_2. To promote attachment of HFL1 cells, growth surfaces were treated with 0.1 mg/mL rat tail collagen (BD Biosciences, Palo Alto, CA) in 0.02 N acetic acid for 10 min and rinsed with PBS prior to use. Cell culture materials were purchased from Corning Inc. (Corning, NY) unless otherwise stated.

4.3.2 Synthesis of 29 variants

All of the **29** variants were synthesized by Ms. Maha Aljowni in the laboratory of Dr. Alex Lippert, in the Chemistry Department at SMU (Wise *et al.* unpublished).

4.3.3 MTT cell viability assay

Cells were trypsinized from monolayers and seeded with 3000 cells in 150 μL of complete medium in a 96 well plate. After 24 hours, cells were treated for 48 hours with paclitaxel (Acros Organics, NJ) and / or P-gp inhibitory compounds dissolved in DMSO, or DMSO controls. All additions were diluted into complete medium. After 48 hours of treatment, MTT assays were performed as described [193] using 5 mg/mL of MTT (Acros Organics, NJ) solution prepared in PBS (137 mM NaCl, 2.7 mM KCl, 10 mM Na_2HPO_4, 1.8 mM KH_2PO_4, pH 7.4). After 4 hours of incubation with MTT, the media was removed and the formazan crystals were dissolved in 100 μL of DMSO. The absorbance at 570 nm was then measured using a BioTek Cytation 5 imaging multi-mode reader (Bio-Tek, Winooski, VT). Percent viability was calculated using

DMSO treated cells as representative for 100% viability. Background absorbance was determined using MTT and complete medium without cells and subtracted from all the test values.

$$\% \text{ Viability} = \frac{\text{Absorbance at 570 nm of test well}}{\text{Absorbance at 570 nm of DMSO treated cells}}$$

The results were plotted as the mean with standard deviation (SD) of eight replicates per concentration from at least two independent experiments. The graphical representations and IC_{50} values were determined using four parameter variable slope non-linear regression, using the following equation: Y=bottom+(top-bottom)/(1+10^((logIC50-X)*Hill Slope) (GraphPad Prism™, La Jolla California, USA, Version 6.05). The reported "fold sensitization" was calculated as follows.

$$\text{Fold sensitization} = \frac{IC_{50} \text{ value of A2780ADR cells treated with chemotherapeutic only}}{IC_{50} \text{ value of A2780ADR or A2780 cells treated with chemotherapeutic and P-gp inhibitory compound}}$$

4.3.4 Calcein AM assay

To assess inhibition of P-gp-catalyzed transport of the P-gp pump substrate, calcein AM, DU145TXR cells were seeded in 96 wells plates and allowed to grow in complete medium until reach confluency. Medium was removed, and cells were treated without 2 μM P-gp inhibitory compounds and 1 μg/mL calcein AM (Life Technologies, OR) and diluted into phenol red free RPMI 1640 media. To study the effect of pre-incubation of compounds cells were treated with just P-gp inhibitory compounds and incubated in 37 °C for six hours before adding calcein AM. Fluorescence excitation at 485 nm with a 20 nm gate and at emission at 535 nm with a 20 nm gate was measured using a BioTek Cytation 5 imaging multi-mode reader (Bio-Tek, Winooski,

VT) over 60 minutes in 20 minute intervals. DMSO was used as vehicle. Results were plotted as the mean with standard deviation (SD) of six replicates per concentration and are representative of at least two independent experiments.

4.3.5 Cellular Accumulation Assays for Experimental P-gp Inhibitors

Cells used (DU145TXR), cell culturing, cell exposure to compounds, cellular handling and extractions were performed as described in [235]. LC-MS/MS methods were performed as described in [201] and as modified in [235].

4.4 Discussion

Compound **29** is a P-gp inhibitor which is not a P-gp substrate [235]. According to Brewer *et al*. there is evidence that inhibitor **29** acts as an allosteric inhibitor of P-glycoprotein [164]. Inhibitor **29** reduces the verapamil stimulated activity of P-gp in proteins assays and it shows the properties of a P-gp inhibitor in *in vitro* cellular assays as well [164], [235]. Nevertheless, it does not affect the ATP binding of P-gp according to electron resonance spectroscopy (ESR) experiments described in [164]. Based on these observations, it was suggested that P-gp inhibitor **29** may be an allosteric inhibitor and this was a main reason why **29** was selected for further development. Our focus was to identify P-gp inhibitors which are not P-gp pump substrates as pump substrates such as verapamil had limited or no success in clinical trials as they were required in high systemic concentrations leading to toxicity [11].

Here we discuss the *in vitro* results of eight variants after lead optimization of original inhibitor **29**. These variants were assigned into two different groups based on how they were derived. The compounds of Group 1 (**216**, **227** and **231**) were generated by ChemGen software, an in-lab production that can generate variants of a given molecule within the controlled parameters such as molecular weight. The resulting **29** variants from ChemGen were submitted

to *in silico* docking and variants that showed higher affinities to NBDs, and low estimated affinity for the DBD of P-gp than did the parental **29** were synthesized by our collaborators from SMU Chemistry (Lippert and Aljowni) (**216**, **227** and **231**). Variants of Group 2 (**238**, **255**, **278**, **280** and **286**) were synthesized by a conventional "rational design" methods, by visualizing the binding poses in complex with P-gp and varying shape, size and physicochemical properties of the original inhibitor **29** following conventional lead optimization methods. All these compounds were chosen for relative ease of synthesis as well as availability and expense of precursors.

All these variants (both Group 1 and 2) reversed MDR in the P-gp overexpressing prostate cell line. According to the calculated IC_{50} values from viability assays, **227** and **231** from Group 1 exhibited nearly 5 and 10 fold improvement respectively in reversing MDR at 10 μM compared to the parental **29** P-gp inhibitor. This correlated with the predicted improved affinities of these variants in computational studies performed by John Wise (computational data is not shown).

In calcein accumulation assays it appeared that Group 2 variants performed better than the Group 1 variants of **29**. We hypothesized that Group 1 compounds were more hydrophobic than 29 which may be delaying the interaction with P-gp by remaining in plasma membrane for a more extended time. The improved efficacy of Group 1 inhibitors in accumulating calcein after 6 hour incubation with inhibitors than without any incubation provided some support for this hypothesis. In addition, **238** from Group 2 exhibited nearly 300 fold improvement of MDR resensitization when compared with parental **29** at 10 μM concentration. However, our strategy in this project was to identify P-gp inhibitors that are not P-gp transport substrates since P-gp substrates have failed in clinical trial settings to reverse MDR [11]. When cellular accumulation

of the inhibitors was assessed in the presence or absence of a strong P-gp inhibitor, tariquidar, the results suggested that all inhibitors in Group 1 were not transport substrates while four out of five of the Group 2 inhibitors likely are transported by the pump. The data suggest that all Group 1 compounds and only 278 from Group 2 seemed to reverse the MDR of the cancer cells by being true enzymological inhibitors of P-gp. P-gp is known to have the ability to transport molecules with very different shapes and properties [7], [53], [268]. This study shows how only subtle differences in very similar molecules can be differentiated by P-gp, making some transport substrates, while others act as real inhibitors of transport by P-gp.

Over all this study produced four more P-gp inhibitors (**216**, **227**, **231** and **278**) that reversed MDR in *in vitro*. These four inhibitors are variants of the original P-gp inhibitor **29** and showed higher efficacy in reversing MDR in P-gp overexpressing prostate cancer cell lines compared to inhibitor **29**. Further experiments are required to evaluate their effectiveness in *in vivo*. Their stability under *in vivo* conditions is especially important as one of the inhibitors (**227**) was found not be stable and was quickly degraded in mouse liver homogenate (data not shown). Analyzing the degraded products of these compounds submitted to *in vivo* conditions will predict the unstable positions of molecules and those position should be modified to increase the stability and but also retaining P-gp inhibitory action of the compound.

This study has clearly shown the effectiveness of computational lead optimization in drug discovery as all three variants from Group 1 reversed MDR without being substrates for P-gp. A computational based method will be much more advantageous in procedures like screening for P-gp inhibitors which are non substrates as proteins like P-gp are evolutionarily adapted to pump various molecules. This approach may reduce the number of compounds

needed to be tested in the laboratory in *in vitro* or *in vivo* conditions saving overall cost and time in identifying drugs. In future the similar approach we used to lead optimize the P-gp inhibitor **29** can be used to optimize the other P-gp inhibitors (**34** and **45**) we have discovered in previous studies [164], [165], [235].

CHAPTER 5: REVERSAL OF BREAST CANCER RESISTANCE PROTEIN-MEDIATED MULTIDRUG RESISTANCE WITH NOVEL COMPOUNDS IN MULTIDRUG RESISTANT BREAST CANCER CELLS

5.1 Introduction

Breast cancer resistance protein (BCRP) is an efflux transporter which belongs to the same ATP-binding cassette (ABC) protein super family as P-glycoprotein [4], [5], [107], [233]. ABC family transporters including BCRP can transport xenobiotics out of the cells thus play a major physiological role in human biological barriers such as blood brain barrier (BBB) [269]–[271] and the placenta [272]–[274]. Overexpression of BCRP in cell culture models has resulted in MDR cell lines [191], [275]. BCRP overexpression has also been correlated with poor prognoses of hematopoietic malignancies and solid tumors, since BCRP can transport a variety of chemotherapeutic classes such as topoisomerase inhibitors, anthracyclines and tyrosine kinase inhibitors [107].

Other than its implication in MDR cancers, BCRP plays a key role in preventing drug penetration through BBB [269], [270], [276]. ABC transporters including BCRP limit the drug entrance to brain thus, in the case of central nervous system (CNS) diseases, preventing the drug from reaching the target. Other than some chemotherapeutics which are used for treating brain tumors [276], several drugs that are used for epilepsy [277] and HIV [278] are also known to be BCRP substrates. Simultaneous inhibition of BCRP and P-gp has been evaluated for increasing the efficacy of therapeutics that target the brain tumors [147], [279]. Furthermore, the use of

BCRP inhibitors has exhibited incremental increases in oral availability of anti-cancer drugs aswell. However, BCRP inhibitors have shown no clinical successes in the few human trials concluded so far [159], although several have proven to be successful in *in vitro* [280] and *in vivo* [151] studies.

In this study, we have screened for BCRP inhibitors from a group of small molecules available in the lab. These molecules were selected and obtained from computational high-throughput screenings of millions of drug-like molecules freely available in online databases [170], [171] by docking studies using homology models of P-gp and/or BCRP. As BCRP and P-gp both belong to the ABC protein super family and P-gp and BCRP inhibitors are known to cross-react with other ABC transporters, we predicted that identifying BCRP inhibitors in a pool of molecules that was originally targeted for P-gp may well be possible. Here we identify and characterize several BCRP modulators and one BCRP inhibitor that have the capability of increasing the accumulation of BCRP substrates and of reversing BCRP mediated MDR in a BCRP overexpressing breast cancer cell line. Furthermore, these inhibitors are shown to increase the intracellular accumulation common substrates of BCRP and P-gp in a human blood brain barrier cell line demonstrating the potentiality of the inhibitors to open the BBB.

5.2 Results

5.2.1 Continuous growth of drug-sensitive MCF-7 cells in mitoxantrone resulted in a BCRP-overexpressing and mitoxantrone-resistant derivative cell line

A mitoxantrone-resistant, BCRP over-expressing breast cancer cell line (MCF-7 M100) was established from a mitoxantrone-sensitive parental cell line (MCF-7) [190] by passaging on media containing increasing concentrations of mitoxantrone essentially as previously described [191][275] (see Methods for details). Initially, the drug sensitive MCF-7 breast cancer cells were cultured in media containing 2 nM of mitoxantrone. Gradually the concentration of mitoxantrone was increased in between passages. After 60 passages, the resultant cells remained viable in up to 100 nM of mitoxantrone in the medium. The tolerability of mitoxantrone by these breast cancer cells was qualitatively evaluated by observing the morphological characteristics and cell doubling time. The overexpression of the BCRP protein in these cells was confirmed by Western blot analysis (**Figure 5.1**, Panel A). According to the Western blot analysis, parental MCF-7 did not express detectable amounts of BCRP, while an intense band corresponding to the size of BCRP (72 Kda) was observed in MCF-7 M100 cell lysate.

These MCF-7 M100 cells also showed reduced viability when they were treated with mitoxantrone in the presence of Ko143, a known inhibitor of BCRP [151], as compared to mitoxantrone treatment alone (**Figure 5.6**, right most histogram). Further, these cells exhibited a higher intracellular accumulation of the BCRP substrate, Hoechst 33342 [88], [281], after treating with Ko143. The P-gp modulator, verapamil [282], in similar experiments did not show any effects on the intracellular accumulation of Hoechst 33342 in these cells (**Figure 5.1**, Panel B). These results strongly suggest that over-expression of BCRP was responsible for the

mitoxantrone resistance observed in the MCF-7 M100 cell line and that over-expression of P-gp did not play a role in their MDR phenotype.

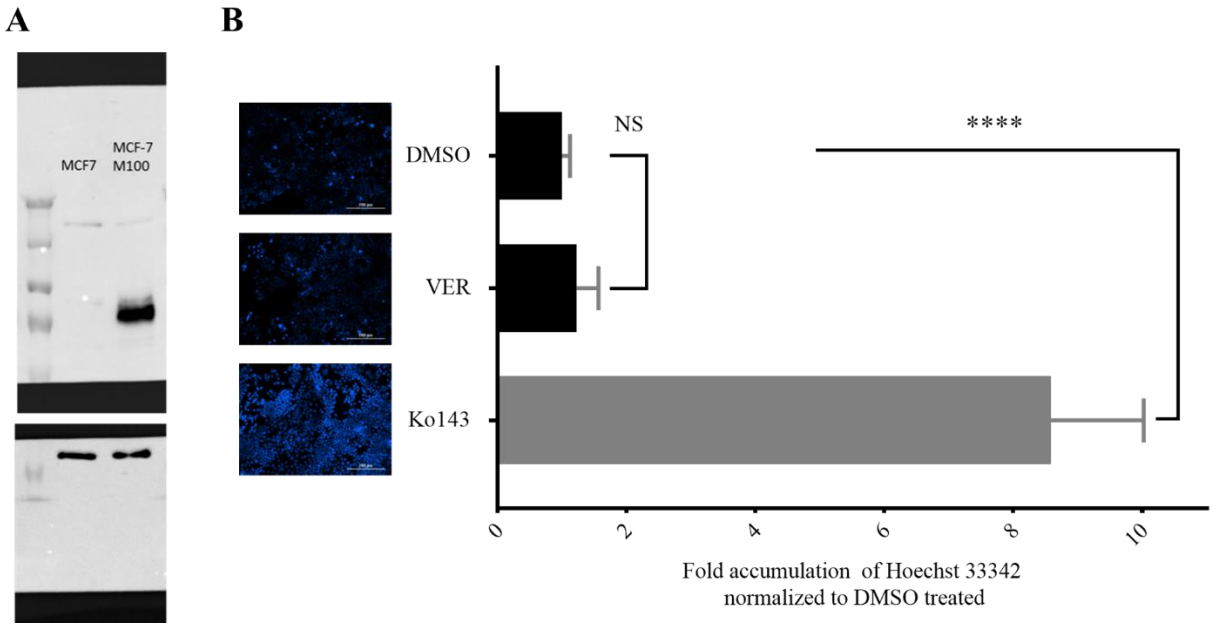

Figure 5.1- **MCF-7 M100 cells are mitoxantrone resistant due to overexpression of BCRP**
A - Western blot analysis of protein expression in cell lysates from breast cancer cell lines MCF-7 (drug sensitive) and MCF-7 M100 (multidrug resistant) performed as described in methods. Top: Western blot analysis of MCF-7 and MCF-7 M100 was performed using anti BCRP antibody B1 (from Santa Cruz Biotechnology, CA). Bottom: The lower half of the same gel was probed with β-actin monoclonal antibody C4 (from Santa Cruz Biotechnology, CA). Lane 1 (from left)- Spectra™ Multicolor Broad Range Protein Ladder (catalog # 26623), Visible bands from top to bottom in the two panels represent 260, 140, 100, 70, 50, 40, 35 kDa, respectively. Lane 2 - total cell extract from cell line MCF-7 (drug sensitive breast cancer cell line), 5 µg. Lane 3 - total cell extract from cell line MCF-7 M100 (multidrug resistant breast cancer cell line), 5 µg.
B – Qualitative and quantitative BCRP transport activity in MCF-7 M100 cells were analyzed using the BCRP substrate, Hoechst 33342, as described in Methods. Approximately 9 fold increase in intracellular Hoechst accumulation (Panel B, right) was observed in MCF-7 M100 cells treated with 1 µM of BCRP inhibitor Ko143 resulting a higher fluorescence (Panel B, left) compared to vehicle (DMSO) treated cells as imaged with a DAPI channel. P-gp modulator verapamil (VER, 10 µM) had no influence in these cells. Each histogram presents the average ± S.D. of the determinations (n>8, Replicates from two individual experiments; **** $P < 0.0001$; NS - not significant).

5.2.2 Compounds 50, 53, 70, 71, 83, 103, and 117 induced higher intracellular accumulation of the BCRP substrate, Hoechst 33342, in BCRP overexpressing MCF-7 M100 breast cancer cells

An assay utilizing the fluorescent dye, Hoechst 33342 (see Methods), which is a good transport substrate of BCRP, was used here to potentially identify small drug-like compounds that inhibit BCRP function. Hoechst 33342 is a cell membrane permeable, nuclear stain that becomes fluorescent upon binding to DNA [283], [284]. The dye can be efficiently effluxed by BCRP as a substrate [285], [286]. Inhibitors of BCRP can interfere with the BCRP-catalyzed efflux of Hoechst 33342 which results in a higher intracellular accumulation of the dye relative to controls without BCRP inhibitors. Differences in fluorescence intensities can then be quantitatively measured and compared to give indications of BCRP-specific inhibition [281].

A collection of small drug-like compounds available in the laboratory (numbered from **11** to **124** including several variants of compound **29** described above) were screened here to identify whether any of these compounds might inhibit BCRP. Each member of the compound library was acquired or synthesized for testing as a potential ABC transporter inhibitor in related studies on P-glycoprotein. Each of these compounds was assayed for intracellular Hoechst 33342 accumulation in the BCRP-overexpressing cell line MCF7 M100 to recognize possible BCRP inhibitors. The results of these assays are presented in **Figure 5.2**, Figure 5.3 and Figure 5.4. Compounds **50**, **53**, **70**, **71**, **83**, **103**, and **117** (shown in the contrasting gray histograms in **Figure 5.2, Figure 5.3** and Figure 5.4) exhibited the highest BCRP modulation activities resulting in an approximately 4-fold fluorescence intensity increase compared to vehicle treated cells. These eight compounds were selected to further analyze their ability reverse the chemotherapeutic resistance in BCRP overexpressing cells.

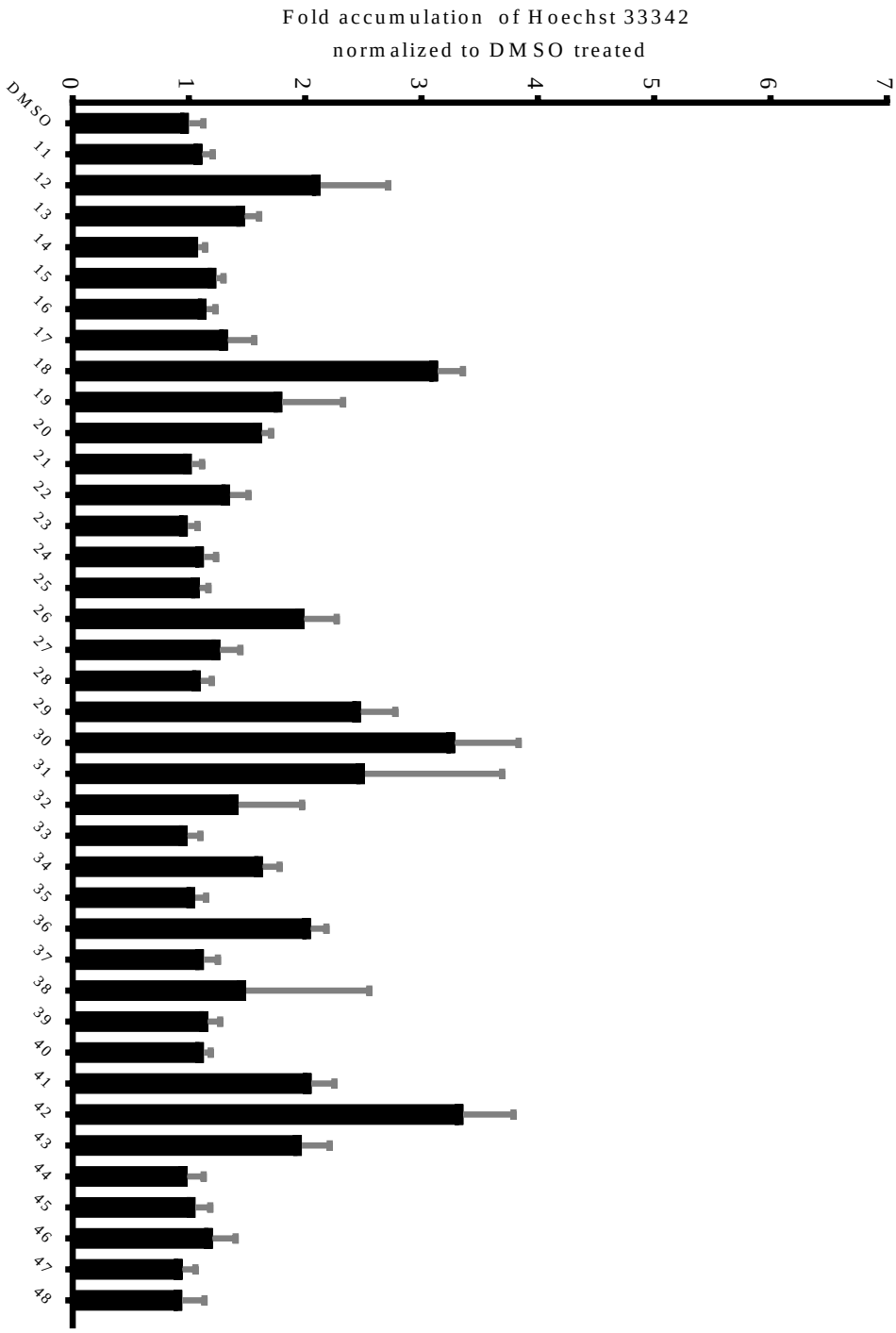

Figure 5.2 - **Hoechst 33342 accumulation by compounds 11-48 in MCF-7 M100 cells**
Fold accumulation of Hoechst 33342 in MCF-7 M100 cells treated with compounds 11 – 48. Data are represented as mean ± s.d., n>6.

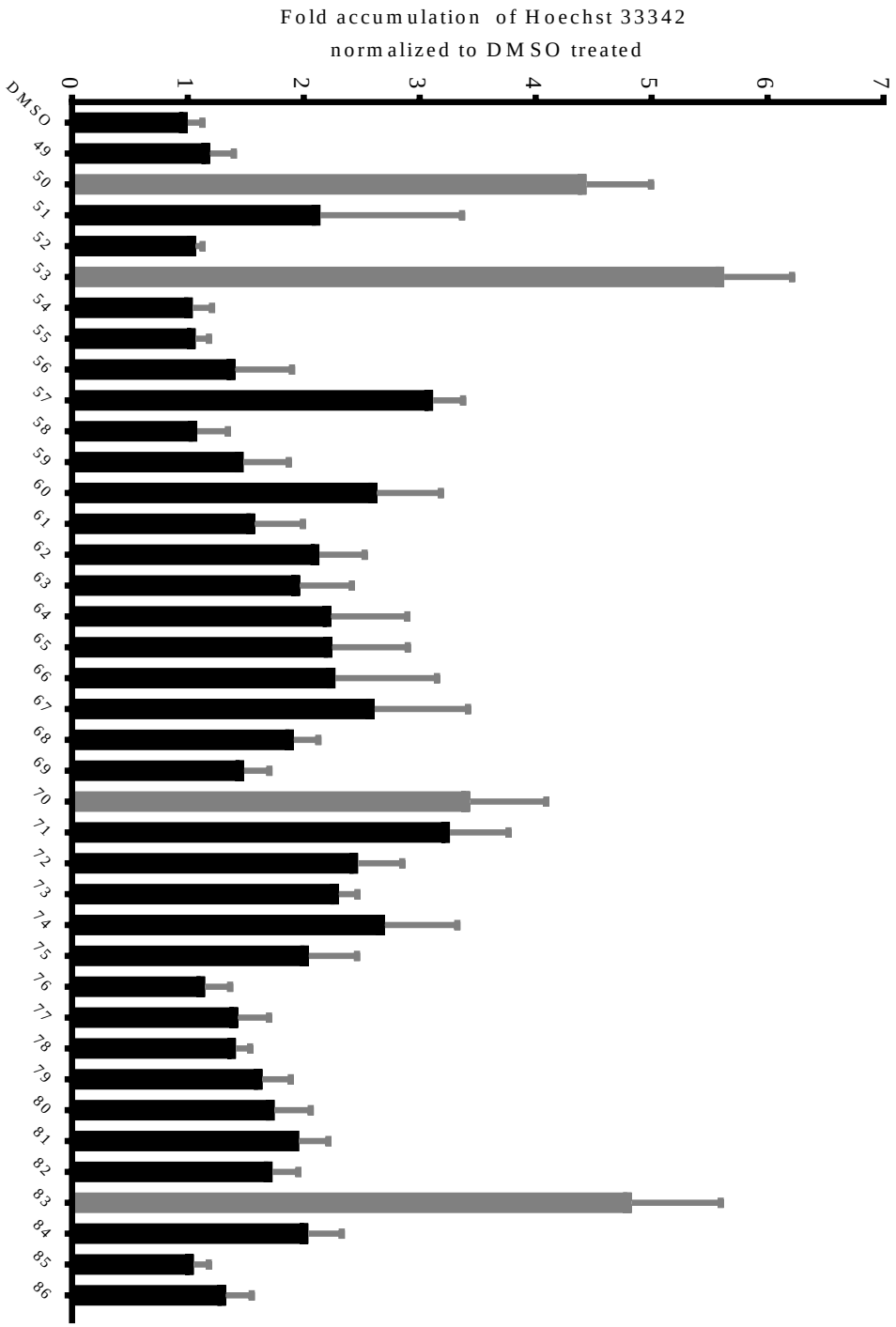

Figure 5.3 **- Hoechst 33342 accumulation by compounds 49-86 in MCF-7 M100 cells**
Fold accumulation of Hoechst 33342 in MCF-7 M100 cells treated with compounds 49-86. Selected BCRP modulators for further studies are indicated in grey bars. Data are represented as mean ± s.d., n>6

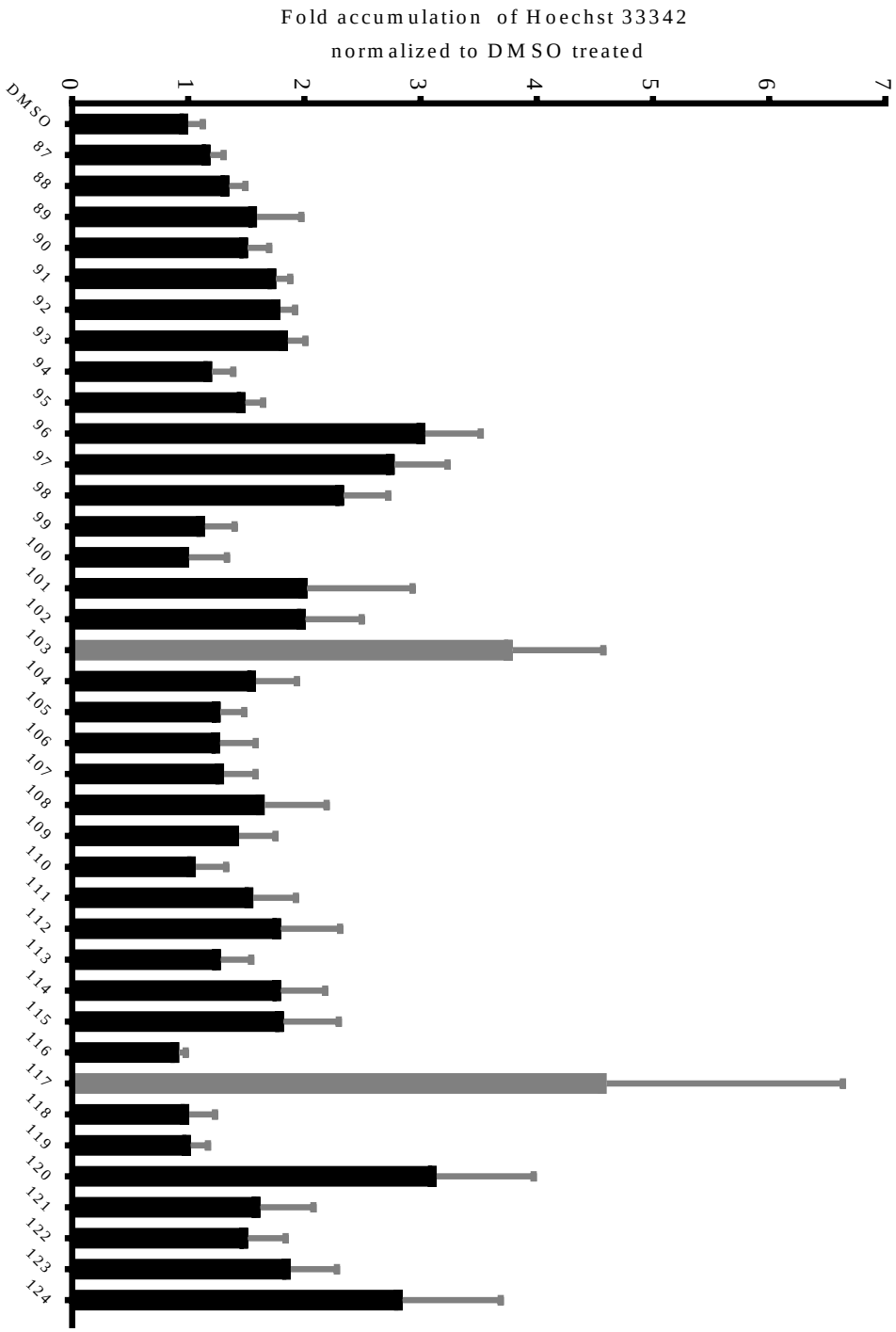

Figure 5.4 **- Hoechst 33342 accumulation by compounds 87-124 in MCF-7 M100 cells**
Fold accumulation of Hoechst 33342 in MCF-7 M100 cells treated with compounds 87-124. Selected BCRP modulators for further studies are indicated in grey bars. Data are represented as mean ± s.d., n>6.

Interestingly, several variants of compound **29**, compounds **231**, **238**, **255** and **286**, which are currently in optimization studies for P-gp inhibition, exhibited the highest BCRP modulation activities of approximately 4-fold fluorescence increases compared to vehicle treated cells (**Figure 5.5**). Variants **231**, **238** and **255** were selected to further analyze their ability reverse the multidrug resistance in BCRP overexpressing cells. Compound **286** exhibited a higher toxicity in a previous study and was therefore not included in the BCRP studies.

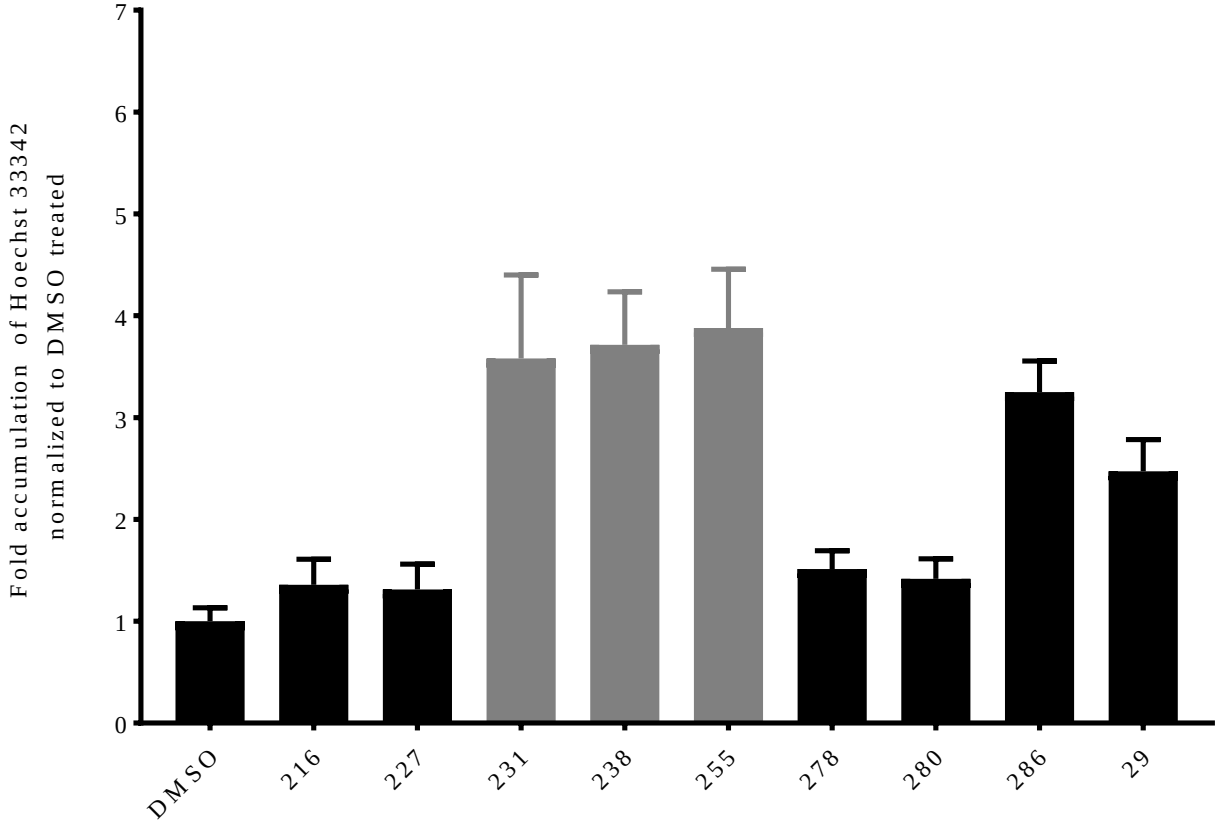

Figure 5.5 **- Hoechst 33342 accumulation by 29 derivatives in MCF-7 M100 cells**
Fold accumulation of Hoechst 33342 in MCF-7 M100 cells treated with 29 derivatives. Selected BCRP modulators for further studies are indicated in grey bars. Data are represented as mean ± s.d., n = 12.

5.2.3 Compounds 50, 71 and 117 reversed the mitoxantrone resistance and showed the least toxicity to the BCRP overexpressing breast cancer cells

Compounds **50**, **53**, **70**, **71**, **83**, **103**, and **117** which were the most promising candidates for BCRP-inhibitors identified in the Hoechst 33342 screening were analyzed for their ability to reverse drug resistance in the MCF-7 M100 cells by interfering with BCRP activity. In these experiments, cells were treated with 10 µM of compounds **50**, **53**, **70**, **71**, **83**, **103**, and **117** individually with or without 200 nM of mitoxantrone and observed with MTT viability assays (Methods) to study both the toxicity of the compounds towards cancer cells and to evaluate their potential to reverse mitoxantrone resistance. Compounds **53**, **70**, **83** and **103** reduced the viability of cancer cells significantly by themselves (no added chemotherapeutic) (**Figure 5.6**), indicating relatively high toxicity towards the MCF-7 M100 cells. In contrast, compounds **50**, **71** and **117** did not show substantial cytotoxicity. Most importantly their combined treatment with mitoxantrone resulted a decreased viability in cells increasing the mitoxantrone toxicity (**Figure 5.6**). Compounds **50**, **71** and **117** therefore assumed to be potential BCRP inhibitors which reverse the BCRP mediated MDR. These three compounds need to be studied further in different BCRP overexpressing cell lines and also need to be confirmed as non BCRP substrates.

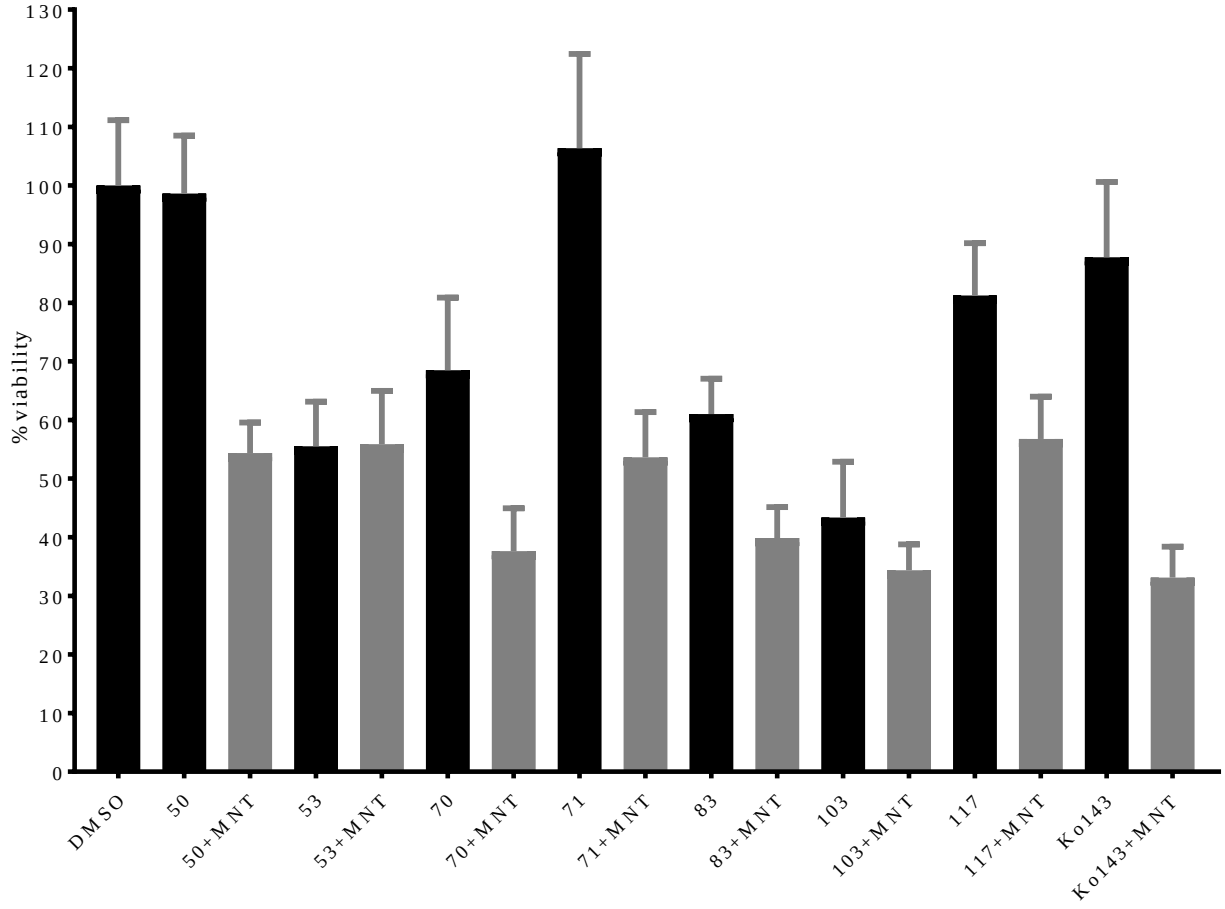

Figure 5.6 - **Reversal of mitoxantrone resistance by predicted BCRP inhibitors**
MCF-7 M100 cells were treated with 200 nM of the chemotherapeutic mitoxantrone (MNT) and either compound **50**, **53**, **70**, **71**, **83**, **103**, or **117** at 10 µM, Ko143 at 1 µM, as indicated in the figure. After 72 hours viability was measured using MTT assay as described in methods. Each histogram presents the average ± S.D. of the determinations (n=8, Replicates from two individual experiments)

5.2.4 29 variants 231, 238 and 255 reversed the MDR phenotype in BCRP overexpressing breast cancer cells

The Hoechst accumulation assay results reported in **Figure 5.5** identified three derivatives of **29** that appeared to be good candidates as BCRP inhibitors. These compounds, **231**, **238** or **255**, were tested in MTT viability assays (Methods) for the ability to reverse multidrug resistances in the MCF-7 M100 cell line. Various concentrations of three different chemotherapeutics (mitoxantrone, topotecan and SN-38), all of which are BCRP substrates, were

tested individually with 10 µM of **231**, **238** or **255** to quantitate their ability to reverse MDR in the BCRP-overexpressing cell line. We observed that all three putative inhibitors reversed the chemotherapeutic resistance to very similar levels in the BCRP overexpressing MCF-7 M100 cells (**Figure 5.7**). The highest efficacy of these inhibitors was exhibited against mitoxantrone (**Figure 5.7,** Panel A) compared to topotecan and SN-38. It should be noted that these cells have shown 100% viability with complete resistance towards ~100 nM of all three of the chemotherapeutics (without inhibitors) used in these viability assays (**Figure 5.7**). We observed that the viabilities dropped to about 50% when the chemotherapeutics (at 100 nM concentration) were combined with the potential BCRP inhibitors at 10 µM. These cells remained viable (~ 50% viability) even at very high concentrations of chemotherapeutics such as 10 µM. But when combined with potential inhibitors, the viability has reduced to almost 0% completely reversing the resistance. Further, in experiments using the MCF-7 drug-sensitive parental cell line, the three putative BCRP inhibitors, 231, 238 and 255 had no effect in viability assays analogous to those performed with MCF-7 M100 cells (**Figure 5.7**, Panel D). These results strongly suggest that the reversal of the MDR phenotype by compounds 231, 238 and 255 was due to their interaction with BCRP.

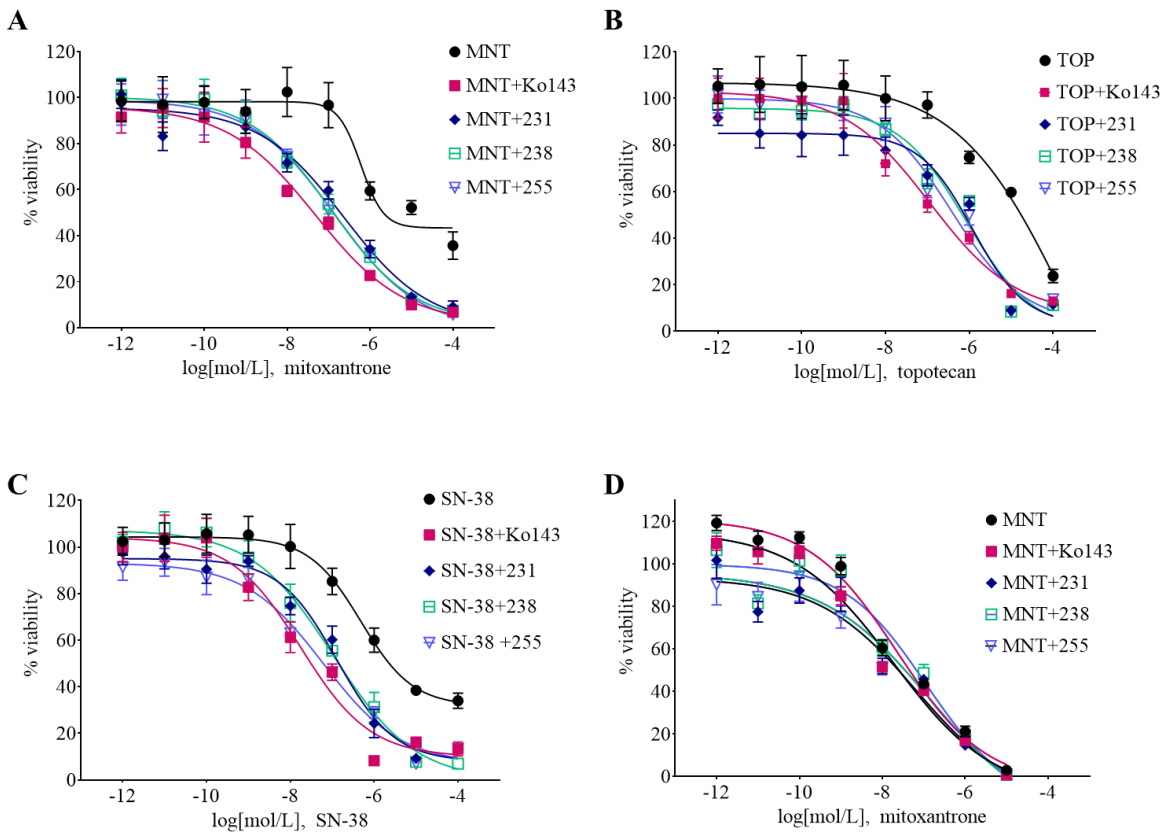

Figure 5.7 - **Compounds 231, 238 and 255 reverse the MDR in BCRP overexpressing breast cancer cells**
MCF-7 M100 (Panel **A**, **B** and **C**) cells were treated in the presence of compounds 231, 238, 255 at 10 µM or Ko143 at 1 µM with the indicated concentrations of chemotherapeutics. **A** – Mitoxantrone (MNT), **B** – Topotecan (TOP), **C** – SN-38. **D** - MCF-7 cells were treated in the presence of compounds 231, 238, 255 at 10 µM concentration or Ko143 at 1 µM with the mitoxantrone. Viability was determined by MTT assay after 72 hours. Experiments were duplicated and representative figures are shown. Data represents the mean ± SD and n=4.

5.2.5 Compound 231, 238 and 255 resulted higher intracellular accumulation of BCRP substrates in BCRP overexpressing breast cancer cells

To understand the kinetic properties of BCRP modulation by compounds **231**, **238** and **255**, the Hoechst 33342 assay (Methods) was utilized with or without a pre-incubation step with the putative inhibitors. The results presented in **Figure 5.8**, Panel A suggested that the effects of compound **238** and **255** in interfering with BCRP transporter activity as demonstrated by the increasing Hoechst 33342 intracellular fluorescence occurred at a rate that was about twice that

of observed for compound **231**(**Figure 5.8**, Panel A). Since all three inhibitors showed indistinguishable effects in the viability assays (**Figure 5.7**) that were performed over 72 hours, we hypothesized that the differences between the inhibitors may be due to their abilities to penetrate the cell membrane and to interact with BCRP. To test this hypothesis, we incubated the BCRP overexpressing MCF-7 M100 cells with potential inhibitors for 3 hours prior to addition of the Hoechst dye. After the 3 hour preincubation step, all three inhibitors produced significantly higher accumulations of Hoechst 33342 compared to vehicle controls, and the level of fluorescence intensity reached for each inhibitor was indistinguishable (**Figure 5.8**, Panel B) supporting the hypothesis. In additional experiments, we observed that the putative inhibition of BCRP for each of the compounds was concentration dependent, resulting in considerable amounts of Hoechst accumulation even at the low concentration of 2.5 μM of each putative inhibitor (**Figure 5.8**, Panel C).

In additional experiments, we correlated the reversal of MDR in MCF-7 M100 cells in viability assays (**Figure 5.7**) with higher intracellular accumulation of chemotherapeutics in the presence of the inhibitors compounds. Treatment with **231**, **238** and **255** increased the intracellular accumulation of mitoxantrone and daunorubicin marginally, but statistically significantly (**Figure 5.8**, Panel E and **Figure 5.9**). It is therefore seemed likely that the observed reversal of MDR in BCRP overexpressing cancer cells in these experiments was due to increased chemotherapeutic accumulation in the presence of the putative BCRP inhibitors.

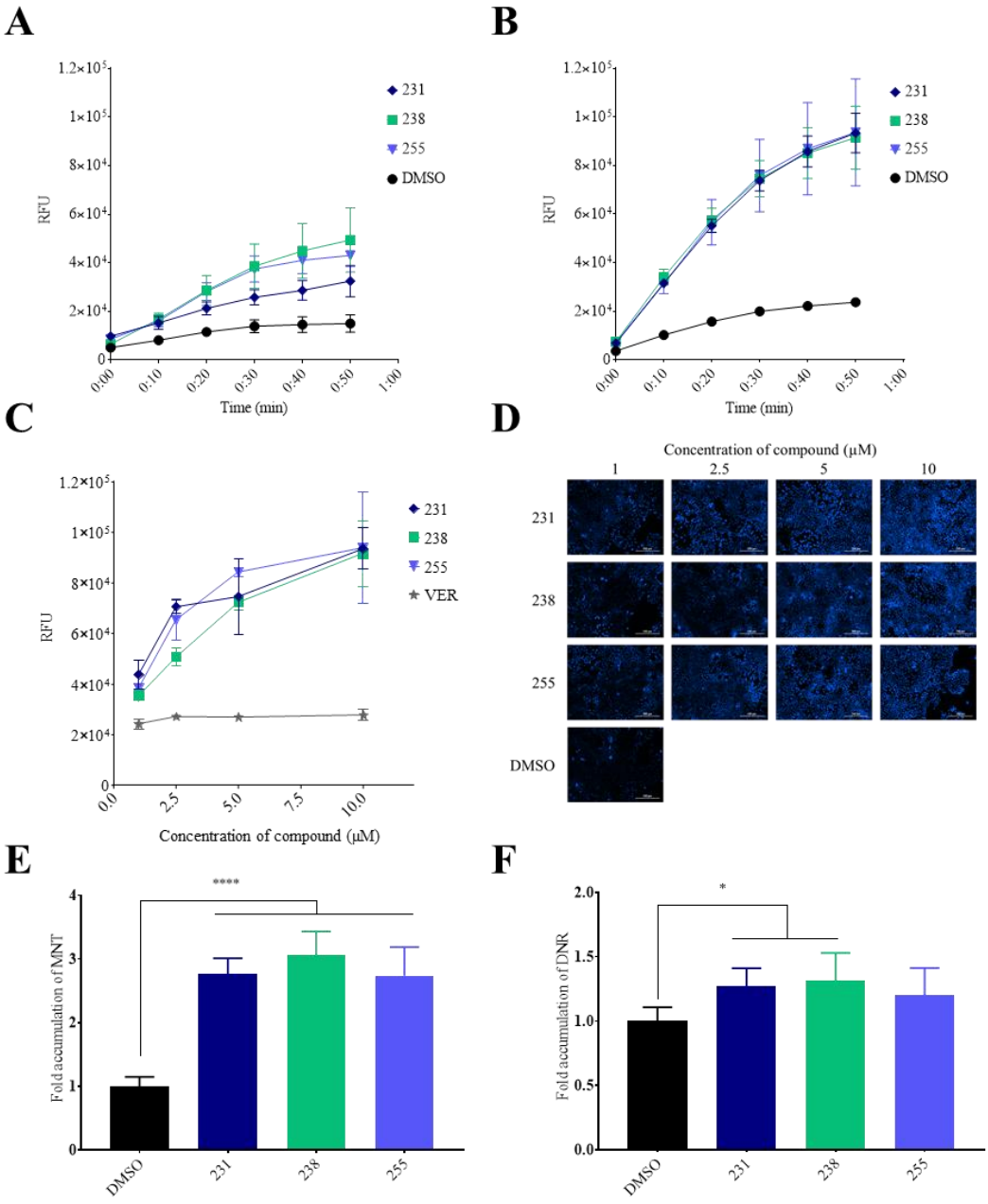

Figure 5.8 - **Compounds 231, 238 and 255 increased the accumulation of BCRP substrates in BCRP overexpressing breast cancer cells**

MCF-7 M100 cells were treated with Hoechst 33342 and without (Panel **A**) or after (Panel **B**) a 3-hr preincubation with 10 μM of the indicated predicted BCRP inhibitors. The effect of concentration of inhibitors was evaluated using a Hoechst assay (Panel **B**) and by measuring fluorescence (Panel **C**) and imaging with a DAPI channel (Panel **D**). Intracellular accumulation of chemotherapeutics, mitoxantrone (Panel **E**) and daunorubicin (Panel **F**) was measured after treating cells with compounds at 25 μM concentration and lysing the cells as described in Methods. Fold accumulation was calculated compared to vehicle (DMSO) treated wells. Experiments were at least duplicated, and representative figures are shown. Data are represented as mean ± s.d., n>6.

5.2.6 Compounds 231, 238 and 255 resulted in higher intracellular accumulation of BCRP and P-gp common transport substrates in immortalized human cerebral microvascular endothelial cells

The human cerebral microvascular endothelial cell line, hCMEC/D3 [287], an *in vitro* blood brain barrier model [288]–[290], was used to analyze the accumulation of transport substrates that are common to both BCRP and P-gp upon simultaneous inhibition of both transporters by compounds **231**, **238** or **255**. As described earlier, we showed that **231** is a P-gp inhibitor and **238** or **255** are P-gp substrates which reversed P-gp mediated MDR. Hence, we predicted that inhibition of both P-gp and BCRP would lead to a higher accumulation of P-gp and BCRP common substrates in the BCRP and P-gp expressing hCMEC/D3 cell line [291]. These results would demonstrate the potential of these new inhibitor compounds to open blood brain barrier for increasing drug penetration to the brain. In these experiments, we used Hoechst 33342 [292] and rhodamine 123 [287] which are both known to be transport substrates of BCRP and P-glycoprotein. After treating the hCMEC/D3 cells as described in Methods, we observed a significantly higher accumulation of rhodamine 123 in a concentration dependent manner compared to vehicle treated cells (**Figure 5.9**, Panel A). Compounds **238** and **255** exhibited a higher efficacy in facilitating accumulation of rhodamine compared to **231**. We also note that treatment of these cells with compounds **231**, **238** and **255** each marginally, but statically significantly increased the intracellular accumulation Hoechst 33342 (**Figure 5.9**, Panel B).

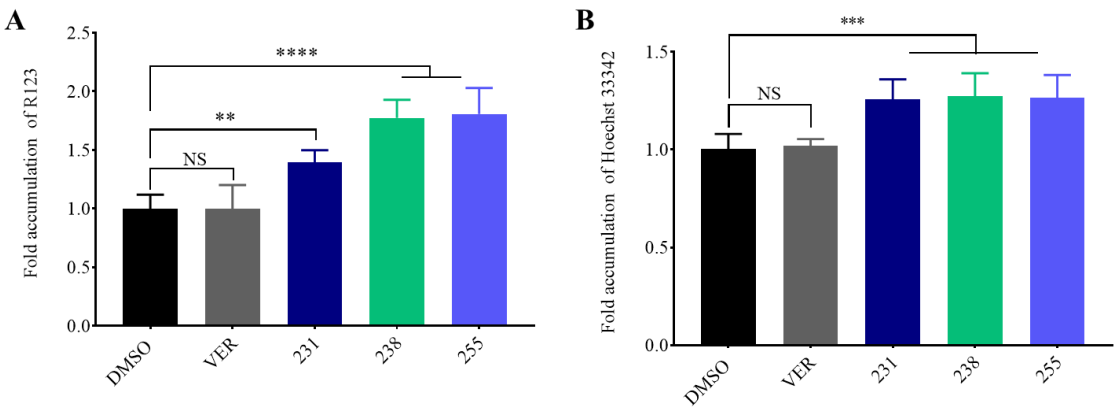

Figure 5.9 - **Compounds 231, 238 and 255 increased the accumulation of P-gp and BCRP common substrates in human cerebral microvascular endothelial cells**
Blood brain barrier model cell line – hCMEC/D3 cells were treated with compounds 231, 238 or 255 for 3 hours and were exposed to either rhodamine 123 (R123) or Hoechst 33342 as described in Methods. Fluorescence was measured as described in Methods and fold accumulation compared to vehicle (DMSO) were calculated and graphed for rhodamine 123 (Panel **A**) and Hoechst 33342 (Panel **B**). Data are represented as mean ± s.d., n=6. (** $P < 0.01$; *** $P < 0.001$; **** $P < 0.0001$; NS - not significant.)

5.2.7 Compound 231 is not a BCRP substrate while compounds 238 and 255 are BCRP substrates.

Cell accumulation assays for **231**, **238** and **255** variants were performed as in [235] (see Methods) to more directly assess whether the compounds were transport substrates for BCRP. These assays measured the intracellular accumulation of the experimental compounds using LC-MS/MS methods after incubation with the BCRP overexpressing cell line, MCF-7 M100, in the absence and presence of the strong BCRP inhibitor, Ko143 [151]. Low levels of cellular accumulation of a compound in the absence of Ko143 accompanied by much higher levels of accumulation in the presence of Ko143 strongly suggests that the compound in question may be a transport substrate of BCRP. Mitoxantrone is an example of a good transport substrate for BCRP and showed very strong cellular accumulation in these assays when BCRP was inhibited by Ko143, but much less accumulation in the cells when BCRP was not inhibited (**Figure 5.10**, Panel B). If a compound is not a substrate of BCRP, no significant difference in intracellular

accumulation of the compound with or without Ko143 would be expected. The results of the accumulation experiments (**Figure 5.10**, Panel A) strongly suggest that compound **231** does not function as a transport substrate for BCRP, i.e. no significant difference in cellular accumulation of compound **231** was observed with or without addition of Ko143. We can state with some assurance that **231** interfered with the transporter activity of BCRP in viability and BCRP substrate accumulation assays by inhibiting BCRP function and not by acting as a BCRP transport substrate. In contrast, compounds **238** and **255** displayed significant increases in their cellular accumulation upon BCRP inhibition by Ko143 (**Figure 5.10**, Panel B and C) indicating they are transport substrates of BCRP. It is likely that these two compounds interfered with BCRP transporter activity of other substrates like the Hoechst dye (**Figure 5.5**) by being a competitor for transport at the drug binding domain of BCRP.

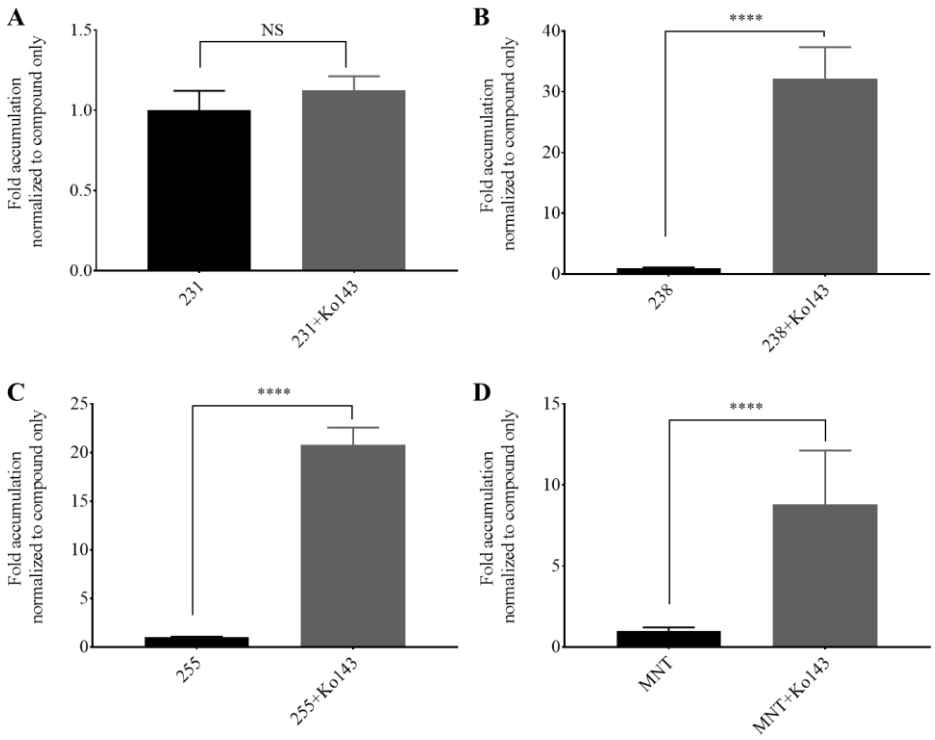

Figure 5.10 - **Compounds 231 is not a transporter substrate for BCRP while compounds 238 and 255 are transport substrates.**
Quantitative LC-MS/MS analysis of intracellular accumulation of 231 (panel **A**), 238 (panel **B**), 255 (panel **C**), or mitoxantrone, MNT (panel **D**) in MCF-7 M100 with or without BCRP inhibitor Ko143 as described in Methods. Each histogram represents the average ± S.D. (n=6 from two independent experiments); **** $P < 0.0001$; NS - not significant).

5.3 Materials and methods

5.3.1 Cell lines and cell culture

A drug sensitive MCF-7 breast cancer cell line (obtained from ATCC) [190] and the mitoxantrone resistant derivative of MCF-7 (MCF-7 M100) were maintained in complete media consisting of RPMI-1640 with L-glutamine, 10% fetal bovine serum (FBS; Corning, NY), 100 U/mL penicillin and 100 µg/mL streptomycin in a humidified incubator at 37 °C and 5% CO_2. The mitoxantrone-resistant line MCF-7 M100 was maintained under positive selection pressure by supplementing complete medium with 100 nM mitoxantrone (Santa Cruz Biotechnology, CA). Immortalized human cerebral microvascular endothelial cell line - hCMEC/D3 [287] was a generous gift from Dr. Ashlee Moses (Oregon Health and Science

University, Oregon, USA). These cells were maintained in EBM-2 medium (Lonza, MD) supplemented with EGM-2 MV medium (Lonza, MD), 1% Chemically defined lipid concentrate (Gibso, USA), 5% fetal FBS (Corning, NY), 100 U/mL penicillin and 100 µg/mL streptomycin in a humidified incubator at 37 °C and 5% CO_2. To promote attachment of hCMEC/D3 cells, growth surfaces were treated with 0.1 mg/mL rat tail collagen (BD Biosciences, Palo Alto, CA) in 0.02 N acetic acid for 10 min and rinsed with PBS prior to use. Other cell culture materials were purchased from Corning Inc. (Corning, NY) unless otherwise stated.

5.3.2 Establishment of a multidrug resistant BCRP overexpressing breast cancer cell line

A BCRP over-expressing breast cancer cell line, MCF-7 M100, was established by us according to previously described methods [191][275]. Briefly, the initially drug sensitive MCF-7 [190] breast cancer cells were exposed to 2 nM of mitoxantrone and the concentration of mitoxantrone was increased gradually in approximately 2-fold increments between 6 – 10 passages according to their tolerance to the chemotherapeutic. After 60 passages, the resultant cells could remain viable and grow up to 100 nM of mitoxantrone in their medium. Thereafter, the MCF-7 M100 cell line was always maintained in medium containing 100 nM of mitoxantrone.

5.3.3 Western blot analyses

Whole cell lysates were prepared using approximately five million cells from each cell line. Cells were lysed with 500 µL of SDS buffer (125 mM Tris HCl pH 6.8, 20% v/v glycerol, 4% w/v SDS and 2% v/v β-mercaptoethanol) containing 5 µL of protease inhibitor cocktail (P8340, Sigma). The lysates were filtered through a spin column (QIAprep ®) by centrifugation at 5000 rpm for 5 minutes and used for Western blot analysis. The lysate

proteins were resolved by denaturing SDS-PAGE [196] for 100 minutes at 110 V and subsequently transferred to a PVDF membrane (Bio-Rad, CA) using a Mini Transblot cell (Bio-Rad) for 70 minutes at 110 V. The transfer buffer contained 192 mM glycine, 25 mM Tris, and 10% methanol. The membrane was blocked overnight at 4 °C with 4% powdered skimmed milk in TBS-T (12 mM Tris–HCl pH 7.5, 0.5 M NaCl, 0.05% Tween 20). Washed membranes were incubated with the BCRP-specific monoclonal antibody B1 (obtained from Santa Cruz Biotechnology, CA), or the β-actin monoclonal antibody C4 (Santa Cruz Biotechnology, CA), diluted to between 1:500 and 1:2000 in TBS-T and 4% powdered skimmed milk. Incubation with the primary antibody solution was performed for 2 hours at room temperature. Washed membranes were subsequently incubated for 1 hour at room temperature with alkaline horseradish peroxidase-conjugated goat anti-mouse secondary antibody sc-2005 (Santa Cruz Biotechnology, CA) diluted to 1:10000 in TBS-T containing 4% milk powder. Membranes were washed in TBS-T, and BCRP or β-actin bands were visualized using an enhanced chemiluminescence detection kit (ECL kit, Thermo Scientific, IL). Images were recorded using a ChemiDoc™ Touch imaging system (Bio-rad, CA).

5.3.4 Screening for BCRP inhibitors from our in house small molecule library

A collection of small molecules (numbered from **11** to **124** and variants of **29**) which were used for several previous studies were rescreened here to identify potential BCRP inhibitors. These compounds were either purchased or synthesized in collaboration with Dr. Alex Lippert and Maha Aljowani from the Chemistry Department at SMU.

The ability of BCRP to efflux the nuclear stain Hoechst 33342 was used as an assay to identify any small molecules which interfere with BCRP transporter activity [88], [281]. In these experiments, about 14,000 MCF-7 M100 breast cancer cells were seeded in each well in 96 well

plates and allowed to grow until nearly 90 % confluency was reached (4-5 days). At this point, the media was replaced with phenol red free RPMI media and cells were treated with or without 10 μM of small molecules (**11**-**124** and SMU29 variants **216**, **227**, **231**, **238**, **255**, **278**, **280** and **286**) in the presence of 5 μg/mL of Hoechst 33342. Fluorescence was measured with excitation at 361/20 nm and at emission 497/20 nm using the BioTek Cytation 5 imaging multi-mode reader (Bio-Tek, Winooski, VT) after 90 minutes of treatment at 37 ^{0}C. DMSO (0.5% v/v) was used as the vehicle control, and 1 μM of the known BCRP inhibitor, Ko143, was used as a positive control [151] and10 μM of P-gp substrate, verapamil, was used as negative control [282]. Any compounds that resulted in more than approximately 4-fold increased Hoechst 33342 accumulation compared to the vehicle controls were selected for further studies.

5.3.5 Evaluation of cytotoxicity and reversal of mitoxantrone resistance by compounds 50, 53, 70, 71, 83, 103, and 117

Cytotoxicity and the ability to reverse the mitoxantrone resistance displayed by MCF-7 M100 cancer cells by compounds **50**, **53**, **70**, **71**, **83**, **103**, and **117** were evaluated using MTT viability assays. About 5000 MCF-7 M100 cells were seeded in each well of 96 well plates for 24 hours and cells were treated with 10 μM compound with or without 200 nM of mitoxantrone for 72 hours before addition of MTT. The MTT assays were performed as described in [193] using 5 mg/mL of MTT (Acros Organics, NJ) solution prepared in PBS (137 mM NaCl, 2.7 mM KCl, 10 mM Na_2HPO_4, 1.8 mM KH_2PO_4, pH 7.4). After 4 hours of incubation with MTT, the media was removed and the formazan crystals that had formed were dissolved in 100 μL of DMSO. The absorbance at 570 nm was then measured using a Cytation 5 instrument. Percent viability was calculated using DMSO treated cells as representative for 100% viability.

Background absorbance was determined using MTT and complete medium without cells. Background absorbance was subtracted from all of the test values.

5.3.6 Reversal of Multidrug resistance by compounds 50, 71, 117 and 29 variants 231, 238 and 255.

Three of the compounds that performed well in the MTT viability assays, **50**, **71**, and **117**, were tested again at differing concentrations of mitoxantrone. These assays were performed as above with mitoxantrone at concentrations of 1 mM, 100 μM, 10 μM, 1 μM, 100 nM, 10 nM, 1 nM, and 100 pM with or without 10 μM of compounds 50, 71, and 117.

The **29** variants (**231**, **238** and **255**) which led to high levels of accumulation of Hoechst 33342 in MCF-7 M100 cells were tested in viability assay with 10 μM concentrations of 29 variants similar to the viability assay procedure described above. To assess the reversal of MDR, viability assays were repeated with two more chemotherapeutics, topotecan and SN-38, as well. Further impact of these putative inhibitors on parental drug sensitive MCF-7 cells were assayed using the same assay conditions as described above. The graphical representations were determined using four parameter variable slope non-linear regression, using the following equation: Y=bottom + (top-bottom)/(1 + 10^((logIC50-X)*Hill Slope (GraphPad Prism™, La Jolla California, USA, Version 6.05).

5.3.7 Evaluation of the accumulation of BCRP substrates in BCRP overexpressing MCF-7 M100 cells by 29 variants

The concentration dependence and time courses of **29** variants (**231**, **238** and **255**) on BCRP inhibitory action were studied using the Hoechst assay as described earlier with the following modifications. Cells were treated with various concentrations (1, 2.5, 5 and 10 μM) of

putative BCRP inhibitors and 5 μg/mL of Hoechst 33342. Immediately after addition, the fluorescence was measured with excitation at 361/20 nm and at emission 497/20 nm using the Cytation 5 every 10 minutes for 50 minutes while maintaining 37 ^{0}C.

To study the influence of the preincubation of inhibitors with the cells, another experiment was performed similar to those described above, but included incubation of the putative inhibitors for 3 hours in 37 ^{0}C before Hoechst 33342 addition. After Hoechst addition, fluorescence was measured every 10 minutes for 50 minutes while maintaining 37 ^{0}C. Imaging of samples was performed after 50 minutes incubation with Hoechst using a DAPI channel of the Cytation 5 to observe the qualitative accumulation of Hoechst in MCF-7 M100 cells.

To measure the cellular accumulation of chemotherapeutics, daunorubicin and mitoxantrone were used. MCF-7 M100 cells were seeded in 96 wells plates at 14,000 cells per well in complete media and allowed to grow until 100% confluency. Medium was removed and cells were treated with or without 25 μM potential BCRP inhibitory compounds in the presence of 15 μM daunorubicin (MP Biomedicals, France) or 25 μM mitoxantrone (Santa Cruz Biotechnology, CA) in complete medium. Vehicle controls were treated with 0.5% DMSO. After 3 hours of incubation, media were removed and cells were washed three times with 200 μL of ice cold PBS. The cells were lysed by addition of 100 μL of PBS containing 0.8% SDS and 0.8% Triton X100 immediately after the washing step. The fluorescence of daunorubicin was measured using excitation at 488 nm (20 nm gate) and emission at 575 nm (20 nm gate). The fluorescence of mitoxantrone was measured using excitation at 640 nm (10 nm gate) and emission at 690 nm (10 nm gate) using the also using the Cytation 5 instrument. Fold accumulation for each of the experiments were calculated compared to vehicle treated cells.

5.3.8 Evaluation of BCRP and P-gp substrate accumulation in the blood brain barrier endothelial cell line hCMEM/d3

The immortalized human cerebral microvascular endothelial cell line, hCMEC/D3, were seeded in 96 well plates with 5000 cells per well and allowed to grow 4 to 5 days until cells become nearly 100% confluent. Cells were treated with 25 µM of **231**, **238** or **255** individually. After 3 hours of incubation, cells were treated with 2.5 µM of rhodamine 123 diluted in media and allowed the cells to accumulate rhodamine 123 for 90 minutes. Then media were removed and cells were washed three times with 200 µL of PBS. Cells were lysed in 100 µL of PBS containing 0.8% SDS and 0.8% Triton X100 immediately after the washing step. The P-gp substrate, verapamil (25 µM), was used as a positive control and vehicle controls were treated with 0.5% DMSO. The fluorescence of rhodamine 123 was measured using excitation at 488 nm with a 20 nm gate and emission at 575 nm with a 20 nm gate using the Cytation 5. Fold accumulations were calculated and normalized to vehicle treated cells.

To analyze the Hoechst 33342 accumulation, cells were seeded as above and after reaching 100% confluence, the media was replaced with phenol red free RPMI media. Cells were then treated with 25 µM of **231**, **238**, or **255** individually diluted in phenol red free RPMI media and incubated at 37 ^{o}C for 3 hours. After the initial incubation, cells were then treated with 1 µg/mL of Hoechst 33342. Fluorescence was measured with excitation at 361/20 nm and at emission 497/20 nm using the Cytation 5 after a 50 minute 37 ^{o}C incubation with the Hoechst dye. Fold accumulations were calculated, and normalized vehicle treated cells.

5.3.9 Cellular accumulation assays for experimental BCRP inhibitors

MCF-7 M100 cells were seeded in 6 well plates with ~200,000 cells per well. After several days when cells were 100% confluent, the media was replaced with fresh media and

cells were treated with 5 μM of compounds (**231**, **238**, or **255** or mitoxantrone) with or without 500 nM of Ko143 (Sigma). Experiments were performed in triplicate. After 2.5 hours of incubation with compounds, cells were washed with Hank's Balanced Salt Solution (HBSS, Corning Inc. NY), harvested using trypsin, and counted. Each sample was then washed with 2 mL of ice-cold HBSS and diluted in cold HBSS at a final concentration of 1 million cells/mL. All samples were frozen with liquid nitrogen and stored at −80 °C until analysis. Samples were analyzed at the University of Texas Southwestern Medical Center Preclinical Pharmacology Laboratory using LC-MS/MS analyses essentially as described in [201] and as modified in [235].

5.4 Discussion

BCRP overexpression is correlated with MDR in cancer and its expression in blood brain barrier (BBB) plays a major functional role by excluding therapeutics away from brain [107]. BCRP inhibitors have been demonstrated to reverse MDR in cell cultures [280] and their use in *in vivo* experiments is correlated with elevated BCRP substrate concentrations in the brain [269]. Nevertheless, these inhibitors have not yet shown success in clinical settings; thus the demand for clinically approved BCRP inhibitors remains [159]. Computational screenings have been deployed to recognize drugs successfully over the decades and have been used in attempts to identify BCRP inhibitors as well [293], [294]. After studying a small library of compounds selected using a computational based screening, we have identified several BCRP modulating compounds including one confirmed BCRP inhibitor and two BCRP substrates in this study.

The toxicity of therapeutics is a major drawback in chemotherapy [295]. Out of the seven compounds which could interfere with BCRP transport activity (**50**, **53**, **70**, **71**, **83**, **103**, and **117)** we selected from screens of a library containing **114** compounds using the Hoechst assays

(**Figure 5.3** and **Figure 5.4**), four of them (**53**, **70**, **83** and **103)** had exhibited significant toxicity by themselves in ealier viability assays (**Figure 5.6**). The viability experiments should be repeated using another BCRP overexpressing cell line to confirm this toxicity is not a cell line specific effect. Although **29** variant **286** exhibited a significant Hoechst accumulation (**Figure 5.5**) we did not include **286** in viability assays as this compound has exhibited toxicity by itself to different cell lines in previous studies (Chapter 4).

Since clinical trials using substrates of P-gp such as verapamil as MDR reversing agent have failed, we wanted to examine whether the **29** variants which modulated BCRP activity were BCRP inhibitors or as transport substrates. In previous work by others, BCRP substrates have been confirmed by using cell lines with directional expression of BCRP on transwell plates [296] or by using vesicle transport assays [93] with BCRP enriched vesicles. Here we have adopted a relatively facile method equivalent to that described in [235] by analyzing the intracellular accumulation of compounds in the presence or the absence of a strong, known BCRP inhibitor (Ko143) to determine whether a given compound functions as a BCRP substrate. As the positive control we used mitoxantrone, which is a very good transport substrate of BCRP. As indicated in **Figure 5.10**, this method cam be reliably used for identification of BCRP substrates with a BCRP overexpressing cell line even without a directional expression pattern. We have confirmed that compound **231** is not a BCRP substrate which is importance since we also demonstrated this compound to not be a substrate of P-glycoprotein. This indicates that **231** reversed the MDR and increased the BCRP substrate accumulation in the BCRP overexpressing cell line by functioning as an inhibitor of BCRP turnover. Similar to what we observed with P-gp in earlier experiments, compounds **238** and **255** accumulated upon BCRP inhibition indicating that both likely are transport substrates for BCRP. According to the accumulation results obtained from these

experiments, compound **238** appeared to be a better substrate than was the positive control, mitoxantrone (**Figure 5.10** Panel B and D). In other work, by colleagues in the lab, the ATPase activity of isolated protein preparations (Gang Chen, data not shown), compound **238** stimulated basal ATPase activity to a higher extend than the known P-gp substrate, verapamil, again suggesting that compound **238** might be an excellent transport substrate for P-gp. If compounds **238** and **255** are stable in *in vivo* conditions, radiolabeled derivatives of these two compounds coupled with positron emission tomography (PET) imaging might be useful for simultaneous analyses of P-gp and BCRP function *in vivo* similar to that described in [297]–[300].

The pool of compounds we analyzed in this study (**11**-**124** and **29** variants) were originally selected by docking compound structures available in databases of commercially available, small molecule drug-like compounds to P-gp [44], [164]or BCRP [unpublished] homology models. We used a BCRP homology model due to the unavailability of a high-resolution structure of the NBD of BCRP at the time these screenings were performed. We hypothesized that compounds that were predicted to be P-gp inhibitors by these computational screenings might also have the potential to show modulatory/inhibitory action on BCRP. This is mainly due to both of these transporters belonging to the ABC super family of proteins, their similarities in function and especially in the structures of the nucleotide binding domains of the two proteins [301]. In support of this assumption, it should be noted that inhibitors like elacridar inhibit both P-gp and BCRP [302], evidencing the predictability of having BCRP inhibitors in a pool of molecules targeted to be P-gp inhibitors. The BCRP modulatory compounds which we have identified in Hoechst accumulation assays using BCRP-overexpressing breast cancer cells in this study (**50**, **53**, **70**, **71**, **83**, **103**, and **117)** all exhibited P-gp modulatory activities in previous studies (McCormick *et al*. unpublished; data not shown). in addition, the **29** variant **231** is a predicted P-

gp inhibitor (Chapter 4) and this study illustrates that **231** also functions as a non-transported BCRP inhibitor as well. Compounds **238** and **255** were identified as BCRP substrates in this study; both of these compounds are also P-gp substrates (Chapter 4). We predicted that these inhibitors would elevate the penetration and accumulation of P-gp and BCRP substrates into the brain through the BBB, as well as in reversing the BCRP and P-gp mediated MDR in cancers. *In vivo* experiments should be performed in future to examine the efficacy of these inhibitors. *In vivo* and preclinical data have demonstrated the increased oral bio-availability of chemotherapeutics by the inhibition of both P-gp and BCRP from elacridar [147]. We believe dual modulation of P-gp and BCRP by the compounds we describe in this study might have the potential to enhance the bio-availability of CNS targeted therapeutics as well.

CHAPTER 6: CONCLUSIONS AND FUTURE DIRECTIONS

6.1 Conclusions

6.1.1 Compound 29, 34 and 45 are P-gp inhibitors

Multidrug resistance is correlated with poor outcome of chemotherapy and P-glycoprotein is one of the main reasons for MDR [303], [304]. P-gp inhibitors have shown success in reversing MDR in *in vitro* and *in vivo*, but only with marginal success in clinical trials. Thus demand for clinically approved P-gp inhibitors remains [305]. One major aim in our studies was to find P-gp inhibitors that are not P-gp substrates. Previous studies from our group have recognized compounds **29**, **34** and **45** as potential P-gp inhibitors. Here we show that these inhibitors can reverse MDR in two different P-gp overexpressing cells lines, A2780ADR ovarian cancer cells and DU145TXR prostate cancer cells, using multiple chemotherapeutics. The reversal of MDR is correlated with the higher accumulation of P-gp substrates when cells are exposed to P-gp inhibitors. P-gp inhibitors **34** and **45** have no impact on BCRP overexpressing breast cancer cells, indicating that no functionally detectable interactions with BCRP occurred. Compound **29** conversely also modulated the BCRP activity. We have proposed a relatively simple and novel assay for recognizing P-gp substrates in *in vitro* conditions based on the accumulation of the compound in the presence or absence of a known P-gp inhibitor tariquidar, when tested with LC-MS/MS approaches. Using this novel assay, we concluded that these three compounds are not P-gp transporter substrates. Hence combining the results from cellular accumulations of these compounds with the results of MDR reversing cell culture assays and

Western blot analyses for P-gp expression, we concluded that compounds **29**, **34** and **45** reverse the MDR by functioning as inhibitors of P-gp.

6.1.2 Extended treatment of P-gp inhibitor 29 significantly increases the efficacy of chemotherapy

P-gp inhibitors had only a limited success in clinical settings and one reason could the treatment strategy [5], [11]. Extended treatment of inhibitor **29** after an initial exposure to both **29** and chemotherapeutics led to a higher retention of chemotherapeutics in the P-gp overexpressing cancer cells *in vitro*. Intracellular retention of chemotherapeutics by P-gp inhibitor **29**, even in the absence of free chemotherapeutics in the medium, significantly improved the outcome of the chemotherapeutic treatments in *in vitro* assays. Extended treatment had no impact on cancer cells that do not overexpress P-gp nor did it impact non-cancerous cells. We can therefore predict that this strategy could be used *in vivo* or potentially clinically in the future to enhance the outcome of chemotherapy treatments.

6.1.3 Lead optimization of compound 29 has yielded improved P-gp inhibitors.

One of the most important steps of computational based drug screenings is the lead optimization. This is the process where "potential" drugs become clinically acceptable by improving the drug-like characteristics [262]. The three variants (**216**, **227** and **238**) generated from computational based lead optimization of parental P-gp inhibitor **29** are not P-gp substrates thus we conclude that these variants reversed the paclitaxel resistance by functioning as P-gp inhibitors. Only **278** out of five variants (**238**, **255**, **278**, **280** and **286**) exhibited the P-gp inhibitor like characteristics which were designed through conventional lead optimization. Although parental P-gp inhibitor **29** modulates the BCRP activity, variants **216**, **227**, **278** and **280** do not modulate BCRP activity, showing the improved specificity towards P-gp in their

variant forms. Improved efficacy of reversing paclitaxel resistance compared to parental P-gp inhibitor **29** and observing that 100% of computationally designed P-gp inhibitors did not function as P-gp substrates provides evidence and a strong example of the advantages of using computationally based lead optimization over more conventional methods.

6.1.4 Potential BCRP inhibitors can reverse BCRP mediated MDR

BCRP is another ABC type transporter which confers MDR in cancer and is also important in extruding xenobiotics away from brain [147], [270]. We have established a BCRP overexpressing breast cancer cell line, MCF-7 M100, from the parental cell line MCF-7 to use in cell-based assays of BCRP inhibitors. Our screenings have resulted in the identification of several BCRP modulators with the potential to be BCRP inhibitors (**50**, **53**, **70**, **71**, **83**, **103**, and **117)**. Further, we have found that three variants of P-gp inhibitor **29**, compounds **231**, **238** and **255,** also reversed BCRP mediated MDR *in vitro*. Their ability to reverse MDR in BCRP overexpressing cancer cells is correlated with increased intracellular accumulation of chemotherapeutics that are BCRP substrates chemotherapeutics. Here we introduce a novel assay using LC-MS/MS instrumentation for determining whether any given compound acted as a BCRP substrate in *in vitro* cell-based experiments. These assays were developed in analogy with those described earlier for determining whether compounds act as P-gp substrates. The tests in this case used cells over-expressing BCRP and LC-MS/MS to quatify the accumulation of the compounds in the presence or absence of a known BCRP inhibitor, Ko143. Results from these assays strongly suggest that compound **231** is not a BCRP substrate and that compounds **238** and **255** do function as BCRP substrates using this novel assay. These compound screens identified two new substrates for both P-gp and BCRP (compounds **238** and **255**). These novel substrates could be useful in the future for various purposes such as determining transporter activity in

normal or cancerous tissues. Further we can predict that dual modulators of P-gp and BCRP may eventually prove useful in opening the BBB to drugs that target brain or CNS pathologies.

6.2 Future Directions

Our aim here was to identify novel P-gp and BCRP inhibitors that are not substrates for the relevant transporters. This study has identified several P-gp inhibitors and BCRP inhibitors that meet this criteria and other compounds that modulate transporter function while acting as substrates. screening for new inhibitors as well as optimizing the leads that we have already identified should continue on to find and / or develop inhibitors with higher binding affinities and better drug-likeness. These novel inhibitors should be able to reverse MDR in P-gp overexpressing cell lines in viability assays, increase P-gp substrate intracellular accumulation, should be tested for the specificity for P-gp, be assessed for their potential of being P-gp substrates. Successful candidates will have to further undergo testing for metabolic stability similar to [172]. Stable inhibitors can then be directed to *in vivo* studies [306]. As described, we have gained significant improvements in P-gp inhibitor **29** in lead optimization studies. The ChemGen process we have used for inhibitor **29** may be applied for computationally based lead optimization of other P-gp inhibitors.

Screening for the identification of novel BCRP inhibitors can be performed efficiently in future using new BCRP structures with a higher resolution as determined by cryo-electron microscopy [307]. Ideally, one should test the potential BCRP inhibitors in at least two different BCRP overexpressing cell lines to confirm that the effects are not cell line specific and the similar process described for P-gp in above can be applied to identify novel BCRP inhibitors that can lead to clinical trials. The compounds with dual modulatory activity of both P-gp and BCRP

can be directed for *in vivo* BBB studies to analyze potentially higher brain targeted accumulation of therapeutics which are P-gp and BCRP substrates.

REFERENCES

[1] H. Lage, “An overview of cancer multidrug resistance: a still unsolved problem,” *Cell. Mol. Life Sci.*, vol. 65, no. 20, pp. 3145–3167, Oct. 2008.

[2] R. Krishna and L. D. Mayer, “Multidrug resistance (MDR) in cancer: Mechanisms, reversal using modulators of MDR and the role of MDR modulators in influencing the pharmacokinetics of anticancer drugs,” *Eur. J. Pharm. Sci.*, vol. 11, no. 4, pp. 265–283, Oct. 2000.

[3] G. Housman, S. Byler, S. Heerboth, K. Lapinska, M. Longacre, N. Snyder, and S. Sarkar, “Drug resistance in cancer: an overview,” *Cancers (Basel)*, vol. 6, no. 3, pp. 1769–1792, Sep. 2014.

[4] H. Zahreddine and K. L. B. Borden, “Mechanisms and insights into drug resistance in cancer.,” *Front. Pharmacol.*, vol. 4, p. 28, 2013.

[5] M. M. Gottesman, T. Fojo, and S. E. Bates, “Multidrug resistance in cancer: role of ATP–dependent transporters,” *Nat. Rev. Cancer*, vol. 2, no. 1, pp. 48–58, Jan. 2002.

[6] G. Housman, S. Byler, S. Heerboth, K. Lapinska, M. Longacre, N. Snyder, and S. Sarkar, “Drug resistance in cancer: an overview,” *Cancers (Basel)*, vol. 6, no. 3, pp. 1769–1792, 2014.

[7] F. J. Sharom, “ABC multidrug transporters: structure, function and role in chemoresistance,” *Pharmacogenomics*, vol. 9, no. 1, pp. 105–127, 2008.

[8] M. Yu, A. Ocana, and I. F. Tannock, “Reversal of ATP-binding cassette drug transporter activity to modulate chemoresistance: why has it failed to provide clinical benefit?,” *Cancer Metastasis Rev*, vol. 32, no. 1–2, pp. 211–227, 2013.

[9] D. Fruci, W. C. Cho, V. Nobili, F. Locatelli, and A. Alisi, “Drug Transporters and Multiple Drug Resistance in Pediatric Solid Tumors,” *Curr Drug Metab*, vol. 17, no. 4, pp. 308–316, 2016.

[10] T. Mukhopadhyay, J. G. Batsakis, and M. T. Kuo, “Expression of the mdr (P-glycoprotein) gene in Chinese hamster digestive tracts.,” *J. Natl. Cancer Inst.*, vol. 80, no. 4, pp. 269–75, Apr. 1988.

[11] A. Palmeira, E. Sousa, M. H. Vasconcelos, and M. M. Pinto, “Three decades of P-gp inhibitors: skimming through several generations and scaffolds,” *Curr Med Chem*, vol. 19, no. 13, pp. 1946–2025, 2012.

[12] S. V Ambudkar, S. Dey, C. A. Hrycyna, M. Ramachandra, I. Pastan, and M. M. Gottesman, “Biochemical, cellular, and pharmacological aspects of the multidrug transporter,” *Annu Rev Pharmacol Toxicol*, vol. 39, pp. 361–398, 1999.

[13] S. Wilkens, “Structure and mechanism of ABC transporters.,” *F1000Prime Rep.*, vol. 7, p. 14, 2015.

[14] M. Dean, Y. Hamon, and G. Chimini, “The human ATP-binding cassette (ABC) transporter superfamily.,” *J. Lipid Res.*, vol. 42, no. 7, pp. 1007–17, Jul. 2001.

[15] E. Dassa and P. Bouige, “The ABC of ABCs: a phylogenetic and functional classification of ABC systems in living organisms,” *Res. Microbiol.*, vol. 152, no. 3–4, pp. 211–229, Apr. 2001.

[16] R. W. Robey, K. M. Pluchino, M. D. Hall, A. T. Fojo, S. E. Bates, and M. M. Gottesman, “Revisiting the role of ABC transporters in multidrug-resistant cancer,” *Nat. Rev. Cancer*, vol. 18, no. 7, pp. 452–464, Jul. 2018.

[17] G. D. Leonard, T. Fojo, and S. E. Bates, “The role of ABC transporters in clinical practice.,” *Oncologist*, vol. 8, no. 5, pp. 411–24, Oct. 2003.

[18] C.-H. Choi, “ABC transporters as multidrug resistance mechanisms and the development of chemosensitizers for their reversal.,” *Cancer Cell Int.*, vol. 5, p. 30, Oct. 2005.

[19] V. Ling and L. H. Thompson, “Reduced permeability in CHO cells as a mechanism of resistance to colchicine,” *J. Cell. Physiol.*, vol. 83, no. 1, pp. 103–116, Feb. 1974.

[20] J. L. Biedler and H. Riehm, “Cellular resistance to actinomycin D in Chinese hamster cells in vitro: cross-resistance, radioautographic, and cytogenetic studies.,” *Cancer Res.*, vol. 30, no. 4, pp. 1174–84, Apr. 1970.

[21] V. Ling, “Drug resistance and membrane alteration in mutants of mammalian cells.,” *Can. J. Genet. Cytol.*, vol. 17, no. 4, pp. 503–15, Dec. 1975.

[22] R. L. Juliano and V. Ling, “A surface glycoprotein modulating drug permeability in Chinese hamster ovary cell mutants.,” *Biochim. Biophys. Acta*, vol. 455, no. 1, pp. 152–62, Nov. 1976.

[23] L. M. Hodges, S. M. Markova, L. W. Chinn, J. M. Gow, D. L. Kroetz, T. E. Klein, and R. B. Altman, “Very important pharmacogene summary: ABCB1 (MDR1, P-glycoprotein).,” *Pharmacogenet. Genomics*, vol. 21, no. 3, pp. 152–61, Mar. 2011.

[24] M. Bodor, E. J. Kelly, and R. J. Ho, “Characterization of the human MDR1 gene.,” *AAPS J.*, vol. 7, no. 1, pp. E1-5, Feb. 2005.

[25] S. V Ambudkar, C. Kimchi-Sarfaty, Z. E. Sauna, and M. M. Gottesman, “P-glycoprotein: from genomics to mechanism,” *Oncogene*, vol. 22, no. 47, pp. 7468–7485, Oct. 2003.

[26] M. E. Goldsmith, J. M. Gudas, E. Schneider, and K. H. Cowan, “Wild type p53 stimulates

expression from the human multidrug resistance promoter in a p53-negative cell line.," *J. Biol. Chem.*, vol. 270, no. 4, pp. 1894–8, Jan. 1995.

[27] K. Katayama, K. Noguchi, and Y. Sugimoto, "Regulations of P-Glycoprotein/ABCB1/ *MDR1* in Human Cancer Cells," *New J. Sci.*, vol. 2014, pp. 1–10, May 2014.

[28] R. C. Bargou, K. Jürchott, C. Wagener, S. Bergmann, S. Metzner, K. Bommert, M. Y. Mapara, K. J. Winzer, M. Dietel, B. Dörken, and H. D. Royer, "Nuclear localization and increased levels of transcription factor YB-1 in primary human breast cancers are associated with intrinsic MDR1 gene expression.," *Nat. Med.*, vol. 3, no. 4, pp. 447–50, Apr. 1997.

[29] J. C. Lim, K. D. Kania, H. Wijesuriya, S. Chawla, J. K. Sethi, L. Pulaski, I. A. Romero, P. O. Couraud, B. B. Weksler, S. B. Hladky, and M. A. Barrand, "Activation of -catenin signalling by GSK-3 inhibition increases P-glycoprotein expression in brain endothelial cells," *J. Neurochem.*, vol. 106, no. 4, pp. 1855–65, Jun. 2008.

[30] J. M. Yang, A. D. Vassil, and W. N. Hait, "Activation of phospholipase C induces the expression of the multidrug resistance (MDR1) gene through the Raf-MAPK pathway.," *Mol. Pharmacol.*, vol. 60, no. 4, pp. 674–80, Oct. 2001.

[31] H. Bark and C.-H. Choi, "PSC833, cyclosporine analogue, downregulates MDR1 expression by activating JNK/c-Jun/AP-1 and suppressing NF-κB," *Cancer Chemother. Pharmacol.*, vol. 65, no. 6, pp. 1131–1136, May 2010.

[32] H. Sui, G.-X. Cai, S.-F. Pan, W.-L. Deng, Y.-W. Wang, Z.-S. Chen, S.-J. Cai, H.-R. Zhu, and Q. Li, "miR200c Attenuates P-gp-Mediated MDR and Metastasis by Targeting JNK2/c-Jun Signaling Pathway in Colorectal Cancer," *Mol. Cancer Ther.*, vol. 13, no. 12,

pp. 3137–3151, Dec. 2014.

[33] F. Lu, Y.-Q. Hou, Y. Song, and Z.-J. Yuan, “TFPI-2 Downregulates Multidrug Resistance Protein in 5-FU-Resistant Human Hepatocellular Carcinoma BEL-7402/5-FU Cells,” *Anat. Rec. Adv. Integr. Anat. Evol. Biol.*, vol. 296, no. 1, pp. 56–63, Jan. 2013.

[34] Y. Wang, D. Zhang, K. Wu, Q. Zhao, Y. Nie, and D. Fan, “Long Noncoding RNA MRUL Promotes ABCB1 Expression in Multidrug-Resistant Gastric Cancer Cell Sublines,” *Mol. Cell. Biol.*, vol. 34, no. 17, pp. 3182–3193, Sep. 2014.

[35] V. Lopes-Rodrigues, H. Seca, D. Sousa, E. Sousa, R. T. Lima, and M. H. Vasconcelos, “The network of P-glycoprotein and microRNAs interactions,” *Int. J. Cancer*, vol. 135, no. 2, pp. 253–263, Jul. 2014.

[36] A. E. Senior, M. K. al-Shawi, and I. L. Urbatsch, “The catalytic cycle of P-glycoprotein,” *FEBS Lett.*, vol. 377, no. 3, pp. 285–289, Dec. 1995.

[37] X. Zhang, K. I. Collins, and L. M. Greenberger, “Functional evidence that transmembrane 12 and the loop between transmembrane 11 and 12 form part of the drug-binding domain in P-glycoprotein encoded by MDR1.,” *J. Biol. Chem.*, vol. 270, no. 10, pp. 5441–8, Mar. 1995.

[38] T. W. Loo, M. C. Bartlett, and D. M. Clarke, “Transmembrane segment 7 of human P-glycoprotein forms part of the drug-binding pocket,” *Biochem. J.*, vol. 399, no. 2, pp. 351–359, Oct. 2006.

[39] ‡ Michel Demeule, ‡ Alain Laplante, § Gérard F. Murphy, ‖ and Roland M. Wenger, and ‡ Richard Béliveau*, “Identification of the Cyclosporin-Binding Site in P-Glycoprotein†,” 1998.

[40] E. P. Bruggemann, S. J. Currier, M. M. Gottesman, and I. Pastan, “Characterization of the azidopine and vinblastine binding site of P-glycoprotein.,” *J. Biol. Chem.*, vol. 267, no. 29, pp. 21020–6, Oct. 1992.

[41] ‡ Christine A. Hrycyna, ‡,§ Lisa E. Airan, ‡,∥ Ursula A. Germann, ‡ Suresh V. Ambudkar, ⊥ and Ira Pastan, and ‡ Michael M. Gottesman*, “Structural Flexibility of the Linker Region of Human P-Glycoprotein Permits ATP Hydrolysis and Drug Transport†,” 1998.

[42] A. Ward, C. L. Reyes, J. Yu, C. B. Roth, and G. Chang, “Flexibility in the ABC transporter MsbA: Alternating access with a twist,” *Proc. Natl. Acad. Sci.*, vol. 104, no. 48, pp. 19005–19010, Nov. 2007.

[43] J. G. Wise, “Catalytic transitions in the human MDR1 P-glycoprotein drug binding sites.,” *Biochemistry*, vol. 51, no. 25, pp. 5125–41, Jun. 2012.

[44] J. W. McCormick, P. D. Vogel, and J. G. Wise, “Multiple Drug Transport Pathways through Human P-Glycoprotein,” *Biochemistry*, vol. 54, no. 28, pp. 4374–4390, Jul. 2015.

[45] D. Fu and I. M. Arias, “Intracellular trafficking of P-glycoprotein.,” *Int. J. Biochem. Cell Biol.*, vol. 44, no. 3, pp. 461–4, Mar. 2012.

[46] E. B. Mechetner, B. Schott, B. S. Morse, W. D. Stein, T. Druley, K. A. Davis, T. Tsuruo, I. B. Roninson, E. Pardon, C. Cregger, D. J. Swartz, P. G. Falson, I. L. Urbatsch, C. Govaerts, J. Steyaert, and G. Chang, “P-glycoprotein function involves conformational transitions detectable by differential immunoreactivity,” *Proc. Natl. Acad. Sci.*, vol. 94, no. 24, pp. 12908–12913, Nov. 1997.

[47] A. T. Fojo, K. Ueda, D. J. Slamon, D. G. Poplack, M. M. Gottesman, and I. Pastan, “Expression of a multidrug-resistance gene in human tumors and tissues.,” *Proc. Natl.*

Acad. Sci. U. S. A., vol. 84, no. 1, pp. 265–9, Jan. 1987.

[48] F. Thiebaut, T. Tsuruo, H. Hamada, M. M. Gottesman, I. Pastan, and M. C. Willingham, "Immunohistochemical localization in normal tissues of different epitopes in the multidrug transport protein P170: evidence for localization in brain capillaries and crossreactivity of one antibody with a muscle protein.," *J. Histochem. Cytochem.*, vol. 37, no. 2, pp. 159–164, Feb. 1989.

[49] L. Su, P. Jenardhanan, D. D. Mruk, P. P. Mathur, Y.-H. Cheng, K.-W. Mok, M. Bonanomi, B. Silvestrini, and C. Y. Cheng, "Role of P-glycoprotein at the blood-testis barrier on adjudin distribution in the testis: a revisit of recent data.," *Adv. Exp. Med. Biol.*, vol. 763, pp. 318–33, 2012.

[50] I. Sugawara, I. Kataoka, Y. Morishita, H. Hamada, T. Tsuruo, S. Itoyama, and S. Mori, "Tissue distribution of P-glycoprotein encoded by a multidrug-resistant gene as revealed by a monoclonal antibody, MRK 16.," *Cancer Res.*, vol. 48, no. 7, pp. 1926–9, Apr. 1988.

[51] F. Staud, M. Ceckova, S. Micuda, and P. Pavek, "Expression and Function of P-Glycoprotein in Normal Tissues: Effect on Pharmacokinetics," in *Methods in molecular biology (Clifton, N.J.)*, vol. 596, Humana Press, 2010, pp. 199–222.

[52] M. Aryal, K. Fischer, C. Gentile, S. Gitto, Y.-Z. Zhang, and N. McDannold, "Effects on P-Glycoprotein Expression after Blood-Brain Barrier Disruption Using Focused Ultrasound and Microbubbles.," *PLoS One*, vol. 12, no. 1, p. e0166061, 2017.

[53] S.-F. Zhou, "Structure, function and regulation of P-glycoprotein and its clinical relevance in drug disposition," *Xenobiotica*, vol. 38, no. 7–8, pp. 802–832, Aug. 2008.

[54] D. Levêque and F. Jehl, "P-glycoprotein and pharmacokinetics.," *Anticancer Res.*, vol. 15,

no. 2, pp. 331–6.

[55] J. H. Lin and M. Yamazaki, “Role of P-Glycoprotein in Pharmacokinetics,” *Clin. Pharmacokinet.*, vol. 42, no. 1, pp. 59–98, 2003.

[56] B. L. Lum and M. P. Gosland, “MDR expression in normal tissues. Pharmacologic implications for the clinical use of P-glycoprotein inhibitors.,” *Hematol. Oncol. Clin. North Am.*, vol. 9, no. 2, pp. 319–36, Apr. 1995.

[57] C. K. van Kalken, H. J. Broxterman, H. M. Pinedo, N. Feller, H. Dekker, J. Lankelma, and G. Giaccone, “Cortisol is transported by the multidrug resistance gene product P-glycoprotein.,” *Br. J. Cancer*, vol. 67, no. 2, pp. 284–9, Feb. 1993.

[58] P. Gros, J. Croop, and D. Housman, “Mammalian multidrug resistance gene: complete cDNA sequence indicates strong homology to bacterial transport proteins.,” *Cell*, vol. 47, no. 3, pp. 371–80, Nov. 1986.

[59] S. I. Hsu, L. Lothstein, and S. B. Horwitz, “Differential overexpression of three mdr gene family members in multidrug-resistant J774.2 mouse cells. Evidence that distinct P-glycoprotein precursors are encoded by unique mdr genes.,” *J. Biol. Chem.*, vol. 264, no. 20, pp. 12053–62, Jul. 1989.

[60] A. Devault and P. Gros, “Two members of the mouse mdr gene family confer multidrug resistance with overlapping but distinct drug specificities.,” *Mol. Cell. Biol.*, vol. 10, no. 4, pp. 1652–63, Apr. 1990.

[61] L. J. Goldstein, “MDR1 gene expression in solid tumours.,” *Eur. J. Cancer*, vol. 32A, no. 6, pp. 1039–50, Jun. 1996.

[62] A. H. Schinkel, U. Mayer, E. Wagenaar, C. A. Mol, L. van Deemter, J. J. Smit, M. A. van

der Valk, A. C. Voordouw, H. Spits, O. van Tellingen, J. M. Zijlmans, W. E. Fibbe, and P. Borst, “Normal viability and altered pharmacokinetics in mice lacking mdr1-type (drug-transporting) P-glycoproteins.,” *Proc. Natl. Acad. Sci. U. S. A.*, vol. 94, no. 8, pp. 4028–33, Apr. 1997.

[63] J. Liu, Y. Liu, D. A. Powell, M. P. Waalkes, and C. D. Klaassen, “Multidrug-resistance mdr1a/1b double knockout mice are more sensitive than wild type mice to acute arsenic toxicity, with higher arsenic accumulation in tissues.,” *Toxicology*, vol. 170, no. 1–2, pp. 55–62, Jan. 2002.

[64] D. R. Bell, J. H. Gerlach, N. Kartner, R. N. Buick, and V. Ling, “Detection of P-glycoprotein in ovarian cancer: a molecular marker associated with multidrug resistance.,” *J. Clin. Oncol.*, vol. 3, no. 3, pp. 311–315, Mar. 1985.

[65] L. J. Goldstein, H. Galski, A. Fojo, M. Willingham, S. L. Lai, A. Gazdar, R. Pirker, A. Green, W. Crist, and G. M. Brodeur, “Expression of a multidrug resistance gene in human cancers.,” *J. Natl. Cancer Inst.*, vol. 81, no. 2, pp. 116–24, Jan. 1989.

[66] M. M. Gottesman and I. H. Pastan, “The Role of Multidrug Resistance Efflux Pumps in Cancer: Revisiting a JNCI Publication Exploring Expression of the MDR1 (P-glycoprotein) Gene,” *J Natl Cancer Inst*, vol. 107, no. 9, Sep. 2015.

[67] S. C. Linn, A. H. Honkoop, K. Hoekman, P. van der Valk, H. M. Pinedo, and G. Giaccone, “p53 and P-glycoprotein are often co-expressed and are associated with poor prognosis in breast cancer.,” *Br. J. Cancer*, vol. 74, no. 1, pp. 63–8, Jul. 1996.

[68] M. R. Raspollini, G. Amunni, A. Villanucci, V. Boddi, and G. L. Taddei, “Increased cyclooxygenase-2 (COX-2) and P-glycoprotein-170 (MDR1) expression is associated with

chemotherapy resistance and poor prognosis. Analysis in ovarian carcinoma patients with low and high survival," *Int. J. Gynecol. Cancer*, vol. 15, no. 2, pp. 255–260, Mar. 2005.

[69] F. J. Hornicek, M. C. Gebhardt, M. W. Wolfe, F. D. Kharrazi, H. Takeshita, S. G. Parekh, D. Zurakowski, and H. J. Mankin, "P-glycoprotein levels predict poor outcome in patients with osteosarcoma.," *Clin. Orthop. Relat. Res.*, no. 373, pp. 11–7, Apr. 2000.

[70] M. Filipits, R. W. Suchomel, S. Zöchbauer, R. Brunner, K. Lechner, R. Pirker, and E. Vellenga, "Multidrug resistance-associated protein in acute myeloid leukemia: No impact on treatment outcome.," *Clin. Cancer Res.*, vol. 3, no. 8, pp. 1419–25, Aug. 1997.

[71] M. Pajic, J. K. Iyer, A. Kersbergen, E. van der Burg, A. O. H. Nygren, J. Jonkers, P. Borst, and S. Rottenberg, "Moderate Increase in Mdr1a/1b Expression Causes In vivo Resistance to Doxorubicin in a Mouse Model for Hereditary Breast Cancer," *Cancer Res.*, vol. 69, no. 16, pp. 6396–6404, Aug. 2009.

[72] L. Pusztai, P. Wagner, N. Ibrahim, E. Rivera, R. Theriault, D. Booser, F. W. Symmans, F. Wong, G. Blumenschein, D. R. Fleming, R. Rouzier, G. Boniface, and G. N. Hortobagyi, "Phase II study of tariquidar, a selective P-glycoprotein inhibitor, in patients with chemotherapy-resistant, advanced breast carcinoma," *Cancer*, vol. 104, no. 4, pp. 682–691, Aug. 2005.

[73] L. A. Doyle, W. Yang, L. V Abruzzo, T. Krogmann, Y. Gao, A. K. Rishi, and D. D. Ross, "A multidrug resistance transporter from human MCF-7 breast cancer cells.," *Proc. Natl. Acad. Sci. U. S. A.*, vol. 95, no. 26, pp. 15665–70, Dec. 1998.

[74] K. Miyake, L. Mickley, T. Litman, Z. Zhan, R. Robey, B. Cristensen, M. Brangi, L. Greenberger, M. Dean, T. Fojo, and S. E. Bates, "Molecular cloning of cDNAs which are

highly overexpressed in mitoxantrone-resistant cells: demonstration of homology to ABC transport genes.," *Cancer Res.*, vol. 59, no. 1, pp. 8–13, Jan. 1999.

[75] N. Khunweeraphong, T. Stockner, and K. Kuchler, "The structure of the human ABC transporter ABCG2 reveals a novel mechanism for drug extrusion," *Sci Rep*, vol. 7, no. 1, p. 13767, 2017.

[76] M. Jani, C. Ambrus, R. Magnan, K. T. Jakab, E. Beéry, J. K. Zolnerciks, and P. Krajcsi, "Structure and function of BCRP, a broad specificity transporter of xenobiotics and endobiotics," *Arch. Toxicol.*, vol. 88, no. 6, pp. 1205–1248, Jun. 2014.

[77] T. Nakanishi and D. D. Ross, "Breast cancer resistance protein (BCRP/ABCG2): its role in multidrug resistance and regulation of its gene expression.," *Chin. J. Cancer*, vol. 31, no. 2, pp. 73–99, Feb. 2012.

[78] Q. Wang, Y. Wang, X. Wang, X. Mo, J. Gu, Z. Lu, Z. Pan, and Y. Zhu, "Survivin up-regulates the expression of breast cancer resistance protein (BCRP) through attenuating the suppression of p53 on NF-κB expression in MCF-7/5-FU cells," *Int. J. Biochem. Cell Biol.*, vol. 45, no. 9, pp. 2036–2044, Sep. 2013.

[79] X. Wang, X. Wu, C. Wang, W. Zhang, Y. Ouyang, Y. Yu, and Z. He, "Transcriptional suppression of breast cancer resistance protein (BCRP) by wild-type p53 through the NF-κB pathway in MCF-7 cells," *FEBS Lett.*, vol. 584, no. 15, pp. 3392–3397, Aug. 2010.

[80] H. Tomiyasu, M. Watanabe, K. Sugita, Y. Goto-Koshino, Y. Fujino, K. Ohno, S. Sugano, and H. Tsujimoto, "Regulations of ABCB1 and ABCG2 expression through MAPK pathways in acute lymphoblastic leukemia cell lines.," *Anticancer Res.*, vol. 33, no. 12, pp. 5317–23, Dec. 2013.

[81] Y.-Z. Pan, M. E. Morris, and A.-M. Yu, “MicroRNA-328 negatively regulates the expression of breast cancer resistance protein (BCRP/ABCG2) in human cancer cells.,” *Mol. Pharmacol.*, vol. 75, no. 6, pp. 1374–9, Jun. 2009.

[82] M. Yoshikawa, S. Kasamatsu, M. Yasunaga, G. Wang, Y. Ikegami, H. Yoshida, S. Tarui, H. Yabuuchi, and T. Ishikawa, “Does ABCG2 Need a Heterodimer Partner? Expression and Functional Evaluation of ABCG2 (Arg 482)*,” *Drug Metab. Pharmacokinet.*, vol. 17, no. 2, pp. 130–135, Jan. 2002.

[83] K. Kage, T. Fujita, and Y. Sugimoto, “Role of Cys-603 in dimer/oligomer formation of the breast cancer resistance protein BCRP/ABCG2,” *Cancer Sci.*, vol. 96, no. 12, pp. 866–872, Dec. 2005.

[84] I. Manolaridis, S. M. Jackson, N. M. I. Taylor, J. Kowal, H. Stahlberg, and K. P. Locher, “Cryo-EM structures of a human ABCG2 mutant trapped in ATP-bound and substrate-bound states,” *Nature*, vol. 563, no. 7731, pp. 426–430, Nov. 2018.

[85] K. Noguchi, K. Katayama, and Y. Sugimoto, “Human ABC transporter ABCG2/BCRP expression in chemoresistance: basic and clinical perspectives for molecular cancer therapeutics.,” *Pharmgenomics. Pers. Med.*, vol. 7, pp. 53–64, 2014.

[86] R. Allikmets, L. M. Schriml, A. Hutchinson, V. Romano-Spica, and M. Dean, “A human placenta-specific ATP-binding cassette gene (ABCP) on chromosome 4q22 that is involved in multidrug resistance.,” *Cancer Res.*, vol. 58, no. 23, pp. 5337–9, Dec. 1998.

[87] M. Maliepaard, G. L. Scheffer, I. F. Faneyte, M. A. van Gastelen, A. C. Pijnenborg, A. H. Schinkel, M. J. van De Vijver, R. J. Scheper, and J. H. Schellens, “Subcellular localization and distribution of the breast cancer resistance protein transporter in normal human

tissues.," *Cancer Res.*, vol. 61, no. 8, pp. 3458–64, Apr. 2001.

[88] Q. Mao and J. D. Unadkat, "Role of the breast cancer resistance protein (BCRP/ABCG2) in drug transport--an update," *AAPS J*, vol. 17, no. 1, pp. 65–82, Jan. 2015.

[89] D. D. Ross, W. Yang, L. V Abruzzo, W. S. Dalton, E. Schneider, H. Lage, M. Dietel, L. Greenberger, S. P. Cole, and L. A. Doyle, "Atypical multidrug resistance: breast cancer resistance protein messenger RNA expression in mitoxantrone-selected cell lines.," *J. Natl. Cancer Inst.*, vol. 91, no. 5, pp. 429–33, Mar. 1999.

[90] D. Westover and F. Li, "New trends for overcoming ABCG2/BCRP-mediated resistance to cancer therapies.," *J. Exp. Clin. Cancer Res.*, vol. 34, p. 159, Dec. 2015.

[91] E. L. Volk and E. Schneider, "Wild-type breast cancer resistance protein (BCRP/ABCG2) is a methotrexate polyglutamate transporter.," *Cancer Res.*, vol. 63, no. 17, pp. 5538–43, Sep. 2003.

[92] G. L. Scheffer, M. Maliepaard, A. C. Pijnenborg, M. A. van Gastelen, M. C. de Jong, A. B. Schroeijers, D. M. van der Kolk, J. D. Allen, D. D. Ross, P. van der Valk, W. S. Dalton, J. H. Schellens, and R. J. Scheper, "Breast cancer resistance protein is localized at the plasma membrane in mitoxantrone- and topotecan-resistant cell lines.," *Cancer Res.*, vol. 60, no. 10, pp. 2589–93, May 2000.

[93] K. Nakatomi, M. Yoshikawa, M. Oka, Y. Ikegami, S. Hayasaka, K. Sano, K. Shiozawa, S. Kawabata, H. Soda, T. Ishikawa, S. Tanabe, and S. Kohno, "Transport of 7-Ethyl-10-hydroxycamptothecin (SN-38) by Breast Cancer Resistance Protein ABCG2 in Human Lung Cancer Cells," *Biochem. Biophys. Res. Commun.*, vol. 288, no. 4, pp. 827–832, Nov. 2001.

[94] C. de Wolf, R. Jansen, H. Yamaguchi, M. de Haas, K. van de Wetering, J. Wijnholds, J. Beijnen, and P. Borst, “Contribution of the drug transporter ABCG2 (breast cancer resistance protein) to resistance against anticancer nucleosides,” *Mol. Cancer Ther.*, vol. 7, no. 9, pp. 3092–3102, Sep. 2008.

[95] D. K. Maurya, R. Ayuzawa, C. Doi, D. Troyer, and M. Tamura, “Topoisomerase I inhibitor SN-38 effectively attenuates growth of human non-small cell lung cancer cell lines in vitro and in vivo.,” *J. Environ. Pathol. Toxicol. Oncol.*, vol. 30, no. 1, pp. 1–10, 2011.

[96] P. L. Bonate, L. Arthaud, W. R. Cantrell, K. Stephenson, J. A. Secrist, and S. Weitman, “Discovery and development of clofarabine: a nucleoside analogue for treating cancer,” *Nat. Rev. Drug Discov.*, vol. 5, no. 10, pp. 855–863, Oct. 2006.

[97] P. Agostinis, K. Berg, K. A. Cengel, T. H. Foster, A. W. Girotti, S. O. Gollnick, S. M. Hahn, M. R. Hamblin, A. Juzeniene, D. Kessel, M. Korbelik, J. Moan, P. Mroz, D. Nowis, J. Piette, B. C. Wilson, and J. Golab, “Photodynamic therapy of cancer: an update.,” *CA. Cancer J. Clin.*, vol. 61, no. 4, pp. 250–81, 2011.

[98] J. Morgan, J. D. Jackson, X. Zheng, S. K. Pandey, and R. K. Pandey, “Substrate affinity of photosensitizers derived from chlorophyll-a: the ABCG2 transporter affects the phototoxic response of side population stem cell-like cancer cells to photodynamic therapy.,” *Mol. Pharm.*, vol. 7, no. 5, pp. 1789–804, Oct. 2010.

[99] W. J. Huss, D. R. Gray, N. M. Greenberg, J. L. Mohler, and G. J. Smith, “Breast Cancer Resistance Protein–Mediated Efflux of Androgen in Putative Benign and Malignant Prostate Stem Cells,” *Cancer Res.*, vol. 65, no. 15, pp. 6640–6650, Aug. 2005.

[100] Z.-F. Ning, Y.-J. Huang, T.-X. Lin, Y.-X. Zhou, C. Jiang, K.-W. Xu, H. Huang, X.-B. Yin, and J. Huang, “Subpopulations of Stem-like Cells in Side Population Cells from the Human Bladder Transitional Cell Cancer Cell Line T24,” *J. Int. Med. Res.*, vol. 37, no. 3, pp. 621–630, May 2009.

[101] D. D. Ross, J. E. Karp, T. T. Chen, and L. A. Doyle, “Expression of breast cancer resistance protein in blast cells from patients with acute leukemia.,” *Blood*, vol. 96, no. 1, pp. 365–8, Jul. 2000.

[102] M. van den Heuvel-Eibrink, E. Wiemer, A. Prins, J. Meijerink, P. Vossebeld, B. van der Holt, R. Pieters, and P. Sonneveld, “Increased expression of the breast cancer resistance protein (BCRP) in relapsed or refractory acute myeloid leukemia (AML),” *Leukemia*, vol. 16, no. 5, pp. 833–839, May 2002.

[103] Z. Benderra, A.-M. Faussat, L. Sayada, J.-Y. Perrot, D. Chaoui, J.-P. Marie, and O. Legrand, “Breast Cancer Resistance Protein and P-Glycoprotein in 149 Adult Acute Myeloid Leukemias,” *Clin. Cancer Res.*, vol. 10, no. 23, pp. 7896–7902, Dec. 2004.

[104] S. L. A. Plasschaert, D. M. van der Kolk, E. S. J. M. de Bont, W. A. Kamps, K. Morisaki, S. E. Bates, G. L. Scheffer, R. J. Scheper, E. Vellenga, and E. G. E. de Vries, “The role of breast cancer resistance protein in acute lymphoblastic leukemia.,” *Clin. Cancer Res.*, vol. 9, no. 14, pp. 5171–7, Nov. 2003.

[105] A. Sauerbrey, W. Sell, D. Steinbach, A. Voigt, and F. Zintl, “Expression of the BCRP gene (ABCG2/MXR/ABCP) in childhood acute lymphoblastic leukaemia.,” *Br. J. Haematol.*, vol. 118, no. 1, pp. 147–50, Jul. 2002.

[106] N. E. Jordanides, H. G. Jorgensen, T. L. Holyoake, and J. C. Mountford, “Functional

ABCG2 is overexpressed on primary CML CD34+ cells and is inhibited by imatinib mesylate," *Blood*, vol. 108, no. 4, pp. 1370–1373, Aug. 2006.

[107] W. Mo and J.-T. Zhang, "Human ABCG2: structure, function, and its role in multidrug resistance.," *Int. J. Biochem. Mol. Biol.*, vol. 3, no. 1, pp. 1–27, 2012.

[108] E. Monzani, F. Facchetti, E. Galmozzi, E. Corsini, A. Benetti, C. Cavazzin, A. Gritti, A. Piccinini, D. Porro, M. Santinami, G. Invernici, E. Parati, G. Alessandri, and C. A. M. La Porta, "Melanoma contains CD133 and ABCG2 positive cells with enhanced tumourigenic potential," *Eur. J. Cancer*, vol. 43, no. 5, pp. 935–946, Mar. 2007.

[109] T. Reya, S. J. Morrison, M. F. Clarke, and I. L. Weissman, "Stem cells, cancer and cancer stem cells," *Nature*, vol. 414, no. 6859, pp. 105–111, Nov. 2001.

[110] M. Yang, P. Liu, and P. Huang, "Cancer stem cells, metabolism, and therapeutic significance," *Tumor Biol.*, vol. 37, no. 5, pp. 5735–5742, May 2016.

[111] X. Ding, J. Wu, and C. Jiang, "ABCG2: A potential marker of stem cells and novel target in stem cell and cancer therapy," *Life Sci.*, vol. 86, no. 17–18, pp. 631–637, Apr. 2010.

[112] M. Díaz-Coránguez, C. Ramos, and D. A. Antonetti, "The inner blood-retinal barrier: Cellular basis and development," *Vision Res.*, vol. 139, pp. 123–137, Oct. 2017.

[113] N. Strazielle and J. F. Ghersi-Egea, "Physiology of Blood–Brain Interfaces in Relation to Brain Disposition of Small Compounds and Macromolecules," *Mol. Pharm.*, vol. 10, no. 5, pp. 1473–1491, May 2013.

[114] F. L. Cardoso, D. Brites, and M. A. Brito, "Looking at the blood–brain barrier: Molecular anatomy and possible investigation approaches," *Brain Res. Rev.*, vol. 64, no. 2, pp. 328–363, Sep. 2010.

[115] Y. Serlin, I. Shelef, B. Knyazer, and A. Friedman, “Anatomy and physiology of the blood-brain barrier.,” *Semin. Cell Dev. Biol.*, vol. 38, pp. 2–6, Feb. 2015.

[116] R. Daneman and A. Prat, “The blood-brain barrier.,” *Cold Spring Harb. Perspect. Biol.*, vol. 7, no. 1, p. a020412, Jan. 2015.

[117] Y. Sharif, F. Jumah, L. Coplan, A. Krosser, K. Sharif, and R. S. Tubbs, “Blood brain barrier: A review of its anatomy and physiology in health and disease,” *Clin. Anat.*, vol. 31, no. 6, pp. 812–823, Sep. 2018.

[118] D. J. Begley, “ABC transporters and the blood-brain barrier.,” *Curr. Pharm. Des.*, vol. 10, no. 12, pp. 1295–312, 2004.

[119] D. S. Miller, “Regulation of ABC transporters at the blood-brain barrier.,” *Clin. Pharmacol. Ther.*, vol. 97, no. 4, pp. 395–403, Apr. 2015.

[120] R. Sane, S. Agarwal, R. K. Mittapalli, and W. F. Elmquist, “Saturable Active Efflux by P-Glycoprotein and Breast Cancer Resistance Protein at the Blood-Brain Barrier Leads to Nonlinear Distribution of Elacridar to the Central Nervous System,” *J. Pharmacol. Exp. Ther.*, vol. 345, no. 1, pp. 111–124, Apr. 2013.

[121] F. Helm and G. Fricker, “Liposomal conjugates for drug delivery to the central nervous system.,” *Pharmaceutics*, vol. 7, no. 2, pp. 27–42, Apr. 2015.

[122] F. E. O’Brien, T. G. Dinan, B. T. Griffin, and J. F. Cryan, “Interactions between antidepressants and P-glycoprotein at the blood-brain barrier: clinical significance of in vitro and in vivo findings.,” *Br. J. Pharmacol.*, vol. 165, no. 2, pp. 289–312, Jan. 2012.

[123] W. Löscher and H. Potschka, “Blood-brain barrier active efflux transporters: ATP-binding cassette gene family.,” *NeuroRx*, vol. 2, no. 1, pp. 86–98, Jan. 2005.

[124] P. Breedveld, D. Pluim, G. Cipriani, P. Wielinga, O. van Tellingen, A. H. Schinkel, and J. H. M. Schellens, “The Effect of Bcrp1 (Abcg2) on the *In vivo* Pharmacokinetics and Brain Penetration of Imatinib Mesylate (Gleevec): Implications for the Use of Breast Cancer Resistance Protein and P-Glycoprotein Inhibitors to Enable the Brain Penetration of Imatinib in Patients,” *Cancer Res.*, vol. 65, no. 7, pp. 2577–2582, Apr. 2005.

[125] K. Kawamura, T. Yamasaki, J. Yui, A. Hatori, F. Konno, K. Kumata, T. Irie, T. Fukumura, K. Suzuki, I. Kanno, and M.-R. Zhang, “In vivo evaluation of P-glycoprotein and breast cancer resistance protein modulation in the brain using [11C]gefitinib,” *Nucl. Med. Biol.*, vol. 36, no. 3, pp. 239–246, Apr. 2009.

[126] E. M. Kemper, A. E. van Zandbergen, C. Cleypool, H. A. Mos, W. Boogerd, J. H. Beijnen, and O. van Tellingen, “Increased penetration of paclitaxel into the brain by inhibition of P-Glycoprotein.,” *Clin. Cancer Res.*, vol. 9, no. 7, pp. 2849–55, Jul. 2003.

[127] N. Shaik, N. Giri, G. Pan, and W. F. Elmquist, “P-glycoprotein-Mediated Active Efflux of the Anti-HIV1 Nucleoside Abacavir Limits Cellular Accumulation and Brain Distribution,” *Drug Metab. Dispos.*, vol. 35, no. 11, pp. 2076–2085, Aug. 2007.

[128] R. B. Kim, M. F. Fromm, C. Wandel, B. Leake, A. J. Wood, D. M. Roden, and G. R. Wilkinson, “The drug transporter P-glycoprotein limits oral absorption and brain entry of HIV-1 protease inhibitors.,” *J. Clin. Invest.*, vol. 101, no. 2, pp. 289–294, Jan. 1998.

[129] J. W. Polli, T. M. Baughman, J. E. Humphreys, K. H. Jordan, A. L. Mote, J. A. Salisbury, T. K. Tippin, and C. J. Serabjit-Singh, “P-glycoprotein Influences the Brain Concentrations of Cetirizine (Zyrtec®), a Second-Generation Non-Sedating Antihistamine,” *J. Pharm. Sci.*, vol. 92, no. 10, pp. 2082–2089, Oct. 2003.

[130] C. Luna-Tortós, M. Fedrowitz, and W. Löscher, “Several major antiepileptic drugs are substrates for human P-glycoprotein,” *Neuropharmacology*, vol. 55, no. 8, pp. 1364–1375, Dec. 2008.

[131] J. S. Lagas, R. W. Sparidans, R. A. B. van Waterschoot, E. Wagenaar, J. H. Beijnen, and A. H. Schinkel, “P-Glycoprotein Limits Oral Availability, Brain Penetration, and Toxicity of an Anionic Drug, the Antibiotic Salinomycin,” *Antimicrob. Agents Chemother.*, vol. 52, no. 3, pp. 1034–1039, Mar. 2008.

[132] S. Agarwal, A. M. S. Hartz, W. F. Elmquist, and B. Bauer, “Breast cancer resistance protein and P-glycoprotein in brain cancer: two gatekeepers team up.,” *Curr. Pharm. Des.*, vol. 17, no. 26, pp. 2793–802, 2011.

[133] K. Yusa and T. Tsuruo, “Reversal mechanism of multidrug resistance by verapamil: direct binding of verapamil to P-glycoprotein on specific sites and transport of verapamil outward across the plasma membrane of K562/ADM cells.,” *Cancer Res.*, vol. 49, no. 18, pp. 5002–6, Sep. 1989.

[134] T. Tsuruo, H. Iida, M. Nojiri, S. Tsukagoshi, and Y. Sakurai, “Circumvention of vincristine and Adriamycin resistance in vitro and in vivo by calcium influx blockers.,” *Cancer Res.*, vol. 43, no. 6, pp. 2905–10, Jun. 1983.

[135] T. Tsuruo, H. Iida, S. Tsukagoshi, and Y. Sakurai, “Overcoming of vincristine resistance in P388 leukemia in vivo and in vitro through enhanced cytotoxicity of vincristine and vinblastine by verapamil.,” *Cancer Res.*, vol. 41, no. 5, pp. 1967–72, May 1981.

[136] M. L. Amin, “P-glycoprotein Inhibition for Optimal Drug Delivery.,” *Drug Target Insights*, vol. 7, pp. 27–34, Aug. 2013.

[137] A. M. Rogan, T. C. Hamilton, R. C. Young, R. W. Klecker, and R. F. Ozols, “Reversal of adriamycin resistance by verapamil in human ovarian cancer.,” *Science*, vol. 224, no. 4652, pp. 994–6, Jun. 1984.

[138] S. Eberl, B. Renner, A. Neubert, M. Reisig, I. Bachmakov, J. König, F. Dörje, T. E. Mürdter, A. Ackermann, H. Dormann, K. G. Gassmann, E. G. Hahn, S. Zierhut, K. Brune, and M. F. Fromm, “Role of P-Glycoprotein Inhibition for Drug Interactions,” *Clin. Pharmacokinet.*, vol. 46, no. 12, pp. 1039–1049, 2007.

[139] W. T. van der Graaf, E. G. de Vries, H. Timmer-Bosscha, G. J. Meersma, G. Mesander, E. Vellenga, and N. H. Mulder, “Effects of amiodarone, cyclosporin A, and PSC 833 on the cytotoxicity of mitoxantrone, doxorubicin, and vincristine in non-P-glycoprotein human small cell lung cancer cell lines.,” *Cancer Res.*, vol. 54, no. 20, pp. 5368–73, Oct. 1994.

[140] X. Zhu, M. Sui, and W. Fan, “In vitro and in vivo characterizations of tetrandrine on the reversal of P-glycoprotein-mediated drug resistance to paclitaxel.,” *Anticancer Res.*, vol. 25, no. 3B, pp. 1953–62.

[141] M. F. Ullah, “Cancer multidrug resistance (MDR): a major impediment to effective chemotherapy.,” *Asian Pac. J. Cancer Prev.*, vol. 9, no. 1, pp. 1–6.

[142] W. H. Wilson, C. Jamis-Dow, G. Bryant, F. M. Balis, R. W. Klecker, S. E. Bates, B. A. Chabner, S. M. Steinberg, D. R. Kohler, and R. E. Wittes, “Phase I and pharmacokinetic study of the multidrug resistance modulator dexverapamil with EPOCH chemotherapy.,” *J. Clin. Oncol.*, vol. 13, no. 8, pp. 1985–1994, Aug. 1995.

[143] L. D. Weidner, K. L. Fung, P. Kannan, J. K. Moen, J. S. Kumar, J. Mulder, R. B. Innis, M. M. Gottesman, and M. D. Hall, “Tariquidar Is an Inhibitor and Not a Substrate of Human

and Mouse P-glycoprotein," *Drug Metab. Dispos.*, vol. 44, no. 2, pp. 275–282, Jan. 2016.

[144] C. Martin, G. Berridge, P. Mistry, C. Higgins, P. Charlton, and R. Callaghan, "The molecular interaction of the high affinity reversal agent XR9576 with P-glycoprotein," *Br. J. Pharmacol.*, vol. 128, no. 2, pp. 403–411, Sep. 1999.

[145] L. Liu, A. C. Collier, J. M. Link, K. B. Domino, D. A. Mankoff, J. F. Eary, C. F. Spiekerman, P. Hsiao, A. K. Deo, and J. D. Unadkat, "Modulation of P-glycoprotein at the Human Blood-Brain Barrier by Quinidine or Rifampin Treatment: A Positron Emission Tomography Imaging Study.," *Drug Metab. Dispos.*, vol. 43, no. 11, pp. 1795–804, Nov. 2015.

[146] N. Ogushi, K. Sasaki, and M. Shimoda, "CAN a P-gp modulator assist in the control of methotrexate concentrations in the rat brain? -inhibitory effects of rhodamine 123, a specific substrate for P-gp, on methotrexate excretion from the rat brain and its optimal route of administration.," *J. Vet. Med. Sci.*, vol. 79, no. 2, pp. 320–327, Feb. 2017.

[147] P. Breedveld, J. H. Beijnen, and J. H. M. Schellens, "Use of P-glycoprotein and BCRP inhibitors to improve oral bioavailability and CNS penetration of anticancer drugs," *Trends Pharmacol. Sci.*, vol. 27, no. 1, pp. 17–24, Jan. 2006.

[148] S. Shukla, R. W. Robey, S. E. Bates, and S. V. Ambudkar, "Sunitinib (Sutent, SU11248), a Small-Molecule Receptor Tyrosine Kinase Inhibitor, Blocks Function of the ATP-Binding Cassette (ABC) Transporters P-Glycoprotein (ABCB1) and ABCG2," *Drug Metab. Dispos.*, vol. 37, no. 2, pp. 359–365, Feb. 2009.

[149] L. N. Eadie, T. P. Hughes, and D. L. White, "Interaction of the Efflux Transporters ABCB1 and ABCG2 With Imatinib, Nilotinib, and Dasatinib," *Clin. Pharmacol. Ther.*,

vol. 95, no. 3, pp. 294–306, Mar. 2014.

[150] S. K. Rabindran, D. D. Ross, L. A. Doyle, W. Yang, and L. M. Greenberger, "Fumitremorgin C reverses multidrug resistance in cells transfected with the breast cancer resistance protein.," *Cancer Res.*, vol. 60, no. 1, pp. 47–50, Jan. 2000.

[151] J. D. Allen, A. van Loevezijn, J. M. Lakhai, M. van der Valk, O. van Tellingen, G. Reid, J. H. M. Schellens, G.-J. Koomen, and A. H. Schinkel, "Potent and specific inhibition of the breast cancer resistance protein multidrug transporter in vitro and in mouse intestine by a novel analogue of fumitremorgin C.," *Mol. Cancer Ther.*, vol. 1, no. 6, pp. 417–25, Apr. 2002.

[152] P. Breedveld, N. Zelcer, D. Pluim, Ö. Sönmezer, M. M. Tibben, J. H. Beijnen, A. H. Schinkel, O. van Tellingen, P. Borst, and J. H. M. Schellens, "Mechanism of the Pharmacokinetic Interaction between Methotrexate and Benzimidazoles," *Cancer Res.*, vol. 64, no. 16, pp. 5804–5811, Aug. 2004.

[153] G. D. Pennock, W. S. Dalton, W. R. Roeske, C. P. Appleton, K. Mosley, P. Plezia, T. P. Miller, and S. E. Salmon, "Systemic toxic effects associated with high-dose verapamil infusion and chemotherapy administration.," *J. Natl. Cancer Inst.*, vol. 83, no. 2, pp. 105–10, Jan. 1991.

[154] T. P. Miller, T. M. Grogan, W. S. Dalton, C. M. Spier, R. J. Scheper, and S. E. Salmon, "P-glycoprotein expression in malignant lymphoma and reversal of clinical drug resistance with chemotherapy plus high-dose verapamil.," *J. Clin. Oncol.*, vol. 9, no. 1, pp. 17–24, Jan. 1991.

[155] R. F. Ozols, R. E. Cunnion, R. W. Klecker, T. C. Hamilton, Y. Ostchega, J. E. Parrillo,

and R. C. Young, “Verapamil and adriamycin in the treatment of drug-resistant ovarian cancer patients.,” *J. Clin. Oncol.*, vol. 5, no. 4, pp. 641–647, Apr. 1987.

[156] A. F. List, K. J. Kopecky, C. L. Willman, D. R. Head, D. L. Persons, M. L. Slovak, R. Dorr, C. Karanes, H. E. Hynes, J. H. Doroshow, M. Shurafa, and F. R. Appelbaum, “Benefit of cyclosporine modulation of drug resistance in patients with poor-risk acute myeloid leukemia: a Southwest Oncology Group study.,” *Blood*, vol. 98, no. 12, pp. 3212–20, Dec. 2001.

[157] T. Saeki, T. Nomizu, M. Toi, Y. Ito, S. Noguchi, T. Kobayashi, T. Asaga, H. Minami, N. Yamamoto, K. Aogi, T. Ikeda, Y. Ohashi, W. Sato, and T. Tsuruo, “Dofequidar fumarate (MS-209) in combination with cyclophosphamide, doxorubicin, and fluorouracil for patients with advanced or recurrent breast cancer.,” *J. Clin. Oncol.*, vol. 25, no. 4, pp. 411–7, Feb. 2007.

[158] J. Abraham, M. Edgerly, R. Wilson, C. Chen, A. Rutt, S. Bakke, R. Robey, A. Dwyer, B. Goldspiel, F. Balis, O. Van Tellingen, S. E. Bates, and T. Fojo, “A Phase I Study of the P-Glycoprotein Antagonist Tariquidar in Combination with Vinorelbine,” *Clin. Cancer Res.*, vol. 15, no. 10, pp. 3574–3582, May 2009.

[159] J. W Ricci, D. Lovato, and R. S. Larson, “ABCG2 Inhibitors: Will They Find Clinical Relevance?,” *J. Depress. Anxiety*, vol. 04, no. 05, pp. 1–6, Oct. 2015.

[160] A. Carrato, A. Swieboda-Sadlej, M. Staszewska-Skurczynska, R. Lim, L. Roman, Y. Shparyk, I. Bondarenko, D. J. Jonker, Y. Sun, J. A. De la Cruz, J. A. Williams, B. Korytowsky, J. G. Christensen, X. Lin, J. M. Tursi, M. J. Lechuga, and E. Van Cutsem, “Fluorouracil, Leucovorin, and Irinotecan Plus Either Sunitinib or Placebo in Metastatic

Colorectal Cancer: A Randomized, Phase III Trial," *J. Clin. Oncol.*, vol. 31, no. 10, pp. 1341–1347, Apr. 2013.

[161] C. C. Wagner, M. Bauer, R. Karch, T. Feurstein, S. Kopp, P. Chiba, K. Kletter, W. Loscher, M. Muller, M. Zeitlinger, and O. Langer, "A Pilot Study to Assess the Efficacy of Tariquidar to Inhibit P-glycoprotein at the Human Blood-Brain Barrier with (R)-11C-Verapamil and PET," *J. Nucl. Med.*, vol. 50, no. 12, pp. 1954–1961, Dec. 2009.

[162] W. C. Kreisl, R. Bhatia, C. L. Morse, A. E. Woock, S. S. Zoghbi, H. U. Shetty, V. W. Pike, and R. B. Innis, "Increased Permeability-Glycoprotein Inhibition at the Human Blood-Brain Barrier Can Be Safely Achieved by Performing PET During Peak Plasma Concentrations of Tariquidar," *J. Nucl. Med.*, vol. 56, no. 1, pp. 82–87, Jan. 2015.

[163] C. M. F. Kruijtzer, J. H. Beijnen, H. Rosing, W. W. ten Bokkel Huinink, M. Schot, R. C. Jewell, E. M. Paul, and J. H. M. Schellens, "Increased oral bioavailability of topotecan in combination with the breast cancer resistance protein and P-glycoprotein inhibitor GF120918.," *J. Clin. Oncol.*, vol. 20, no. 13, pp. 2943–50, Jul. 2002.

[164] F. K. Brewer, C. A. Follit, P. D. Vogel, and J. G. Wise, "In silico Screening for Inhibitors of P-Glycoprotein that Target the Nucleotide Binding Domains," *Mol. Pharmacol.*, vol. 86, no. 6, pp. 716–726, Dec. 2014.

[165] C. A. Follit, F. K. Brewer, J. G. Wise, P. D. Vogel, and D. Vogel, "In silico identified targeted inhibitors of P-glycoprotein overcome multidrug resistance in human cancer cells in culture," *Pharmacol Res Perspect*, vol. 3, no. 5, p. e00170, Oct. 2015.

[166] M. M. van den Heuvel-Eibrink, P. Sonneveld, and R. Pieters, "The prognostic significance of membrane transport-associated multidrug resistance (MDR) proteins in leukemia.," *Int.*

J. Clin. Pharmacol. Ther., vol. 38, no. 3, pp. 94–110, Mar. 2000.

[167] R. J. Ferreira, D. J. dos Santos, and M.-J. J. U. Ferreira, "P-glycoprotein and membrane roles in multidrug resistance," *Futur. Med Chem*, vol. 7, no. 7, pp. 929–946, Jun. 2015.

[168] C. F. Higgins, "Multiple molecular mechanisms for multidrug resistance transporters," *Nature*, vol. 446, no. 7137, pp. 749–757, 2007.

[169] S. Ou-Yang, J. Lu, X. Kong, Z. Liang, C. Luo, and H. Jiang, "Computational drug discovery," *Acta Pharmacol. Sin.*, vol. 33, no. 9, pp. 1131–1140, Sep. 2012.

[170] J. J. Irwin and B. K. Shoichet, "ZINC - A free database of commercially available compounds for virtual screening," *J. Chem. Inf. Model.*, vol. 45, no. 1, pp. 177–182, 2005.

[171] J. J. Irwin, T. Sterling, M. M. Mysinger, E. S. Bolstad, and R. G. Coleman, "ZINC: A Free Tool to Discover Chemistry for Biology," *J Chem Inf Model*, vol. 52, no. 7, pp. 1757–1768, 2012.

[172] M. Takeda, A. Mizokami, K. Mamiya, Q. L. You, J. Zhang, E. T. Keller, and M. Namiki, "The establishment of two paclitaxel-resistant prostate cancer cell lines and the mechanisms of paclitaxel resistance with two cell lines," *Prostate*, vol. 67, no. 9, pp. 955–967, Jun. 2007.

[173] S. D. Breul, K. H. Bradley, A. J. Hance, M. P. Schafer, R. A. Berg, and R. G. Crystal, "Control of collagen production by human diploid lung fibroblasts," *J Biol Chem*, vol. 255, no. 11, pp. 5250–5260, 1980.

[174] A. Eva, K. C. Robbins, P. R. Andersen, A. Srinivasan, S. R. Tronick, E. P. Reddy, N. W. Ellmore, A. T. Galen, J. A. Lautenberger, T. S. Papas, E. H. Westin, F. Wong-Staal, R. C. Gallo, and S. A. Aaronson, "Cellular genes analogous to retroviral onc genes are

transcribed in human tumour cells.," *Nature*, vol. 295, no. 5845, pp. 116–9, Jan. 1982.

[175] T. L. Riss, R. A. Moravec, A. L. Niles, H. A. Benink, T. J. Worzella, and L. Minor, "Cell Viability Assays," in *Assay Guidance Manual*, G. S. Sittampalam, N. Gal-Edd, M. Arkin, D. Auld, C. Austin, B. Bejcek, M. Glicksman, J. Inglese, V. Lemmon, Z. Li, J. McGee, O. McManus, L. Minor, A. Napper, T. Riss, O. J. Trask, and J. Weidner, Eds. Bethesda (MD), 2004.

[176] J. O'Brien, I. Wilson, T. Orton, and F. Pognan, "Investigation of the Alamar Blue (resazurin) fluorescent dye for the assessment of mammalian cell cytotoxicity.," *Eur. J. Biochem.*, vol. 267, no. 17, pp. 5421–6, Sep. 2000.

[177] C. H. Yang, Y. C. Chen, and M. L. Kuo, "Novobiocin sensitizes BCRP/MXR/ABCP overexpressing topotecan-resistant human breast carcinoma cells to topotecan and mitoxantrone," *Anticancer Res*, vol. 23, no. 3B, pp. 2519–2523, 2003.

[178] M. Issandou and T. Grand-Perret, "Multidrug resistance P-glycoprotein is not involved in cholesterol esterification," *Biochem Biophys Res Commun*, vol. 279, no. 2, pp. 369–377, 2000.

[179] D. Ribble, N. B. Goldstein, D. A. Norris, and Y. G. Shellman, "A simple technique for quantifying apoptosis in 96-well plates," *BMC Biotechnol*, vol. 5, p. 12, 2005.

[180] K. Liu, P. C. Liu, R. Liu, and X. Wu, "Dual AO/EB staining to detect apoptosis in osteosarcoma cells compared with flow cytometry," *Med Sci Monit Basic Res*, vol. 21, pp. 15–20, 2015.

[181] Y. Sun, Y.-X. X. Li, H.-J. J. Wu, S.-H. H. Wu, Y. A. Wang, D.-Z. Z. Luo, and D. J. Liao, "Effects of an Indolocarbazole-Derived CDK4 Inhibitor on Breast Cancer Cells," *J*

Cancer, vol. 2, no. 2, pp. 36–51, 2011.

[182] C. P. Evans, F. Elfman, G. Cunha, and M. A. Shuman, "Decreased prostate cancer cell migration by inhibition of the insulin-like growth factor II/Mannose-6-Phosphate receptor," *Urol Oncol*, vol. 3, no. 5–6, pp. 166–170, 1997.

[183] M. L. Valero, F. Mello de Queiroz, W. Stuhmer, F. Viana, L. A. Pardo, W. Stü Hmer, F. Viana, and L. A. Pardo, "TRPM8 ion channels differentially modulate proliferation and cell cycle distribution of normal and cancer prostate cells," *PLoS One*, vol. 7, no. 12, p. e51825, 2012.

[184] C. C. Liang, A. Y. Park, and J. L. Guan, "In vitro scratch assay: a convenient and inexpensive method for analysis of cell migration in vitro," *Nat Protoc*, vol. 2, no. 2, pp. 329–333, 2007.

[185] L. Homolya, Z. Holló, U. A. Germann, I. Pastan, M. M. Gottesman, and B. Sarkadi, "Fluorescent cellular indicators are extruded by the multidrug resistance protein," *J. Biol. Chem.*, vol. 268, no. 29, pp. 21493–21496, 1993.

[186] S. Y. Shin, B. H. Choi, J. R. Kim, J. H. Kim, and Y. H. Lee, "Suppression of P-glycoprotein expression by antipsychotics trifluoperazine in adriamycin-resistant L1210 mouse leukemia cells," *Eur J Pharm Sci*, vol. 28, no. 4, pp. 300–306, 2006.

[187] B. H. Choi, C. G. Kim, Y. Lim, S. Y. Shin, and Y. H. Lee, "Curcumin down-regulates the multidrug-resistance mdr1b gene by inhibiting the PI3K/Akt/NF kappa B pathway," *Cancer Lett*, vol. 259, no. 1, pp. 111–118, 2008.

[188] F. Di Nicolantonio, L. A. Knight, S. Glaysher, P. A. Whitehouse, S. J. Mercer, S. Sharma, L. Mills, A. Prin, P. Johnson, P. A. Charlton, D. Norris, and I. A. Cree, "Ex vivo reversal

of chemoresistance by tariquidar (XR9576)," *Anticancer Drugs*, vol. 15, no. 9, pp. 861–869, 2004.

[189] A. Tamaki, C. Ierano, G. Szakacs, R. W. Robey, and S. E. Bates, "The controversial role of ABC transporters in clinical oncology," *Essays Biochem*, vol. 50, no. 1, pp. 209–232, 2011.

[190] H. D. Soule, J. Vazguez, A. Long, S. Albert, and M. Brennan, "A human cell line from a pleural effusion derived from a breast carcinoma.," *J. Natl. Cancer Inst.*, vol. 51, no. 5, pp. 1409–16, Nov. 1973.

[191] M. Nakagawa, E. Schneider, K. H. Dixon, J. Horton, K. Kelley, C. Morrow, and K. H. Cowan, "Reduced intracellular drug accumulation in the absence of P-glycoprotein (mdr1) overexpression in mitoxantrone-resistant human MCF-7 breast cancer cells.," *Cancer Res.*, vol. 52, no. 22, pp. 6175–81, Nov. 1992.

[192] J. van Meerloo, G. J. Kaspers, and J. Cloos, "Cell sensitivity assays: the MTT assay," *Methods Mol Biol*, vol. 731, pp. 237–245, 2011.

[193] M. V Berridge and A. S. Tan, "Characterization of the cellular reduction of 3-(4,5-dimethylthiazol-2-yl)-2,5-diphenyltetrazolium bromide (MTT): subcellular localization, substrate dependence, and involvement of mitochondrial electron transport in MTT reduction," *Arch Biochem Biophys*, vol. 303, no. 2, pp. 474–482, 1993.

[194] K. R. Stone, D. D. Mickey, H. Wunderli, G. H. Mickey, and D. F. Paulson, "Isolation of a human prostate carcinoma cell line (DU 145).," *Int. J. cancer*, vol. 21, no. 3, pp. 274–81, Mar. 1978.

[195] T. C. Hamilton, R. C. Young, and R. F. Ozols, "Experimental model systems of ovarian

cancer: applications to the design and evaluation of new treatment approaches.," *Semin. Oncol.*, vol. 11, no. 3, pp. 285–98, Sep. 1984.

[196] U. K. Laemmli, "Cleavage of structural proteins during the assembly of the head of bacteriophage T4," *Nature*, vol. 227, no. 5259, pp. 680–685, 1970.

[197] S. N. Rampersad, "Multiple applications of Alamar Blue as an indicator of metabolic function and cellular health in cell viability bioassays," *Sensors (Basel)*, vol. 12, no. 9, pp. 12347–12360, Sep. 2012.

[198] M.-T. Ma, M. He, Y. Wang, X.-Y. Jiao, L. Zhao, X.-F. Bai, Z.-J. Yu, H.-Z. Wu, M.-L. Sun, Z.-G. Song, and M.-J. Wei, "MiR-487a resensitizes mitoxantrone (MX)-resistant breast cancer cells (MCF-7/MX) to MX by targeting breast cancer resistance protein (BCRP/ABCG2)," *Cancer Lett.*, vol. 339, no. 1, pp. 107–115, Oct. 2013.

[199] W. S. Rasband, "ImageJ." [Online]. Available: https://imagej.nih.gov/ij/.

[200] J. Friedrich, C. Seidel, R. Ebner, L. A. Kunz-Schughart, & Leoni, and A. Kunz-Schughart, "Spheroid-based drug screen: considerations and practical approach," *Nat Protoc*, vol. 4, no. 3, pp. 309–324, 2009.

[201] C.-Y. Wu, Y. Feng, E. R. Cardenas, N. Williams, P. E. Floreancig, J. K. De Brabander, and M. G. Roth, "Studies toward the unique pederin family member psymberin: structure–activity relationships, biochemical studies, and genetics identify the mode-of-action of psymberin," *J. Am. Chem. Soc.*, vol. 134, no. 46, pp. 18998–19003, 2012.

[202] F. Bray, J. Ferlay, I. Soerjomataram, R. L. Siegel, L. A. Torre, and A. Jemal, "Global cancer statistics 2018: GLOBOCAN estimates of incidence and mortality worldwide for 36 cancers in 185 countries," *CA. Cancer J. Clin.*, vol. 68, no. 6, pp. 394–424, Nov. 2018.

[203] W. P. McGuire, M. Markman, and M. Markman, “Primary ovarian cancer chemotherapy: current standards of care.,” *Br. J. Cancer*, vol. 89 Suppl 3, no. Suppl 3, pp. S3-8, Dec. 2003.

[204] M. Hurwitz, “Chemotherapy in Prostate Cancer,” *Curr. Oncol. Rep.*, vol. 17, no. 10, p. 44, Oct. 2015.

[205] F. Ren, J. Shen, H. Shi, F. J. Hornicek, Q. Kan, and Z. Duan, “Novel mechanisms and approaches to overcome multidrug resistance in the treatment of ovarian cancer,” *Biochim. Biophys. Acta - Rev. Cancer*, vol. 1866, no. 2, pp. 266–275, Dec. 2016.

[206] T. Kato, K. Mizutani, K. Kameyama, K. Kawakami, Y. Fujita, K. Nakane, Y. Kanimoto, H. Ehara, H. Ito, M. Seishima, T. Deguchi, and M. Ito, “Serum exosomal P-glycoprotein is a potential marker to diagnose docetaxel resistance and select a taxoid for patients with prostate cancer,” *Urol. Oncol. Semin. Orig. Investig.*, vol. 33, no. 9, p. 385.e15-385.e20, Sep. 2015.

[207] K. Stefan, S. M. Schmitt, and M. Wiese, “9-Deazapurines as Broad-Spectrum Inhibitors of the ABC Transport Proteins P-Glycoprotein, Multidrug Resistance-Associated Protein 1, and Breast Cancer Resistance Protein,” *J. Med. Chem.*, vol. 60, no. 21, pp. 8758–8780, Nov. 2017.

[208] C. Battistella and H.-A. Klok, “Reversion of P-gp-Mediated Drug Resistance in Ovarian Carcinoma Cells with PHPMA-Zosuquidar Conjugates,” *Biomacromolecules*, vol. 18, no. 6, pp. 1855–1865, Jun. 2017.

[209] M. S. Singh and A. Lamprecht, “Cargoing P-gp inhibitors via nanoparticle sensitizes tumor cells against doxorubicin,” *Int. J. Pharm.*, vol. 478, no. 2, pp. 745–752, Jan. 2015.

[210] F. Li, M. Danquah, S. Singh, H. Wu, and R. I. Mahato, “Paclitaxel- and lapatinib-loaded lipopolymer micelles overcome multidrug resistance in prostate cancer,” *Drug Deliv. Transl. Res.*, vol. 1, no. 6, pp. 420–428, Dec. 2011.

[211] S. Singh, D. Chitkara, R. Mehrazin, S. W. Behrman, R. W. Wake, and R. I. Mahato, “Chemoresistance in prostate cancer cells is regulated by miRNAs and Hedgehog pathway.,” *PLoS One*, vol. 7, no. 6, p. e40021, 2012.

[212] Y. Li, Y. Zeng, S. M. Mooney, B. Yin, A. Mizokami, M. Namiki, and R. H. Getzenberg, “Resistance to paclitaxel increases the sensitivity to other microenvironmental stresses in prostate cancer cells.,” *J. Cell. Biochem.*, vol. 112, no. 8, pp. 2125–37, Aug. 2011.

[213] R. Dreicer, T. A. Lallas, J. K. Joyce, B. Anderson, J. I. Sorosky, and R. E. Buller, “Vinblastine, ifosfamide, gallium nitrate, and filgrastim in platinum- and paclitaxel-resistant ovarian cancer: a phase II study.,” *Am. J. Clin. Oncol.*, vol. 21, no. 3, pp. 287–90, Jun. 1998.

[214] G. Hudes, L. Einhorn, E. Ross, A. Balsham, P. Loehrer, H. Ramsey, J. Sprandio, M. Entmacher, W. Dugan, R. Ansari, F. Monaco, M. Hanna, and B. Roth, “Vinblastine Versus Vinblastine Plus Oral Estramustine Phosphate for Patients With Hormone-Refractory Prostate Cancer: A Hoosier Oncology Group and Fox Chase Network Phase III Trial,” *J. Clin. Oncol.*, vol. 17, no. 10, pp. 3160–3166, Oct. 1999.

[215] C. Obasaju and G. R. Hudes, “Paclitaxel and docetaxel in prostate cancer.,” *Hematol. Oncol. Clin. North Am.*, vol. 15, no. 3, pp. 525–45, Jun. 2001.

[216] A. Kumar, P. J. Hoskins, and A. V. Tinker, “Dose-dense Paclitaxel in Advanced Ovarian Cancer,” *Clin. Oncol.*, vol. 27, no. 1, pp. 40–47, Jan. 2015.

[217] T. Murphy and K. W. L. Yee, “Cytarabine and daunorubicin for the treatment of acute myeloid leukemia,” *Expert Opin. Pharmacother.*, vol. 18, no. 16, pp. 1765–1780, Nov. 2017.

[218] C. Paul, U. Tidefelt, J. Liliemark, and C. Peterson, “Increasing the accumulation of daunorubicin in human leukemic cells by prolonging the infusion time.,” *Leuk. Res.*, vol. 13, no. 2, pp. 191–6, 1989.

[219] P. Pophali and M. Litzow, “What Is the Best Daunorubicin Dose and Schedule for Acute Myeloid Leukemia Induction?,” *Curr. Treat. Options Oncol.*, vol. 18, no. 1, p. 3, Jan. 2017.

[220] J. Marie, R. Zittoun, and B. Sikic, “Multidrug resistance (mdr1) gene expression in adult acute leukemias: correlations with treatment outcome and in vitro drug sensitivity,” *Blood*, vol. 78, no. 3, 1991.

[221] J. J. Marin, O. Briz, G. Rodriguez-Macias, J. L. Diez-Martin, and R. I. Macias, “Role of drug transport and metabolism in the chemoresistance of acute myeloid leukemia,” *Blood Rev*, vol. 30, no. 1, pp. 55–64, 2016.

[222] O. Legrand, G. Simonin, J. Y. Perrot, R. Zittoun, and J. P. Marie, “Pgp and MRP activities using calcein-AM are prognostic factors in adult acute myeloid leukemia patients,” *Blood*, vol. 91, no. 12, pp. 4480–4488, 1998.

[223] M. V Berridge, A. S. Tan, K. D. McCoy, and R. Wang, “The biochemical and cellular basis of cell proliferation assays that use tetrazolium salts,” *Biochemica*, vol. 4, no. 1, pp. 14–19, 1996.

[224] L. Huyck, C. Ampe, and M. Van Troys, “The XTT cell proliferation assay applied to cell

layers embedded in three-dimensional matrix," *Assay Drug Dev Technol*, vol. 10, no. 4, pp. 382–392, 2012.

[225] X. Li and J. Gong, "Chapter 2 Assays of Cell Viability: Discrimination of Cells Dying by Apoptosis," *Methods Cell Biol.*, vol. 41, pp. 15–38, Jan. 1994.

[226] D. Shum, C. Radu, E. Kim, M. Cajuste, Y. Shao, V. E. Seshan, and H. Djaballah, "A high density assay format for the detection of novel cytotoxic agents in large chemical libraries," *J Enzym. Inhib Med Chem*, vol. 23, no. 6, pp. 931–945, 2008.

[227] B. Galateanu, A. Hudita, C. Negrei, R.-M. Ion, M. Costache, M. Stan, D. Nikitovic, A. W. Hayes, D. A. Spandidos, A. M. Tsatsakis, and O. Ginghina, "Impact of multicellular tumor spheroids as an in vivo-like tumor model on anticancer drug response," *Int. J. Oncol.*, vol. 48, no. 6, pp. 2295–2302, Jun. 2016.

[228] K. L. M. Boylan, B. Misemer, M. S. DeRycke, J. D. Andersen, K. M. Harrington, S. E. Kalloger, C. B. Gilks, S. E. Pambuccian, and A. P. N. Skubitz, "Claudin 4 is differentially expressed between ovarian cancer subtypes and plays a role in spheroid formation," *Int J Mol Sci*, vol. 12, no. 2, pp. 1334–1358, 2011.

[229] H. Sun, E. C. Chow, S. Liu, Y. Du, and K. S. Pang, "The Caco-2 cell monolayer: usefulness and limitations," *Expert Opin. Drug Metab. Toxicol.*, vol. 4, no. 4, pp. 395–411, Apr. 2008.

[230] D. Hanahan and R. A. Weinberg, "The Hallmarks of Cancer," *Cell*, vol. 100, no. 1, pp. 57–70, Jan. 2000.

[231] P. Hainaut and A. Plymoth, "Targeting the hallmarks of cancer," *Curr. Opin. Oncol.*, vol. 25, no. 1, pp. 50–51, Jan. 2013.

[232] A. Siddiqa and R. Marciniak, “Cancer Biology & Therapy Targeting the hallmarks of cancer,” 2008.

[233] K. O. Alfarouk, C.-M. Stock, S. Taylor, M. Walsh, A. K. Muddathir, D. Verduzco, A. H. H. Bashir, O. Y. Mohammed, G. O. Elhassan, S. Harguindey, S. J. Reshkin, M. E. Ibrahim, and C. Rauch, “Resistance to cancer chemotherapy: failure in drug response from ADME to P-gp.,” *Cancer Cell Int.*, vol. 15, p. 71, 2015.

[234] G. W. Sledge and K. D. Miller, “Exploiting the hallmarks of cancer: the future conquest of breast cancer.,” *Eur. J. Cancer*, vol. 39, no. 12, pp. 1668–75, Aug. 2003.

[235] A. K. Nanayakkara, C. A. Follit, G. Chen, N. S. Williams, P. D. Vogel, and J. G. Wise, “Targeted inhibitors of P-glycoprotein increase chemotherapeutic-induced mortality of multidrug resistant tumor cells,” *Sci. Rep.*, vol. 8, no. 1, 2018.

[236] L. Chen, Y. Liang, J. Ruan, Y. Ding, X. Wang, Z. Shi, L.-Q. Gu, X. Yang, and L. Fu, “Reversal of P-gp mediated multidrug resistance in-vitro and in-vivo by FG020318,” *J. Pharm. Pharmacol.*, vol. 56, no. 8, pp. 1061–1066, Aug. 2004.

[237] P. Mistry, A. J. Stewart, W. Dangerfield, S. Okiji, C. Liddle, D. Bootle, J. A. Plumb, D. Templeton, and P. Charlton, “In vitro and in vivo reversal of P-glycoprotein-mediated multidrug resistance by a novel potent modulator, XR9576.,” *Cancer Res.*, vol. 61, no. 2, pp. 749–58, Jan. 2001.

[238] M. M. Gottesman, T. Fojo, and S. E. Bates, “Multidrug resistance in cancer: role of ATP-dependent transporters,” *Nat Rev Cancer*, vol. 2, no. 1, pp. 48–58, 2002.

[239] S. Shugarts and L. Z. Benet, “The role of transporters in the pharmacokinetics of orally administered drugs.,” *Pharm. Res.*, vol. 26, no. 9, pp. 2039–54, Sep. 2009.

[240] U. I. Schwarz, T. Gramatté, J. Krappweis, R. Oertel, and W. Kirch, “P-glycoprotein inhibitor erythromycin increases oral bioavailability of talinolol in humans.,” *Int. J. Clin. Pharmacol. Ther.*, vol. 38, no. 4, pp. 161–7, Apr. 2000.

[241] J. S. Woo, C. H. Lee, C. K. Shim, and S.-J. Hwang, “Enhanced oral bioavailability of paclitaxel by coadministration of the P-glycoprotein inhibitor KR30031.,” *Pharm. Res.*, vol. 20, no. 1, pp. 24–30, Jan. 2003.

[242] S. Shukla, S. Ohnuma, and S. V Ambudkar, “Improving cancer chemotherapy with modulators of ABC drug transporters.,” *Curr. Drug Targets*, vol. 12, no. 5, pp. 621–30, May 2011.

[243] M. Kirby, C. Hirst, and E. D. Crawford, “Characterising the castration-resistant prostate cancer population: a systematic review,” *Int. J. Clin. Pract.*, vol. 65, no. 11, pp. 1180–1192, Nov. 2011.

[244] D. R. Berthold, G. R. Pond, F. Soban, R. de Wit, M. Eisenberger, and I. F. Tannock, “Docetaxel plus prednisone or mitoxantrone plus prednisone for advanced prostate cancer: updated survival in the TAX 327 study.,” *J. Clin. Oncol.*, vol. 26, no. 2, pp. 242–5, Jan. 2008.

[245] D. P. Petrylak, C. M. Tangen, M. H. A. Hussain, P. N. Lara, J. A. Jones, M. E. Taplin, P. A. Burch, D. Berry, C. Moinpour, M. Kohli, M. C. Benson, E. J. Small, D. Raghavan, and E. D. Crawford, “Docetaxel and Estramustine Compared with Mitoxantrone and Prednisone for Advanced Refractory Prostate Cancer,” *N. Engl. J. Med.*, vol. 351, no. 15, pp. 1513–1520, Oct. 2004.

[246] I. F. Tannock, R. de Wit, W. R. Berry, J. Horti, A. Pluzanska, K. N. Chi, S. Oudard, C.

Théodore, N. D. James, I. Turesson, M. A. Rosenthal, M. A. Eisenberger, and TAX 327 Investigators, “Docetaxel plus Prednisone or Mitoxantrone plus Prednisone for Advanced Prostate Cancer,” *N. Engl. J. Med.*, vol. 351, no. 15, pp. 1502–1512, Oct. 2004.

[247] C. Sánchez, A. Mercado, H. R. Contreras, P. Mendoza, J. Cabezas, C. Acevedo, C. Huidobro, and E. A. Castellón, “Chemotherapy sensitivity recovery of prostate cancer cells by functional inhibition and knock down of multidrug resistance proteins,” *Prostate*, vol. 71, no. 16, pp. 1810–1817, Dec. 2011.

[248] C. Shanholtz, “ACUTE LIFE-THREATENING TOXICITY OF CANCER TREATMENT,” *Crit. Care Clin.*, vol. 17, no. 3, pp. 483–502, Jul. 2001.

[249] L. S. Schwartzberg, “Chemotherapy-induced nausea and vomiting: clinician and patient perspectives.,” *J. Support. Oncol.*, vol. 5, no. 2 Suppl 1, pp. 5–12, Feb. 2007.

[250] K. S. Khoo, P. T. Ang, and A. G. Lim, “Common toxicities of cancer chemotherapy.,” *Singapore Med. J.*, vol. 34, no. 5, pp. 418–20, Oct. 1993.

[251] J. Abraham, M. Edgerly, R. Wilson, C. Chen, A. Rutt, S. Bakke, R. Robey, A. Dwyer, B. Goldspiel, F. Balis, O. Van Tellingen, S. E. Bates, and T. Fojo, “A phase I study of the P-glycoprotein antagonist tariquidar in combination with vinorelbine.,” *Clin. Cancer Res.*, vol. 15, no. 10, pp. 3574–82, May 2009.

[252] E. Fox, B. C. Widemann, D. Pastakia, C. C. Chen, S. X. Yang, D. Cole, and F. M. Balis, “Pharmacokinetic and pharmacodynamic study of tariquidar (XR9576), a P-glycoprotein inhibitor, in combination with doxorubicin, vinorelbine, or docetaxel in children and adolescents with refractory solid tumors,” *Cancer Chemother. Pharmacol.*, vol. 76, no. 6, pp. 1273–1283, Dec. 2015.

[253] B. L. Samuels, D. R. Hollis, G. L. Rosner, D. L. Trump, C. L. Shapiro, N. J. Vogelzang, and R. L. Schilsky, “Modulation of Vinblastine Resistance in Metastatic Renal Cell Carcinoma with Cyclosporine A or Tamoxifen: A Cancer and Leukemia Group B Study’,” 1977.

[254] S. C. Linn, C. K. van Kalken, O. van Tellingen, P. van der Valk, C. J. van Groeningen, C. M. Kuiper, H. M. Pinedo, and G. Giaccone, “Clinical and pharmacologic study of multidrug resistance reversal with vinblastine and bepridil.,” *J. Clin. Oncol.*, vol. 12, no. 4, pp. 812–819, Apr. 1994.

[255] G. Sliwoski, S. Kothiwale, J. Meiler, E. W. Lowe, and Jr., “Computational methods in drug discovery.,” *Pharmacol. Rev.*, vol. 66, no. 1, pp. 334–95, 2014.

[256] J. H. Van Drie, “Computer-aided drug design: the next 20 years,” *J. Comput. Aided. Mol. Des.*, vol. 21, no. 10–11, pp. 591–601, Oct. 2007.

[257] L. Mak, S. Liggi, L. Tan, K. Kusonmano, J. M. Rollinger, A. Koutsoukas, R. C. Glen, and J. Kirchmair, “Anti-cancer drug development: computational strategies to identify and target proteins involved in cancer metabolism.,” *Curr. Pharm. Des.*, vol. 19, no. 4, pp. 532–77, 2013.

[258] D. Prada-Gracia, “Application of computational methods for anticancer drug discovery, design, and optimization,” *Bol. Med. Hosp. Infant. Mex.*, vol. 73, no. 6, pp. 411–423, Nov. 2016.

[259] M. Jiao, G. Liu, Y. Xue, and C. Ding, “Computational drug repositioning for cancer therapeutics.,” *Curr. Top. Med. Chem.*, vol. 15, no. 8, pp. 767–75, 2015.

[260] K.-H. Lee, J.-H. Lee, S.-W. Han, S.-A. Im, T.-Y. Kim, D.-Y. Oh, and Y.-J. Bang,

"Antitumor activity of NVP-AUY922, a novel heat shock protein 90 inhibitor, in human gastric cancer cells is mediated through proteasomal degradation of client proteins," *Cancer Sci.*, vol. 102, no. 7, pp. 1388–1395, Jul. 2011.

[261] P. A. Brough, W. Aherne, X. Barril, J. Borgognoni, K. Boxall, J. E. Cansfield, K.-M. J. Cheung, I. Collins, N. G. M. Davies, M. J. Drysdale, B. Dymock, S. A. Eccles, H. Finch, A. Fink, A. Hayes, R. Howes, R. E. Hubbard, K. James, A. M. Jordan, A. Lockie, V. Martins, A. Massey, T. P. Matthews, E. McDonald, C. J. Northfield, L. H. Pearl, C. Prodromou, S. Ray, F. I. Raynaud, S. D. Roughley, S. Y. Sharp, A. Surgenor, D. L. Walmsley, P. Webb, M. Wood, P. Workman, and L. Wright, "4,5-Diarylisoxazole Hsp90 Chaperone Inhibitors: Potential Therapeutic Agents for the Treatment of Cancer," *J. Med. Chem.*, vol. 51, no. 2, pp. 196–218, Jan. 2008.

[262] K.-C. Cheng, W. A. Korfmacher, R. E. White, and F. G. Njoroge, "Lead Optimization in Discovery Drug Metabolism and Pharmacokinetics/Case study: The Hepatitis C Virus (HCV) Protease Inhibitor SCH 503034.," *Perspect. Medicin. Chem.*, vol. 1, pp. 1–9, Jun. 2007.

[263] K. H. Bleicher, H.-J. Böhm, K. Müller, and A. I. Alanine, "Hit and lead generation: beyond high-throughput screening," *Nat. Rev. Drug Discov.*, vol. 2, no. 5, pp. 369–378, May 2003.

[264] R. Deprez-Poulain and B. Deprez, "Facts, figures and trends in lead generation.," *Curr. Top. Med. Chem.*, vol. 4, no. 6, pp. 569–80, 2004.

[265] S. C. Basak, "Chemobioinformatics: the advancing frontier of computer-aided drug design in the post-genomic era.," *Curr. Comput. Aided. Drug Des.*, vol. 8, no. 1, pp. 1–2, Mar.

2012.

[266] L. Kupcsik, “Estimation of cell number based on metabolic activity: the MTT reduction assay,” *Methods Mol Biol*, vol. 740, pp. 13–19, 2011.

[267] C. Martin, G. Berridge, P. Mistry, C. Higgins, P. Charlton, and R. Callaghan, “The molecular interaction of the high affinity reversal agent XR9576 with P-glycoprotein,” *Br J Pharmacol*, vol. 128, no. 2, pp. 403–411, 1999.

[268] N. Subramanian, K. Condic-Jurkic, and M. L. O’Mara, “Structural and dynamic perspectives on the promiscuous transport activity of P-glycoprotein,” *Neurochem. Int.*, vol. 98, pp. 146–152, Sep. 2016.

[269] A. L. Iorio, M. da Ros, O. Fantappiè, M. Lucchesi, L. Facchini, A. Stival, S. Becciani, M. Guidi, C. Favre, M. de Martino, L. Genitori, and I. Sardi, “Blood-Brain Barrier and Breast Cancer Resistance Protein: A Limit to the Therapy of CNS Tumors and Neurodegenerative Diseases.,” *Anticancer. Agents Med. Chem.*, vol. 16, no. 7, pp. 810–5, 2016.

[270] P. Garg, R. Dhakne, and V. Belekar, “Role of breast cancer resistance protein (BCRP) as active efflux transporter on blood-brain barrier (BBB) permeability,” *Mol. Divers.*, vol. 19, no. 1, pp. 163–172, Feb. 2015.

[271] A. Mahringer and G. Fricker, “BCRP at the Blood−Brain Barrier: Genomic Regulation by 17β-Estradiol,” *Mol. Pharm.*, vol. 7, no. 5, pp. 1835–1847, Oct. 2010.

[272] N. Memon, K. M. Bircsak, F. Archer, C. J. Gibson, P. Ohman-Strickland, B. I. Weinberger, M. M. Parast, A. M. Vetrano, and L. M. Aleksunes, “Regional expression of the BCRP/ABCG2 transporter in term human placentas,” *Reprod. Toxicol.*, vol. 43, pp.

72–77, Jan. 2014.

[273] Q. Mao, “BCRP/ABCG2 in the Placenta: Expression, Function and Regulation,” *Pharm. Res.*, vol. 25, no. 6, pp. 1244–1255, Jun. 2008.

[274] J. T. Szilagyi, A. M. Vetrano, J. D. Laskin, and L. M. Aleksunes, “Localization of the placental BCRP/ ABCG2 transporter to lipid rafts: Role for cholesterol in mediating efflux activity,” *Placenta*, vol. 55, pp. 29–36, Jul. 2017.

[275] N. Ji, J. Yuan, J. Liu, and S. Tian, “Developing multidrug-resistant cells and exploring correlation between BCRP/ABCG2 over-expression and DNA methyltransferase,” *Acta Biochim. Biophys. Sin. (Shanghai).*, vol. 42, no. 12, pp. 854–862, Dec. 2010.

[276] H. Kodaira, H. Kusuhara, J. Ushiki, E. Fuse, and Y. Sugiyama, “Kinetic Analysis of the Cooperation of P-Glycoprotein (P-gp/Abcb1) and Breast Cancer Resistance Protein (Bcrp/Abcg2) in Limiting the Brain and Testis Penetration of Erlotinib, Flavopiridol, and Mitoxantrone,” *J. Pharmacol. Exp. Ther.*, vol. 333, no. 3, pp. 788–796, Jun. 2010.

[277] H. Nakanishi, A. Yonezawa, K. Matsubara, and I. Yano, “Impact of P-glycoprotein and breast cancer resistance protein on the brain distribution of antiepileptic drugs in knockout mouse models,” *Eur. J. Pharmacol.*, vol. 710, no. 1–3, pp. 20–28, Jun. 2013.

[278] X. Wang, T. Furukawa, T. Nitanda, M. Okamoto, Y. Sugimoto, S.-I. Akiyama, and M. Baba, “Breast cancer resistance protein (BCRP/ABCG2) induces cellular resistance to HIV-1 nucleoside reverse transcriptase inhibitors.,” *Mol. Pharmacol.*, vol. 63, no. 1, pp. 65–72, Jan. 2003.

[279] T. Kilic, J. A. Alberta, P. R. Zdunek, M. Acar, P. Iannarelli, T. O’Reilly, E. Buchdunger, P. M. Black, and C. D. Stiles, “Intracranial inhibition of platelet-derived growth factor-

mediated glioblastoma cell growth by an orally active kinase inhibitor of the 2-phenylaminopyrimidine class.," *Cancer Res.*, vol. 60, no. 18, pp. 5143–50, Sep. 2000.

[280] N. Hussein, C. Ashby, H. Amawi, A. Nyinawabera, A. Vij, V. Khare, C. Karthikeyan, and A. Tiwari, "Cariprazine, A Dopamine D2/D3 Receptor Partial Agonist, Modulates ABCG2-Mediated Multidrug Resistance in Cancer," *Cancers (Basel).*, vol. 10, no. 9, p. 308, Sep. 2018.

[281] K. M. Bircsak, C. J. Gibson, R. W. Robey, and L. M. Aleksunes, "Assessment of drug transporter function using fluorescent cell imaging.," *Curr. Protoc. Toxicol.*, vol. 57, p. Unit 23.6., Sep. 2013.

[282] K. Römermann, T. Wanek, M. Bankstahl, J. P. Bankstahl, M. Fedrowitz, M. Müller, W. Löscher, C. Kuntner, and O. Langer, "(R)-[(11)C]verapamil is selectively transported by murine and human P-glycoprotein at the blood-brain barrier, and not by MRP1 and BCRP.," *Nucl. Med. Biol.*, vol. 40, no. 7, pp. 873–8, Oct. 2013.

[283] M. Sriram, G. A. van der Marel, H. L. Roelen, J. H. van Boom, and A. H. Wang, "Conformation of B-DNA containing O6-ethyl-G-C base pairs stabilized by minor groove binding drugs: molecular structure of d(CGC[e6G]AATTCGCG complexed with Hoechst 33258 or Hoechst 33342.," *EMBO J.*, vol. 11, no. 1, pp. 225–32, Jan. 1992.

[284] I. Parrilla, J. M. Vázquez, C. Cuello, M. A. Gil, J. Roca, D. Di Berardino, and E. A. Martínez, "Hoechst 33342 stain and u.v. laser exposure do not induce genotoxic effects in flow-sorted boar spermatozoa," *Reproduction*, vol. 128, no. 5, pp. 615–621, Nov. 2004.

[285] C. W. Scharenberg, M. A. Harkey, and B. Torok-Storb, "The ABCG2 transporter is an efficient Hoechst 33342 efflux pump and is preferentially expressed by immature human

hematopoietic progenitors.," *Blood*, vol. 99, no. 2, pp. 507–12, Jan. 2002.

[286] M. Kim, H. Turnquist, J. Jackson, M. Sgagias, Y. Yan, M. Gong, M. Dean, J. G. Sharp, and K. Cowan, "The multidrug resistance transporter ABCG2 (breast cancer resistance protein 1) effluxes Hoechst 33342 and is overexpressed in hematopoietic stem cells.," *Clin. Cancer Res.*, vol. 8, no. 1, pp. 22–8, Jan. 2002.

[287] B. B. Weksler, E. A. Subileau, N. Perrière, P. Charneau, K. Holloway, M. Leveque, H. Tricoire-Leignel, A. Nicotra, S. Bourdoulous, P. Turowski, D. K. Male, F. Roux, J. Greenwood, I. A. Romero, and P. O. Couraud, "Blood-brain barrier-specific properties of a human adult brain endothelial cell line," *FASEB J.*, vol. 19, no. 13, pp. 1872–1874, Nov. 2005.

[288] C. J. Czupalla, S. Liebner, and K. Devraj, "In vitro models of the blood-brain barrier," *Methods Mol. Biol.*, 2014.

[289] H. C. Helms, N. J. Abbott, M. Burek, R. Cecchelli, P. O. Couraud, M. A. Deli, C. Förster, H. J. Galla, I. A. Romero, E. V. Shusta, M. J. Stebbins, E. Vandenhaute, B. Weksler, and B. Brodin, "In vitro models of the blood-brain barrier: An overview of commonly used brain endothelial cell culture models and guidelines for their use," *Journal of Cerebral Blood Flow and Metabolism*. 2015.

[290] B. Weksler, I. A. Romero, and P. O. Couraud, "The hCMEC/D3 cell line as a model of the human blood brain barrier," *Fluids and Barriers of the CNS*. 2013.

[291] S. Dauchy, F. Miller, P.-O. Couraud, R. J. Weaver, B. Weksler, I.-A. Romero, J.-M. Scherrmann, I. De Waziers, and X. Declèves, "Expression and transcriptional regulation of ABC transporters and cytochromes P450 in hCMEC/D3 human cerebral microvascular

endothelial cells," *Biochem. Pharmacol.*, vol. 77, no. 5, pp. 897–909, Mar. 2009.

[292] F. Tang, H. Ouyang, J. Z. Yang, and R. T. Borchardt, "Bidirectional Transport of Rhodamine 123 and Hoechst 33342, Fluorescence Probes of the Binding Sites on P-glycoprotein, across MDCK-MDR1 Cell Monolayers," *J. Pharm. Sci.*, 2004.

[293] F. Montanari, A. Cseke, K. Wlcek, and G. F. Ecker, "Virtual Screening of DrugBank Reveals Two Drugs as New BCRP Inhibitors," *SLAS Discov. Adv. Life Sci. R&D*, vol. 22, no. 1, pp. 86–93, Jan. 2017.

[294] Y. Pan, P. P. Chothe, and P. W. Swaan, "Identification of Novel Breast Cancer Resistance Protein (BCRP) Inhibitors by Virtual Screening," *Mol. Pharm.*, vol. 10, no. 4, pp. 1236–1248, Apr. 2013.

[295] I. H. Plenderleith, "Treating the treatment: toxicity of cancer chemotherapy.," *Can. Fam. Physician*, vol. 36, pp. 1827–30, Oct. 1990.

[296] Y. Imai, S. Asada, S. Tsukahara, E. Ishikawa, T. Tsuruo, and Y. Sugimoto, "Breast Cancer Resistance Protein Exports Sulfated Estrogens but Not Free Estrogens," *Mol. Pharmacol.*, vol. 64, no. 3, pp. 610–618, Sep. 2003.

[297] G. Pottier, S. Marie, S. Goutal, S. Auvity, M.-A. Peyronneau, S. Stute, R. Boisgard, F. Dollé, I. Buvat, F. Caillé, and N. Tournier, "Imaging the Impact of the P-Glycoprotein (ABCB1) Function on the Brain Kinetics of Metoclopramide.," *J. Nucl. Med.*, vol. 57, no. 2, pp. 309–14, Feb. 2016.

[298] W. Löscher and O. Langer, "Imaging of P-glycoprotein function and expression to elucidate mechanisms of pharmacoresistance in epilepsy.," *Curr. Top. Med. Chem.*, vol. 10, no. 17, pp. 1785–91, 2010.

[299] S. Eyal, F. S. Chung, M. Muzi, J. M. Link, D. A. Mankoff, A. Kaddoumi, F. O'Sullivan, M. F. Hebert, and J. D. Unadkat, "Simultaneous PET imaging of P-glycoprotein inhibition in multiple tissues in the pregnant nonhuman primate.," *J. Nucl. Med.*, vol. 50, no. 5, pp. 798–806, May 2009.

[300] S. Syvänen and J. Eriksson, "Advances in PET imaging of P-glycoprotein function at the blood-brain barrier.," *ACS Chem. Neurosci.*, vol. 4, no. 2, pp. 225–37, Feb. 2013.

[301] V. Vasiliou, K. Vasiliou, and D. W. Nebert, "Human ATP-binding cassette (ABC) transporter family.," *Hum. Genomics*, vol. 3, no. 3, pp. 281–90, Apr. 2009.

[302] R. Sane, S. Agarwal, R. K. Mittapalli, and W. F. Elmquist, "Saturable active efflux by p-glycoprotein and breast cancer resistance protein at the blood-brain barrier leads to nonlinear distribution of elacridar to the central nervous system.," *J. Pharmacol. Exp. Ther.*, vol. 345, no. 1, pp. 111–24, Apr. 2013.

[303] G. Lehne, "P-glycoprotein as a drug target in the treatment of multidrug resistant cancer.," *Curr. Drug Targets*, vol. 1, no. 1, pp. 85–99, Jul. 2000.

[304] K. Nooter and G. Stoter, "Molecular Mechanisms of Multidrug Resistance in Cancer Chemotherapy," *Pathol. - Res. Pract.*, vol. 192, no. 7, pp. 768–780, Jan. 1996.

[305] F. S. Chung, J. S. Santiago, M. Francisco, M. De Jesus, C. V Trinidad, M. Floyd, and E. See, "Disrupting P-glycoprotein function in clinical settings: what can we learn from the fundamental aspects of this transporter?," 2016.

[306] J. P. Hughes, S. Rees, S. B. Kalindjian, and K. L. Philpott, "Principles of early drug discovery.," *Br. J. Pharmacol.*, vol. 162, no. 6, pp. 1239–49, Mar. 2011.

[307] N. M. I. Taylor, I. Manolaridis, S. M. Jackson, J. Kowal, H. Stahlberg, and K. P. Locher,

"Structure of the human multidrug transporter ABCG2," *Nature*, vol. 546, no. 7659, pp. 504–509, May 2017.